Bio-inspired soft robotic systems: Exploiting environmental interactions using embodied mechanics and sensory coordination

Josie A. E. Hughes

Department of Engineering

University of Cambridge

This dissertation is submitted for the degree of

Doctor of Philosophy

Downing College

July 2018

Declaration

I hereby declare that except where specific reference is made to the work of others, the contents of this dissertation are original and have not been submitted in whole or in part for consideration for any other degree or qualification in this, or any other University. This dissertation is the result of my own work and includes nothing which is the outcome of work done in collaboration, except where specifically indicated in the text. This dissertation contains 42,581 words including appendices, bibliography, footnotes, tables and equations and has 70 figures.

Josie A. E. Hughes
July 2018

Acknowledgements

Thanks to my supervisor Dr. Fumiya Iida from whom I have learnt so much. Thanks also to my family, friends and all those who have supported me over the years, in particular to Holly, Henry and Rufus.

Preface

The content of this dissertation is based on a number of peer-reviewed publications. The content of the publications has been edited and extended to match this thesis. The publications from which the content of a chapter is derived are indicated on the first page of the respective chapter. All projects are the result of collaborative work with Dr. Fumiya Iida. My personal contribution to the project will be identified when the papers are introduced. The papers accepted for publication in peer-reviewed journals include:

- Hughes, Josie, and Fumiya Iida. "Localized differential sensing of soft deformable surfaces." Robotics and Automation (ICRA), 2017 IEEE International Conference on. IEEE, 2017. (pp. 4959-4964)

- Hughes, Josie, and Fumiya Iida. Tactile Sensing applied to the Universal Gripper using Conductive Thermoplastic Elastomer. Soft Robotics Journal. (In Press).

- Hughes, Josie, and Fumiya Iida. Tack and Deformation Based Sensorised Gripping Using Conductive Hot Melt Adhesive. *RoboSoft IEEE Confernce, Livirno, Italy (2018).*

- Hughes, Josie, and Fumiya Iida. "3D Printed Sensorized Soft Robotic Manipulator Design." *Conference Towards Autonomous Robotic Systems. Springer, Cham, 2017.*

- Hughes, Josie, et al. "Soft manipulators and grippers: a review." *Frontiers in Robotics and AI 3 (2016): pp. 69.*

Additionally, I have worked alongside others on a number of published papers which contribute to the larger research concepts and ideology:

- Josie Hughes, Luca Scimeca, Ioana Ifrim, Perla Maiolino and Fumiya Iida, "Achieving Robotically Peeled Lettuce", *Robotics and Automation Letters.*

- Cheah, Michael, Hughes, Josie and Iida, Fumiya. "Data Synthesization for Classification in Autonomous Robotic Grasping System Using 'Catalogue'-Style

Images" *Conference Towards Autonomous Robotic Systems. Springer, Cham, 2018.* (Accepted)

- Watson, Joe, Hughes, Josie and Iida, Fumiya. "Real-World, Real-Time Robotic Grasping with Convolutional Neural Networks." *Conference Towards Autonomous Robotic Systems. Springer, Cham, 2017.* (pp. 617-626)

A a number of papers have also been submitted for review:

- Josie Hughes, Perla Maolino and Fumiya Iida. An Anthropomorphic Soft Skeleton Hand Exploiting Conditional Stiffness for Piano Playing. *Science Robotics.*
- Josie Hughes and Fumiya Iida. Soft tactile sensing for wearable health monitoring devices.
- Glday, Kieran, Hughes, Josie, and Fumiya Iida. "Achieving Flexible Assembly Using Autonomous Robotic Systems" *IROS, 2018*

Abstract

Despite the widespread development of highly intelligent robotic systems exhibiting great precision, reliability, and dexterity, robots remain incapable of performing basic manipulation tasks that humans take for granted. Manipulation in unstructured environments continues to be acknowledged as a significant challenge. Soft robotics, the use of less rigid materials in robots, has been proposed as one means of addressing these limitations. The technique enables more compliant interactions with the environment, allowing for increasingly adaptive behaviours better suited to more human-centric applications.

Embodied intelligence is a biologically inspired concept in which intelligence is a function of the entire system, not only the controller or 'brain'. This thesis focuses on the use of embodied intelligence for the development of soft robots, with a particular focus on how it can aid both perception and adaptability. Two main hypotheses are raised: first, that the mechanical design and fabrication of soft-rigid hybrid robots can enable increasingly environmentally adaptive behaviours, and second, that sensing materials and morphology can provide intelligence that assists perception through embodiment. A number of approaches and frameworks for the design and development of embodied systems are presented that address these hypotheses.

It is shown how embodiment in soft sensor morphology can be used to perform localised processing and thereby distribute the intelligence over the body of a system. Specifically in soft robots, sensor morphology utilises the directional deformations created by interactions with the environment to aid in perception. Building on and formalising these ideas, a number of morphology-based frameworks are proposed for detecting different stimuli.

The multifaceted role of materials in soft robots is demonstrated through the development of materials capable of both sensing and changes in material property. Such materials provide additional functionality beyond their integral scaffolding and static mechanical characteristics. In particular, an integrated material has been created exhibiting both sensing capabilities and also variable stiffness and 'tack' force, thereby enabling complex single-point grasping.

To maximise the intelligence that can be gained through embodiment, a design approach to soft robots, 'soft-rigid hybrid' design is introduced. This approach exploits passive behaviours and body dynamics to provide environmentally adaptive behaviours and sensing.

It is leveraged by multi-material 3D printing techniques and novel approaches and frameworks for designing mechanical structures.

The findings in this thesis demonstrate that an embodied approach to soft robotics provides capabilities and behaviours that are not currently otherwise achievable. Utilising the concept of 'embodiment' results in softer robots with an embodied intelligence that aids perception and adaptive behaviours, and has the potential to bring the physical abilities of robots one step closer to those of animals and humans.

Contents

Chapter 1

Introduction

It has been predicted that by 2050 40% of current jobs will be replaced with robots [1], and that robots will beat the champion world cup football team [2]. Although intentionally provocative claims, these reflect the societal need for robotics [3] and also the significant technological advancements being made in the field. Despite the development of many highly intelligent and capable robotic systems, outside of closely controlled environments, robots cannot perform basic manipulation tasks that humans take for granted [4]. Manipulation in unstructured environments is still acknowledged as a significant challenge [5]. Typically, robotic manipulation has been performed using rigid, high precision manipulators working in ordered, factory-style environments, with the system tailored for a specific, niche task [6]. The development of robots that have the ability to work alongside humans and perform a variety of tasks and behaviours in non-uniform and dynamic environments would represent a step change in the abilities, capabilities and the ubiquity of robotics [7].

The soft and compliant nature of biological systems is one of the most distinguishing differences between them and existing conventional robotic systems [8]. This use of compliance is one factor that enables complexity, variety and subtlety in behaviour that can be seen in animals. Compliance extends the range of movement and behaviours that can be performed, relaxing the typical one-to-one mapping between actuation and the degree of freedom of movement seen in rigid robotics [9]. The softness also amplifies the reciprocal coupling between the environment and the mechanical system, such that interactions with the environment can aid the output behaviour [10]. The increased complexity and environmentally deterministic behaviour also allows some local mechanical 'processing' to be performed to achieve global co-ordination of highly complex soft biological systems [11]. Bio-inspiration and the inclusion of softer more compliant material provides potential mechanisms to allow robotics to achieve the required environmentally adaptive behaviours.

Soft robotics provides a potential paradigm shift, encouraging the use of alternative materials, methods and approaches to those of typical 'rigid robotics.' Soft, deformable and variable stiffness technologies are used alongside new design ideologies and methodologies [9]. This approach utilises the compliance and adaptability of soft structures to develop highly adaptive robots that can exploit the environment to achieve complex and adaptive output behaviours. Soft robotics has the potential to support development of robotic systems which can address many unsolved research problems, and enable dexterous and complex manipulation [12, 13]. For example it can enable development of highly dexterous, variable stiffness manipulators for minimally invasive surgery [14, 15]. The potential for soft interactions allows for safer robot-human interactions [16] and allows robots to interact more intelligently in an unstructured environment with applications in service roles [17, 18] and rehabilitation [19, 20].

Although soft robots offer exciting possibilities, current frameworks impose limitations on the achievable ranges of behaviours, actuation capabilities and perception abilities [21]. The inherent softness introduces trade-offs in the complexity of control required and the achievable precision. Output forces generated by softer systems can be limited and challenging to control. Compliance results in mechanical structures with potentially infinite degrees of freedom, such that typical sensing approaches using a one-to-one mapping between degrees of freedom and sensors are not possible [22]. Therefore, new approaches to sensing and control are required that incorporate an understanding of a compliant system without restricting its natural kinematics.

Approaches and technologies have been developed to address these individual technological challenges at a sub-system level. For example, to extend the range of behaviours of soft bodies without increasing complexity, methods have been developed including underactuation of mechanical systems and exploiting synergies between the mechanics of the system and actuation (motor synergy) [23, 24]. Similarly, sensing technologies that allow high sensitivity detection of high strains have been developed [25, 26]. Many of these problems stem from the advantageous characteristic of soft robotics, compliance. To develop soft solutions which address these challenges, system level design approaches and philosophies for soft robotics are required which embrace inherent compliance rather than fighting it.

A key element of biological systems is the distribution of intelligent behaviour throughout the entire system, ranging from the wrinkles on finger tips for texture detection to complex bone structures which enable passive behaviours. This embodiment of 'intelligence' throughout the entire body (material, mechanical and control systems) enables localised processing and allows exploitation of the interactions between the controller, mechanical systems and the external environment. By applying this concept to soft robotics, a new design approach and accompanying technologies can be developed, in which the different elements of the robot are no longer considered in isolation. The interplay between the brain (controller), materials and the environment must be considered as fundamental to the design of the system. The embodiment of the mechanics and the properties of the materials work cooperatively together to determine the resultant output behaviour and also the perception of both the environment and its own state.

1.1 A Design Approach for Soft Robots using Embodied Intelligence

To address many of the limitations of existing soft robotics approaches, an approach for the design and development of soft robots which considers the embodiment and interplay between the different physical systems and the environment is proposed (Fig. 1.1). Embodied intelligence is a philosophical approach, which believes that many aspects of cognition are shaped by the entire body of the organism, including the materials and mechanics. The brain interacts with the materials and mechanics of the system, which in turn interact with the environment. Thus, computation can be distributed over the entire system, with the embodiment providing intelligence, with the materials and morphology aiding and dictating the output behaviour and interaction with the environment. Under this philosophy, intelligent behaviour emerges from the dynamic physical and sensory interaction of the material, morphology and mechanics of the robot and the environment.

Embodied intelligence can be observed widely in biology. Octopuses in particular are highly embodied and dexterous animals: their arms are fully flexible, can bend in any direction, grasp objects and modulate stiffness along their length [27]. The material and mechanical processes combined with self-organization can result in the emergence of an efficient adaptive behaviour in a specific environment. Embodied intelligence can also be observed in human locomotion and grasping. The morphology and materials, the musculoskeletal system, provides some passive behaviours enabling highly nuanced and complex actions.

The intelligence gained from the embodiment of materials and mechanics also contributes to sensing and perception. Perception, gaining an understanding of the surroundings, involves additional cognition or intelligence after sensing, i.e. the transduction of a stimulus, has been performed. Materials and mechanics can provide embodied intelligence which helps reduce the additional understanding or processing required to achieve perception.

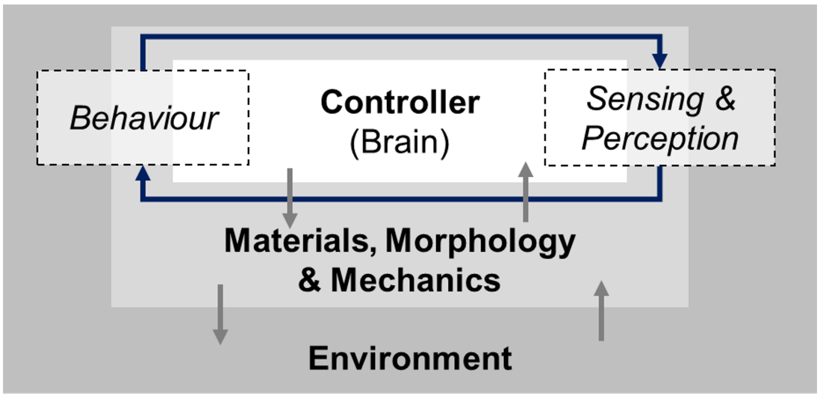

Figure 1.1 Embodied framework for developing soft robots where perception and actuation are dependent on the interaction between materials, environment and the controller.

In this approach, the output behaviour is dependent on the controller, materials and mechanics, and the environment, with all of these components affecting the output behaviour. Perception and behaviour are dependant on the 'embodied' properties of the materials and mechanics, which interact with each other and the environment. To achieve a diverse range of complex output behaviours,the material and morphology and interaction with the environment contribute strongly.

Perception is not only dependent on the controller, materials and mechanics but also dependent on the behaviour of the system and its interaction with the environment. To address the sensing challenging posed by soft robotics (infinite degrees of freedom, flexibility and elasticity) the materials, mechanics, morphology and environmental interaction of the systems should all contribute to and aid perception. Additionally, the embodiment of sensing materials should be used to aid in perception, such that the required stimuli can be detected with minimal post-processing. The mechanical system should aid perception and sensing, with the mechanical system acting as a transducer or enabling specific sensing or perception. This is a bio-inspired approach, with direct comparison to the human body possible. For example, in the human hand, the skin, bone structure and environment all contribute to the achievable behaviour and perception.

To achieve physically implementable solutions, and to address many of the limitations of purely soft robots 'soft-rigid hybrid' mechanical design is proposed as part of the embodied approach. Many high functioning, land-based biological systems use both soft and rigid elements. This offers a trade-off between the compliance and controllability (Fig. 1.2). The increased compliance of soft robotics offers a larger potential range of behaviours, however, these are only achievable with increased control. Soft-rigid hybrid mechanical

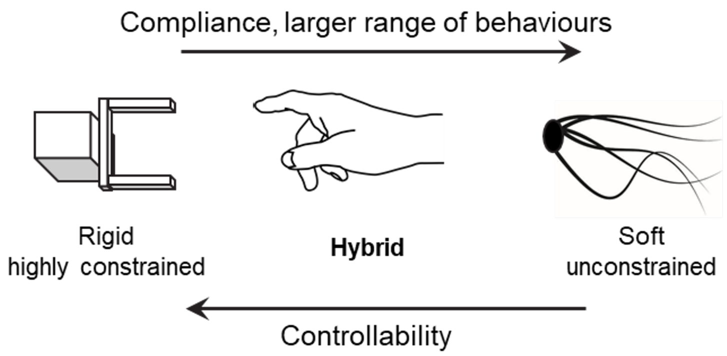

Figure 1.2 Hybrid mechanical offers a compromise in terms of the compliance and range of behaviours and also the control-ability.

design, referred to as hybrid design in this work, offers a compromise; a larger range of behaviours is possible with a lower reduction in controllability and precision.

Hybrid design extends beyond the inclusion of rigid materials into softer bodies. It is a mechanical design approach where the soft and rigid materials work cooperatively to augment their individual capabilities. Taking inspiration from nature, the rigid human skeleton is aided by soft ligaments which keep the joints aligned and limit the range of movement and determine the observable stiffness and characteristics.

This framework for approaching the development of soft robotics includes the use of soft-rigid hybrid mechanics to address the challenge of achieving adaptive behavioural diversity and perceptual acuity. Mechanics and materials are used to achieve embodied localised computation. The methods, technologies and approaches developed will allow robotics to be produced with a wide range of behaviours. The behaviours are adaptable to varying environments and allows perception to be achieved that is scale-able and focuses on the direct detection of the state of the interaction between the body and the environment.

1.2 Research Hypotheses

The overall goal of this research is to understand the role of material and mechanics when developing soft robotics using an embodied approach to design. There are two key hypotheses:

Hypothesis 1: The design and fabrication of soft-rigid hybrid robots can enable increasingly environmentally adaptive behaviours. This can be achieved by:

- Exploiting the mechanical behaviours provided by passive dynamics

- Using integrated materials to provide sensing and functional behaviour (for example change in shape or stiffness)

Hypothesis 2: Sensing materials and morphology can provide intelligence that assists perception through embodiment.

- Materials properties can aid sensing, such as variable stiffness or stickiness
- Sensor morphology in soft bodies can perform localised pre-processing to aid the detection of environmental stimuli
- The mechanical design of a system can provide environmental awareness by sensing body dynamics

To develop the theoretical frameworks and methodologies required to address these hypotheses, the general area of robotic manipulation was chosen as a focus. This area was selected as there are many unsolved challenges against which to validate new and novel approaches.

1.3 Contributions

To address these hypotheses, there are four key areas of research. These develop the necessary technologies and frameworks, each having an original research contribution. In line with the embodied approach (Fig. 1.1), the research contributions consider all aspects of the development of soft robots.

1.3.1 Sensor Morphology for Soft Systems

Sensing of soft deformable surfaces is challenging. Using sensor morphology to perform localised processing of the deformation of a soft body can enable sensors that allow detection of the deformation of the surface without restricting its intrinsic flexibility. The embodied intelligence provided by complex morphologies removes some of the need for the additional post-processing, aiding the conversion between sensor signal and perceived output.

To demonstrate the abilities of sensor morphology three frameworks have been developed that provide large area soft sensing, each building upon the previous. The first uses a grid morphology to provide systematic understanding of large area soft surfaces. The second framework, ‘differential sensing’, uses pairs of sensors with different morphologies to identify specific characteristic of deformation (direction, location or magnitude). The final framework enables dynamic sensing. This allows the creation of unique, large-scale, flexible and deformable soft dynamic motion sensors.

Unlike other sensing technologies or morphologies, the frameworks introduced are scalable to large areas. Sensor morphology utilises the large deformations exhibited by soft bodies, enabling sensor morphology to be particularly powerful in soft systems. The frameworks developed have been applied to the 'Universal Gripper' to enable sensing of objects grasped [28]. This is a complex sensing problem due to the physical dynamics of the gripper. The proposed frameworks enable the inclusion of sensing without limiting the capabilities of the gripper.

In summary, the main contribution of this work to the wider research community is the development of the grid morphology, 'differential sensing' morphology and motion sensing morphology. Of particular interest is the 'differential sensing' morphology which performs localised processing of deformation. When applied to the Universal Gripper this allows sensing of the deformable surface. This is believed to be one of the first implementations of soft sensing on the surface of the Universal Gripper.

1.3.2 Embodied Perception & Behaviour in Materials

Material selection is particularly important for soft robotics, as it determines the environmental interaction. To extend the role of materials beyond that of providing mechanical or scaffolding properties, they can be functionalised to provide sensing and enable control of material properties such as stiffness or shape. This further leverages the interaction with the environment. To demonstrate how functionalised materials can aid soft robotics systems, two sensing materials have been developed.

The first material, Conductive Hot Melt Adhesive (CHMA), shows novel integration of controllable sensing (through the inclusion of conductive particles) and also controllable properties (tackiness and stiffness). This allows detection of environmental interaction, and provides the ability to change how the material interacts with the environment. This material has been used to develop a universal single point gripper that has inherent sensing abilities and picks up objects using 'tackiness'. This implementation demonstrates how materials can be used to reduce the control requirements for complex manipulation problems. The embodied intelligence reduces the requirement for centralised control intelligence, with materials providing some distributed intelligence to the system.

The second soft material developed is a conductive silicone-based material that offers flexibility in implementation allowing both pressure and strain sensing. The capabilities of this material have been demonstrated through a case study on wearable physiological devices. By varying the physical implementation of the material this allows different stimuli to be detected ranging from high force pressure detection (gait analysis) to high sensitivity strain detection (heart rate detection).

In particular, the main research contribution of this work is the functionalisation of a soft material (CHMA) to provide integrated sensing and change in material properties. The variable stiffness and 'tack' force of the material allows single-point grasping of objects. Additionally, a highly versatile strain and pressure sensing material have been developed which has been used to create a number of wearable sensing devices.

1.3.3 Soft-Rigid Hybrid Mechanical Design for Adaptive Robotic Behaviours

Typically, for classical control and robotics, behaviour is a direct function of the control input. However, for complex soft-rigid hybrid mechanical systems behavioural diversity can arise from the passive dynamics and the coupling between the mechanical behaviour and the environment, triggered by external actuation of the whole body. The distribution of intelligence departs from a typical model of robotics where control is emergent from the 'brain' to a model where localised computation is performed in the mechanics. Soft-rigid hybrid mechanical systems provide a compromise between sufficient rigidity to allow meaningful environmental interactions and sufficient compliance to enable complex passive behaviours.

To demonstrate how this approach can be used, a complex multi-material 3D printed anthropomorphic hand has been produced were passive behaviour can be used to achieve piano playing of varying styles. To achieve this a framework named Conditional Stiffness is proposed which enables this exploitation of the coupling between passive mechanics and the environment.

The main research contribution of this work is the exploitation of the passive behaviours of anisotropic stiffness soft rigid hybrid structures manufactured using multi-material 3D printing. Specifically, this enables a soft-rigid hybrid anthropomorphic skeleton hand to perform piano playing of various styles. In addition to this, joint design parameters that affect the resultant behaviours of hybrid systems has been demonstrated through the development of a bio-inspired hand which uses chopsticks to enable object grasping.

1.3.4 Soft Rigid Hybrid Body Dynamics for Perception

In addition to sensor morphology aiding perception, the mechanical properties and passive dynamics of the system can contribute. The interaction between the mechanical system and the environment allows the body dynamics to act as a transducer for environmental stimuli. The increased compliance offered by hybrid systems in comparison to rigid robotics enables greater environmental interaction and hence potential for environmental perception through body dynamics.

The mechanics of the physical body can also aid perception and exploration by exploiting the dynamics of the interaction between mechanics and the environment. In this area of research, the ability of mechanics to directly contribute to perception is considered. In particular, the interaction between hybrid mechanical systems and the environment is understood.

The postural response of soft-rigid hybrid systems changes when interacting with the environment, with the response dependant on environmental properties (stiffness, friction, object size.) Integrating soft sensors to allow posture detection allows the mechanical system to provide environmental information. This is a novel approach to prioproception, with hybrid robotic systems used to optimise the response.

This work brings together many of the previous contributions (materials, sensor morphology and soft-rigid hybrid design) with perception aided by the intelligence provided by embodiment. **The key research contribution is the integration of soft sensors to allow postural sensing of a soft-rigid hybrid system to provide environmental awareness.**

1.4 Structure of Thesis

A design approach for soft robotics that utilises embodied intelligence has been introduced, with the research hypotheses stated. In the next chapter a review of the relevant technologies and existing models and frameworks for the development of soft robotics is presented. The following chapters each focus on the main research contributions of this thesis, using an embodied approach to soft robot development (Fig. 1.1).

Chapter 3 provides three morphological frameworks for assisting perception. The frameworks are demonstrated through integration into robotic manipulation platforms. Following on from this Chapter 4 focuses on the abilities that can be provided by embodiment when using materials to perform both sensing and behavioural capabilities. Two novel materials are presented. The use of sensor materials to perform localised processing through material morphology is discussed.

The next two chapters focus on the role of mechanics in behaviour and perception. Chapter 5 presents the development of 'hybrid' robotic systems, including fabrication methods and theoretical methods for using hybrid systems to extend the range of behaviours. The role of mechanics in perception and exploration is then presented in Chapter 6, focusing on optimising the mechanical systems for proprioception.

The final chapter, Chapter 7, discusses the potential impact of the presented work and places the work in context of robotic manipulation. Future research directions to extend the existing work are also presented.

Chapter 2

Embodied Soft Robots: Prior Art[1]

This chapter presents a review of current state-of-the art research relating to existing models and approaches to soft robotics. Methods and limitations of existing soft robotics models, sensing, perception and behavioural range are discussed.

2.1 Models & Approaches of Soft Robotics

Typical rigid models of robots have centralised control with well defined sub-systems which can be considered in isolation [29]. Rigid systems are deterministic and allow behaviour to be predicted. Typically, actuation affects a single, or quantifiable number of degrees of freedom. This model no-longer holds for soft robotics. The flexibility and compliance of soft robotics, in for particular continuum body systems, makes the modelling of soft robotics challenging. Finite Element Analysis (FEA) is often used to estimate or predict movements of behaviours [30], enabling the development of control for soft robots [4].

Soft robots are typically modelled or defined by the fabrication technique opposed to the functionality of overall development approach [31, 32]. The focus of the design is often on the technologies used. In this approach, similarly to rigid robotics, sub-systems are considered in isolation to the whole system. Alternatively, bio-inspired ‘animal specific‘ models are often proposed, for example a model of a soft octopus robot [33], or a Caterpillar [34]. Both these approaches have advantages, but do not provide a generalised model for designing or understanding soft robotic behaviour.

[1]This chapter includes part of work written in collaboration with others and my supervisor. The peer-reviewed publications which contributes to this chapter is:

- Hughes, Josie, et al. "Soft manipulators and grippers: a review." *Frontiers in Robotics and AI 3 (2016): 69.*

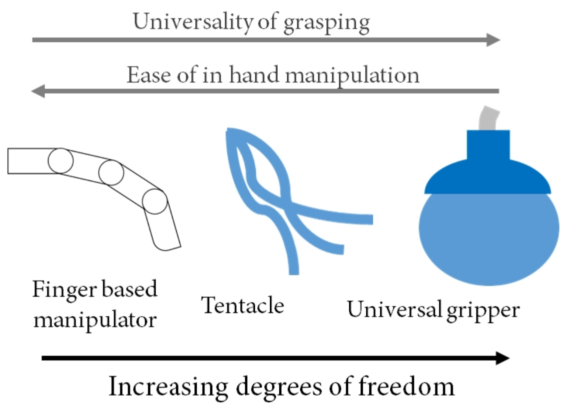

Figure 2.1 Spectrum of soft manipulators demonstrating how morphology affects the manipulator properties.

The similarities between biology and soft robotics has lead to a bio-inspired model being proposed for soft robotics. In this model, embodiment is a key ideology: all aspects of the physical system contribute to the intelligence and output behaviour [11]. Using this concept allows for the understanding of complex animal behaviours, and provides models for distributed intelligence and control across a soft system. Within this approach, concepts of morphological computation [35], synergies [36, 37], self-organisation [11] and self-stability [38] are considered. Although these concepts have been suggested as a potential direction for soft robotics, there has been limited development of more generalised frameworks. Additionally there are limited approaches for developing soft robots using these underlying philosophical ideologies.

2.2 Soft Manipulation

Soft manipulators are designed with many varying morphologies and forms. Most often, the morphology is dependant on the application for which they are required. There can be considered to be a spectrum of morphologies with varying degrees of freedom. This spectrum can be thought of as loosely affecting the qualitative measure of the degree of universality with which objects can be grasped and also the 'in hand' abilities to manipulate objects (Fig. 2.1).

A manipulator with infinite degrees is the universal gripper morphology, which uses the principle of jamming to alter the stiffness and rigidity of the gripper allowing objects to be gripped and released [28]. This morphology allows many objects of varying mass, size, material and shape to be grasped which is a key strength of this morphology. It does not, however, allow for any ‘in-hand’ manipulation of objects which could be required for some applications.

By contrast, bio-inspired muscular hydrostat type manipulators, such as octopus arms or elephant trunks, have a morphology with many degrees of freedom but not infinitely many like the jamming gripper. This still allows for grasping of many objects, with an increased ability to manipulate objects in hand. There is considerable work in the development of octopus inspired robotic manipulators [31, 32, 39] as they have the potential to achieve highly dexterous movement with applications such as robotic surgery.

There are also ‘limb’ based multi-finger soft manipulators such as the MIT hand [40], which introduce a finger based morphology, drawing inspiration from human hands. Some limbed manipulators are highly anthropomorphic [41] and seek to replicate the high dexterity of manipulation which is seen with the human hand. This allows for grasping of a wide variety of objects and highly intricate in-hand manipulation of objects.

The morphology of the manipulator hugely affects the performance of the system. The available materials and design processes allow for significant variation in the morphology of a manipulator, and should be chosen to meet the specific application for which the manipulator is required.

2.3 Sensing & Perception

Sensing for soft robotics is acknowledged as a significant challenge [42]. Sensors are required to sense both intrinsically, to detect body posture and structure, and also extrinsically, to obtain tactile information. Development in soft robotic sensors has the potential to significantly improve the control systems and assist with obtaining information from the environment. Soft sensing is focused on detecting deformations; this could be small deformation required for obtaining tactile information or significantly larger deformations such as obtaining posture information. However, this is challenging as soft systems are not limited by the traditional mechanics of rigid systems, whereby there is a limited and carefully controlled number of degrees of freedom (DOF), so a single sensor can be used to correspond to a given DOF. Soft systems have the potential to have infinite degrees of freedom, this means that there can no longer be a one-to-one pairing of sensor to DOF, and alternative methods and approaches must be developed. Existing methods of strain and deformation sensing for both posture and tactile sensing, their applications and potential limitations are now discussed.

2.3.1 Sensing Materials & Technologies

The sensing material and technologies which have provided the biggest impact and greatest potential for sensing of soft robots are introduced in this section.

Ionic Sensors Highly flexible strain sensors have been developed using ionic and liquid metals. Typically sensors can undergo strains up to 100% [26], with some able to achieve 250% strains [43] whilst displaying high accuracy and reliability [44]. The sensors are developed by producing 3D printed moulds to form flexible polymers (typically PDMS) with embedded microchannels. A conductive liquid is injected into the microchannels such that the resistance of the liquid varies with strain applied to the sensor. Different sensors exist using this technology. A flexible 'skin' sensor has been developed which allows pressure and strains to be identified independently [43] by using multiple layers of sensor, and choosing a specific morphology. Soft multi-axis force sensors have been also developed [45]. These sensors require careful design of the ionic channels, and the morphology must be designed to measure a particular deformation or degree of freedom. Using these sensors, strain and pressure can not be uniquely identified and electrode attachment to the sensor can be technically challenging.

Flexible Electronics Flexible electronics allow pressure to be detected using highly flexible polymer transistors which use a PDMS substrate [46–48]. Such flexible pressure-sensitive organic thin film transistors have a high sensitivity, low power consumption and have been demonstrated to have a high stability over time [49]. There are also carbon-nanotube film-based flexible electronic sensors [50, 51], but there has been limited integration of these sensors into robotics systems. Flexible electronic sensors have applications for use in skin sensing but the sensors can undergo only extremely limited strain, so their applications are mostly limited to pressure sensing. Current applications include mobile health monitoring and remote diagnostics in medicine.

Piezoelectric and Piezeocapacitive Strain Sensors A range of flexible piezoelectric sensors have been developed, including piezoelectric fine-wires which can demonstrate extremely high sensitivity to strains but the range of strains which they can undergo is limited [52, 53]. Other methods investigate embedding crystalline piezoelectric material into other materials such as a cellulose mesh (paper) which allows the sensor to undergo greater strains [54].

Capacitive Strain Sensors Capacitive fibre sensors are comprised of four concentric, alternating layers of conductor and dielectric [55]. These wearable sensors provide accurate and hysteresis-free strain measurements under both static and dynamic conditions. They are, however, difficult to integrate into existing systems, and allow little flexibility in varying the morphology. Carbon nanotube based capacitive strain sensors which can detect strains up to 300% with excellent durability over many cycles of strain have also been developed [56].

Conductive Thermoplastic Sensors There are a number of sensors which incorporate conductive particles such as carbon black, carbon fibre or carbon nanotubes into a matrix of thermoplastic or other elastic material. Carbon black has been integrated into thermoplastics [25] and silicone materials to enable the production of conductive sensing materials. By contrast, the integration of carbon nanotubes has limited repeatability and sensitivity [57]. Models for the conductivity of materials with the inclusion of conductive particles have been suggested [58].

Strain sensitive textiles and fibres Due to the increasing usage and interest in wearable devices, there has been a recent research focus on textile strain sensors, these sensors primarily have been developed to detect posture, position and gait. Current sensing systems include thermoplastic thread used to detect upper body posture [59], thermoplastic integrated into a nylon fabric [60], a strain sensing polymer printed onto fabric [61] and stretchable carbon nanotube strain sensors integrated into fabrics [62]. The strains measured by strain sensing technologies are significantly lower than measured ionic based strain sensors.

Alternative Sensing Methods Alternative methods for tactile sensing have also been developed. These include TACTIP [63], a tactile fingertip which has a soft compliant outer surface. A camera to detect the deformations of the inner side of the soft fingertip has a particular texture which allows deformations to be identified with accuracy and sensitivity [64]. Although powerful for tactile sensing, this technique cannot sense larger scale deformations, and requires the inclusion of a highly rigid camera close to the source of the deformation. Other alternative methods include using fibre optics and photo detectors to detect deformation due to the changing in transmission through the fibre, however, this requires the inclusion of a non-elastic fibre into the soft system [65, 66].

2.3.2 Sensor Morphology

The embodiment of sensing materials to perform some localised ‘processing’ by varying the morphology or implementation of the sensor is a bio-inspired approach [11]. Additionally, the combination of multi-modal sensing through the inclusion of sensors of multiple morphologies (for example different receptor types in the skin) has the potential to detect a range of various stimuli.

Soft ionic and microfluid sensors have been developed which use morphology to detect strains in different axes [67]. This utilises 2D layering of sensors with different morphologies. The ability to vary the morphology of sensors to respond to varying stimuli has also been proposed [68]. The importance of morphology to aid tactile sensing, in particular performing morphological computation has been demonstrated through the wrinkle in fingertips [69]. This has been applied to the generation of a number of texture detection sensors, and for the development of slip sensors [70].

One key challenge that remains is developing sensors which can differentiate between proprioception and extraception. Morphology provides one way in which this could be achieved, by developing sensors that respond to different stimuli.

2.3.3 Sensing Through Proprioception: Mechanical Optimisation

Proprioceptive sensors measure values internal to the system to provide some observation or understanding of the environment. In rigid robots this is typically in the form of encoders, gyroscopes or accelerometers [71]. Due to the compliant nature of soft robots and the accompanying interaction with the environment, there is far more physical environmental interaction which provides many opportunities for using proprioception to gain environmental information.

In soft robots, proprioception is typically in the form of curvature sensors which measure joint angles which can be used to provide shape information about the system [72]. There has been some integration into soft robotic systems, including prosthesis [73] and also haptic systems where soft proprioception is used to provide feedback when grasping [74].

Currently there is little exploration of how the mechanics of a system can aid the proprioception, and how mechanics can be used to aid exploration through proprioception. This exploits the embodiment and compliance which can be achieved with soft robotic systems and can not be seen in rigid systems.

2.4 Achieving Complex Behaviours

In this section, the technologies and approaches for using materials and mechanics and morphology to achieve a diverse range of behaviours is discussed.

2.4.1 Materials

It has been proposed that materials can make an active contribution to robotics opposed to providing specific structural or material support [75]. Materials could enable the construction of more intelligent robots and contribute to the control, intelligence and behaviours through the role of materials in sensing, actuation, computation and communication. Materials have shown the abilities to perform actuation [76], and sensing, hence increasing the range of behaviours or systems.

2.4.2 Mechanics & Morphology

Mechanical design of systems plays a considerable role in the intelligent functioning of animals and machines, which can be observed in passivity-based robot control [77]. Passivity can be used to achieve a pendulum-like swing of legs for locomotion, where no explicit active control is required to achieve stable bipedal walking [78]. High functioning passively-controlled robots have achieved a range of different behaviours such as robotic swimming, flying and manipulation [79]. Smart mechanical design enables systems to show exquisite and complex behaviours that are self-stabilizing and energetically efficient at reduced computation cost [80].

Achieving functional behaviours through passivity is crucial and necessary for biological systems to survive in the natural environment, however, as a design method for robotic systems, it is known to intrinsically restrict the range of behaviour [81]. Underactuated control provides a compromise; it can expand the range of behaviours by introducing a coupling between passive mechanics and limited joint actuation [23, 24]. This creates behaviours which are highly environmentally dependant and sensitive to changes. There is limited behavioural diversity, typically with a one-to-one mapping between environment and behaviour [38, 82]. This limitation can be particularly seen in robotic manipulation and hand design where passive control and underactuated mechanical design allows only a single [83, 84], or at best, a limited number of behaviours to be achieved [85, 86]. To leverage the intelligence of passive mechanical bodies a method for generating a range of behaviours in variable environments is required.

Achieving behavioural diversity in robotics, while utilising passive dynamics, remains a fundamental challenge. There have been several recent approaches to address this challenge. Firstly, actively controlling the mechanical dynamics of the robots by implementing variable stiffness mechanisms allows adaption of the passive behaviours to varying environments [87, 88]. While this approach allows varying behaviours to be achieved, the inclusion of actuators limits the scalability and introduces additional complexity [89, 90]. A second approach centres on the use of materials to alter or adapt the behaviour [75]. Soft deformable materials can be integrated into robots to expand the diversity of achievable behavioural patterns [91, 92]. Behaviours of robots using soft deformable materials are generated through the mechanical dynamics of interactions between the environment and materials [93]. The increased compliance of the soft materials provides more flexibility, enabling a wider variety of mechanical dynamics. However, the inherent flexibility of soft materials can result in behaviours which are ill-defined and highly variable. A key challenge therefore, is controlling the mechanical flexibility when using softer materials [16]. Soft robots can use variable-stiffness materials to achieve a range of movements and to modulate interactions with the environment [94]. The synergy between soft bodies and actuation methods can then be utilised. This allows the movement of soft bodies to be limited or constrained, in turn limiting the requirement for complex additional actuation sources. In particular, work on adaptive synergies and tendon routing shows significant breakthroughs and developments with respect to robotic manipulators [95–97]. Although these approaches provide methods for exploiting mechanical passive dynamics, they do not provide a framework for significantly scaling complexity and behavioural diversity.

Chapter 3

Sensor Morphology for Soft Robotics[1]

This chapter focuses on the role of sensor morphology in soft sensing. By varying the morphology of a sensor, the embodiment of the sensor can enable the morphology to perform some localised computation or processing, aiding sensing and perception. This extends the typical model of a sensor, where the sensing element and signal processing enable perception, to a model where the physical implementation and morphology aid perception, performing embedded sensory processing. This embodiment can improve sensitivity and allow detection of specific stimuli in a scaleable manner. It is an approach suited to soft robotics due to compliance and hence large deformations experienced in soft systems. A number of frameworks providing embodied intelligence are presented in this chapter, each designed to perceive different stimuli. The frameworks developed utilise embodiment of the sensor validating Hypothesis 2, the utilisation the embodied intelligence to perform localised computation for perception.

The novel contribution of the research presented in this chapter is the development of an embodied differential sensing framework for scaleable sensing of soft structures to enable perception of objects. Additionally, a morphology which enables the development of slip sensors that are uniquely stretchable is demonstrated. The sensing frameworks developed

[1]This chapter presents work developed collaboratively with my supervisor F. Iida. I have initiated the problem statement, framework, prepared the figures in the experiment section, and wrote the paper. F. Iida helped with formulating and revising the paper. The peer-reviewed publications which forms the basis of this chapter are:

- Hughes, Josie, and Fumiya Iida. "Localized differential sensing of soft deformable surfaces." Robotics and Automation (ICRA), 2017 IEEE International Conference on. IEEE, 2017.
- Tactile Sensing applied to the Universal Gripper using Conductive Thermoplastic Elastomer. *Soft Robotics Journal.*

have enabled one of the first implementations of deformation sensing of the surface of the 'Universal Gripper', a challenging requirement for soft sensors.

3.1 Requirement for Sensor Morphology in Soft Robotics

One of the most fundamental challenges in soft robots is the development of soft tactile sensors. This arises from the limited flexibility and deformability of traditional sensing receptors and devices. For soft body sensing many receptors can be required to accurately detect deformations, negating the favourable soft mechanical properties of the body. There have been many attempts to address the challenge of sensing large deformable structures with a focus on the development and fabrication of soft sensors. The main body of literature relates to the use of polymer-based conductive layered sheet [98–100], fabric-based approaches [101], resistive ionic or conductive fluids [26, 43] and conductive rubber or elastomers [25, 102–104]. While this work provides important initial development, there are limitations in terms of the flexibility, range of sensing and ability to integrate into soft structures.

Soft structures have the potential to deform in an infinite manner, making sensing challenging. To address this challenge, the use of sensor morphology to provide embodied intelligence is investigated. The morphology of the sensor can be used to perform local 'processing' of the environmental interaction aiding detection of deformation, and reducing the dimensionality of the sensing challenge. In this approach, sensing is no longer dependant on only the sensing receptor and the signal processing, but also the physical mechanics and integration of the sensor.

There have been attempts to automate sensor morphology design for a given application[105–107]. Recent work has used experimentally gathered data to optimise sensor placement for a given task and to identify particular patterns of manipulation [108]. However, these technological frameworks or are not suitable for soft robotics applications or do not fully exploit the large deformations of soft bodies. By using novel materials, an morphology which provides embodied intelligence can be designed to exploit the interactions with the environment. This reflects the approach to soft robot design proposed in the introduction of this thesis (Fig. 1.1).

The methods in this section use a polymer based strain sensor, Conductive Thermoplastic Elastomer (CTPE) [25, 103]. These sensors can be integrated into a deforming surface with minimal changes to the mechanical properties of the soft body allowing significant flexibility in the placement and morphology of the sensors. The framework and theories are transferable to other sensing technologies. This work focuses on the design principles for morphologies which provide embodied intelligence for perception of deformation. There are two groups of frameworks developed:

- **Deformation sensing morphologies.** Using morphology to aid the detection of deformation of large scale soft systems, two frameworks are presented: a grid based system and a new technique termed 'differential sensing' where pairs of sensors are used to perceive specific deformation characteristics. As a case study, sensors of theoretically designed morphologies are applied to the Universal Gripper [109] to allow for improved pick-and-place of objects. The Universal Gripper is a particularly challenging and interesting platform as it has a large area structure which undergoes significant deformation and maintaining the inherent softness is crucial for its functionality[110, 111].

- **Dynamic sensing morphologies.** The previous frameworks can be extended to allow detection of dynamic movement. Sensor morphologies are developed which allow for slip speed, direction and location to be identified on large scale areas.

In this chapter, the material used (CTPE) for sensor development is first introduced, with comment made to other equivalent materials and how their morphologies can be controlled or changed to develop embodied systems. After this, the sensor frameworks are introduced, with experimental results validating the proposed frameworks presented.

3.1.1 Conductive Thermoplastic Elastomer (CTPE)

CTPE is a thermoplastic elastic matrix that is homogeneously mixed with carbon black powder under high pressure and temperature [25]. This process produces an electrically conductive material whose resistance varies with the strain applied [112]. CTPE can be extruded into a wide range of shapes or morphologies, including highly elastic fibres typically of 0.3mm diameter, which can undergo strains of above 80% without reaching their tensile limit. The ease with which the morphology of CTPE sensors can be varied provides high versatility. This section further explains the mechanical properties of CTPE and discusses the advantages of this approach in comparison to similar strain sensing solutions.

3.1.2 CTPE Material Properties

The simplest implementation of CTPE as a strain sensor is to extrude the material into a thread and measure the change in resistance that corresponds to the applied longitudinal strain [112]. Assuming the length of thread to be x_0 with a base resistance of R_0, the relation

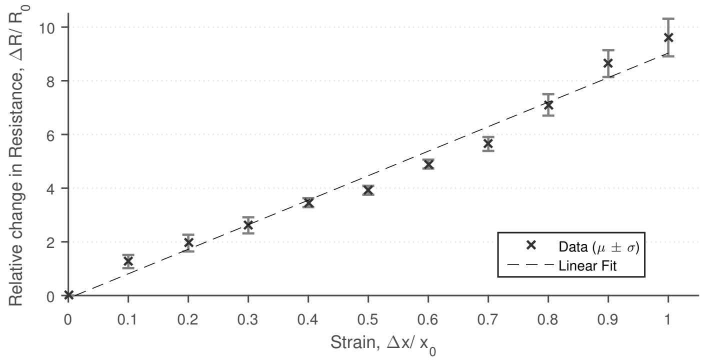

Figure 3.1 Relative change in resistance when strain is applied to CTPE for ten samples of CTPE varying in length from 20mm to 60mm. The gauge factor, $\sigma = 9.5$.

between applied longitudinal strain $\varepsilon = \Delta x / x_0$ and the resistance change ΔR can be described by:

$$\frac{\Delta R}{R_0} = \sigma \varepsilon \tag{3.1}$$

where σ represents the gauge factor, the ratio of relative change in electrical resistance to the mechanical strain.

Fig. 3.1 shows experimental results of the relationship between change in resistance with respect to applied strain. This figure reflects the linear relationship given in Eq. (3.1), with the gauge factor σ found experimentally to be 9.5. The sensitivity of the materials is analytically determined by the gauge factor; however, it can also be influenced by the shape of the same material. For CTPE threads the gauge factor increases in proportion to the diameter of fibre (i.e. the thicker, the more sensitive); but, thicker fibres are less elastic and as such pose a greater restriction to the mechanical properties of the soft structure.

3.1.3 Comparison of Resistivity-based Soft Sensors

The theory and methods introduced in this work are intended to be general, such that many other strain sensing technologies can be employed in a similar manner. Nevertheless, the mechanical characteristics vary for different sensing technologies, hence the scalability and applicability of different implementations should be considered. A summary of resistive sensors is given in Table 3.1, in which three metrics are compared: gauge factor, minimum width of thread, and maximum strain. In additional to the gauge factor, which provides an indication of sensitivity, the minimum width is an important measure which practically indicates the maximum theoretical resolution of sensing. Additionally, the maximum strain which the sensors can undergo provides an indication of the flexibility of sensors and a

Table 3.1 Comparison of gauge factor, minimum achievable diameters and the maximum strain that resistive based sensors can undergo

Sensor Type	Gauge Factor	Minimum Width	Maximum Strain
Strain Gauge [113]	1-2	∼2mm	5%
Ionic Liquid Sensors [26][43]	3-5	0.6mm	100%+
ZnO Nanowire Films [114]	200	∼2mm	50%
Graphene Foam [115]	15 - 29	3mm	75%
Silver Nanocomposite [116]	2-14	3mm	70%
CTPE [25] [112]	9-20	0.5mm	100%

measure of the ability to prevent unwanted mismatches in mechanical impedance between the sensor and soft structure.

This table demonstrates the favourable mechanical characteristics of CTPE in comparison to other solutions. The gauge factor, a measure of the base sensitivity, shows that CTPE is comparable with or better than other alternative sensors. CTPE is also capable of undergoing significant strains. The minimum fabrication width of the sensor is given, as this affects the maximum achievable number of sensor loops in a given area and hence the overall sensitivity of a sensor. For CTPE this width is significantly less than other sensors as it is possible to extrude into fibres with a low diameter. Many of the other sensors materials are formed as films or strips, limiting the possibility for varying the morphology. The ability of CTPE to be easily formed into different morphologies allows the sensitivity to be increased above the base value and tailored to respond to a specific stimuli.

3.2 Theoretical Framework of Soft Deformation Sensing

This section considers a theoretical framework to optimise strain-sensitive sensor placement on large area soft bodies, to allow identification of objects physically in contact with the soft body. The overall aim is to develop a method to place the sensor materials to gain maximum information about the object in contact with the soft body (it is assumed that the object causes an deformation in the soft body). Using this sensor responses an estimation of the environment or object corresponding to the deformation detected and the location of this deformation is generated (Fig. 3.2).

Under this framework we are using the deformation resulting from environmental interaction to provide a means of understanding perception. Thus, the true strain is never identified, however, the surface profile of the soft body is reconstructed. This approach assumes the condition that the surface profile reflects the environmentally interaction is met, and is limited in that it only provides the estimated cross sectional area.

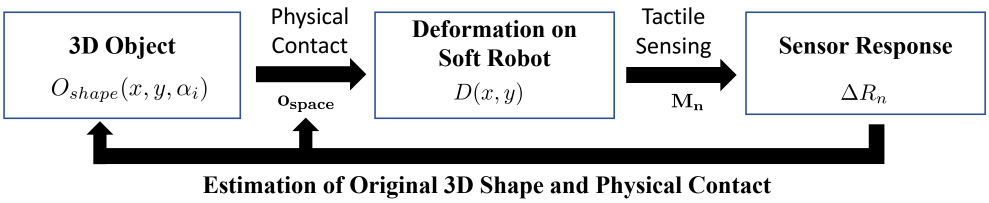

Figure 3.2 Framework of soft tactile sensing of 3D object where the sensor response to used to provide indication of the object in contact with the soft body.

3.2.1 General Framework

An object can be described by the height profile, and is considered to be in contact with the soft body such that it causes a corresponding surface profile. The height in the z direction of the shape for a given (x, y) co-ordinate is described by:

$$O_{shape} = O_{shape}(x, y, \alpha_i), \quad i = 1, 2, ..., j \tag{3.2}$$

which represents the height of object at each point on the x-y plane with α representing factors which determine the objects shape. The object has a set of parameters which describe the state in space, the state is represented by the vector $\mathbf{o_{space}} = [\theta_x, \theta_y, \theta_z, x_c, y_c, z_c]^T$, with the origin of coordinate system being located on the x-y plane of the soft surface.

Given the object shape and state (O_{shape} and $\mathbf{o_{space}}$), the profile of the soft surface can be determined. For the sake of simplicity, it is assumed that deformation of soft sensing surface is perfectly identical to the negative of the object shape. Under this assumption, the profile of the deformed surface D can be given as:

$$D(x, y) = \mathbf{R_x}(\theta_\mathbf{x})\mathbf{R_y}(\theta_\mathbf{y})\mathbf{R_z}(\theta_\mathbf{z}) \begin{bmatrix} x + x_c \\ y + y_c \\ z_c + O_{shape}(x + x_c, y + y_c) \end{bmatrix} \tag{3.3}$$

To identify this deformation induced surface profile, it is first necessary to determine the morphology of the sensor. Starting with the simplest case, where the sensor material is placed in one dimensional lines, the morphology of nth sensor can therefore be described by:

$$\mathbf{M_n} = [m_x^n(l), m_y^n(l)]^T \quad a_n \leq l \leq b_n \tag{3.4}$$

where $(m_x^n(l), m_y^n(l))$ determines the routing and length of nth sensor on the soft surface, and a_n and b_n describe the start and end point of each sensor string.

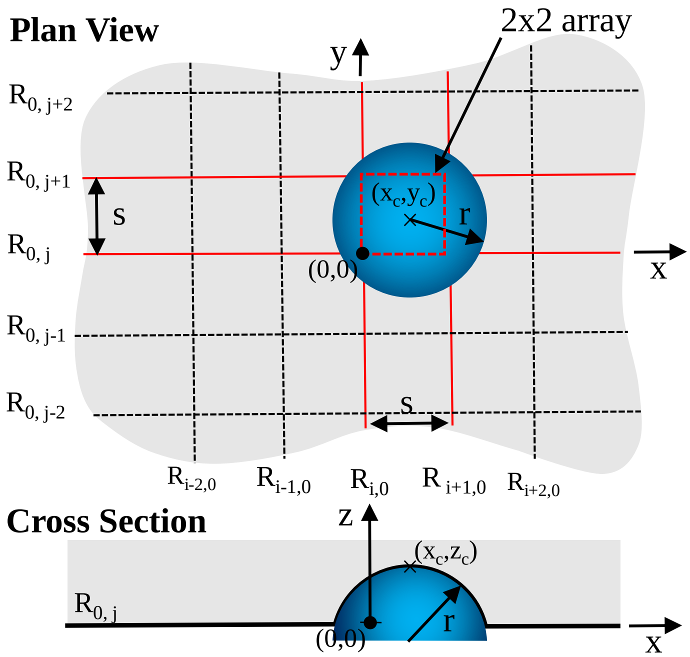

Figure 3.3 Schematic illustration of soft tactile sensing framework. A hemisphere object with the radius r is assumed to be located at (x_c, y_c, z_c) and to deform a soft structure with CTPE sensing grid implemented (represented by $R_{i,j}$).

The response from each sensor is proportional to the strain experienced as a result of the deformation of the soft body. Thus, the sensor response is proportional to the difference in length of the sensor when deformed and before deformation:

$$\Delta R_n = R_0 \sigma \left(\int_{a_n}^{b_n} D(m_x^n, m_y^n) ds \right) \tag{3.5}$$

$$ds = \sqrt{\left(\frac{dx}{dl}\right)^2 + \left(\frac{dy}{dl}\right)^2} dl \tag{3.6}$$

Given this framework, the task of identifying an object through sensing of the new profile can be described as the derivation of $D(x,y)$ from ΔR from which it is possible to obtain O_{shape} and $\mathbf{o_{space}}$. The remainder of the section considers the optimisation of determining $\mathbf{M_n}$ while minimising the number of sensor n and the error in the sensing measurements.

Object sensing with a single sensor

This subsection shows the simplest case study of the framework introduced above, the identification of an object by using a single sensor under the condition of some prior knowledge.

The target object is assumed to be a hemisphere with only one parameter, radius r:

$$O_{shape}(x,y,r) = (r^2 - x^2 - y^2)^{1/2} \tag{3.7}$$

Considering the object location $\mathbf{o_{space}} = [x_c, y_c, z_c]^T$, the profile can be expressed as:

$$D(x,y) = z_c + (r^2 - (x-x_c)^2 - (y-y_c)^2)^{1/2} \tag{3.8}$$

The simplest case is when a single line sensor is placed along the y-axis as:

$$\mathbf{M} = [0,l]^T \qquad -k < l < k \tag{3.9}$$

with k being an arbitrary length larger than r. In this arrangement, the deformation of sensor can be described as $\Delta L = r_x'(\pi - 2)$ where $r_x' = (r^2 - x_c^2)^{\frac{1}{2}}$ when $z_c = 0$. Therefore the signal of this sensor should be described by:

$$\Delta R = R_0 \sigma \Delta L = R_0 \sigma (\pi - 2)(r^2 - x_c^2)^{\frac{1}{2}} \tag{3.10}$$

From this expression, an object can be identified from the sensor signal:

$$r \Big|_{x_c=0, y_c=0, z_c=0} = \frac{\Delta R}{R_0 \sigma (\pi - 2)} \tag{3.11}$$

$$x_c \Big|_{y_c=0, z_c=0, r=r_{known}} = \sqrt{r_{known}^2 - \frac{\Delta R^2}{(R_0 \sigma (\pi - 2))^2}} \tag{3.12}$$

Grid Sensor Morphology

By introducing a second sensor to form a 1×1 grid, it is possible to identify two parameters of the target object. Here it is assumed that the two sensors have the morphology $M_1 = [l,0]^T$ and $M_2 = [0,l]^T$ (where $-k < l < k$), and the cross section $D(x,y)$ of soft surface is the same as Eq. (3.8). By following the same process as earlier, the location of the object can be determined:

$$\Delta R_1 = R_1 \sigma (\pi - 2)(r^2 - x_c^2)^{\frac{1}{2}} \tag{3.13}$$

$$\Delta R_2 = R_2 \sigma (\pi - 2)(r^2 - y_c^2)^{\frac{1}{2}} \tag{3.14}$$

From these equations, it is possible to identify the location and size of object:

$$x_c \Big|_{z_c=0, r=r_{known}} = \sqrt{r_{known}^2 - \left(\frac{\Delta R_1}{R_1 \sigma(\pi - 2)}\right)^2} \tag{3.15}$$

$$y_c \Big|_{z_c=0, r=r_{known}} = \sqrt{r_{known}^2 - \left(\frac{\Delta R_2}{R_2 \sigma(\pi - 2)}\right)^2} \tag{3.16}$$

With a two-by-two grid of sensors, more information about the object can be obtained. When a separation of s between the sensors is applied, the following sensor responses are obtained:

$$\Delta R_1 = R_1 \sigma(\pi - 2(\alpha + cos\alpha))(r^2 - x_c^2)^{\frac{1}{2}} \tag{3.17}$$

$$\Delta R_2 = R_2 \sigma(\pi - 2(\alpha + cos\alpha))(r^2 - y_c^2)^{\frac{1}{2}} \tag{3.18}$$

$$\Delta R_3 = R_3 \sigma(\pi - 2(\alpha + cos\alpha))(r^2 - (x_c + s)^2)^{\frac{1}{2}} \tag{3.19}$$

$$\Delta R_4 = R_4 \sigma(\pi - 2(\alpha + cos\alpha))(r^2 - (y_c + s)^2)^{\frac{1}{2}} \tag{3.20}$$

where $\alpha = sin^{-1}(z_c/r)$. From these equations, it is possible to derive $o_{space} = [x_c, y_c, z_c]^T$ in addition to $o_{shape} = [r]$ either numerically or analytically, where the physical separation of sensors is given as s.

A larger sensor grid would be necessary when detecting a smaller object on a larger surface as the sensor spacing, s, must be lower for detecting smaller objects. However, such a configuration only enables object detection within a given range of the two-by-two grid. To expand the area of sensing, sensors can be assembled into a $n \times m$ array. When the object deforms the grid, the four sensors which form a 2×2 sensing grid around the central location of the object (x_c, y_c) are used to identify the four parameters as above using the same method as the 2×2 grid. These two sensor responses should be the largest magnitude sensor response in each direction, such that the deformation can be determined with highest precision.

In this arrangement a trade-off exists between the number of sensors, the minimum detectable size of hemisphere and the sensing area covered. Assuming that sensors are equally spaced, and for a separation distance s, the minimum radius of object to be detected can be given as:

$$s_{max} \leq \sqrt{r_{min}^2 + (r_{min} - z_{c,min})^2} \tag{3.21}$$

From this calculation it is possible to determine the number of sensors required, given the expected location of object in the x-y plane $[x_{c,min}, y_{c,min}]$ and $[x_{c,max}, y_{c,max}]$.

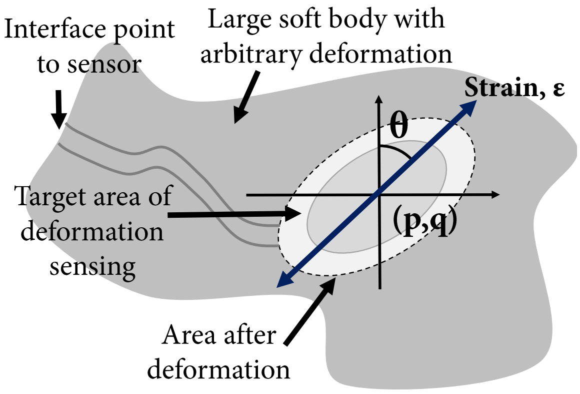

Figure 3.4 Model of localized soft body deformation on a large soft deformable body.

3.2.2 Differential Sensing

Although the sensor grid approach above is a general solution to detect an object on deformable surface, it is not efficient for many applications due to the large number of sensors necessary to cover a large deforming surface. For applications where only limited information about the object is required, there are simpler and more efficient sensor morphologies. A novel embodied, efficient sensing model termed *differential sensing* is proposed.

Fig. 3.4 shows a model for localized soft body deformation on a large surfaces. In this model, a deformation induces a strain, ε, at a location of (p,q) which is at an angle of θ to the global coordinate system. As such, a framework for modelling and understanding the key, and relevant characteristics of deformation can be developed which is described by three characteristic: magnitude (ε), orientation (θ) and location (p,q). Three differential sensor models to identify these characteristics are developed.

Differential sensing is a method which uses pairs of sensors, and considers the difference between the sensors to gain sensory information about the localised deformation. The following three sections explain specific case studies when only partial information about the object is required with substantially simpler sensor arrangement.

1D Differential Sensing One-dimensional strain information at a particular location on soft surface can be obtained by using a pair of sensors in a differential configuration as shown in Fig. 3.5(a). The deformation in the localized area can be isolated by considering the difference between the sensor responses. Sensor 1 covers only the path over the body to the localized area. In the area of localized deformation, Sensor 2 has a morphology designed to achieve maximum sensitivity.

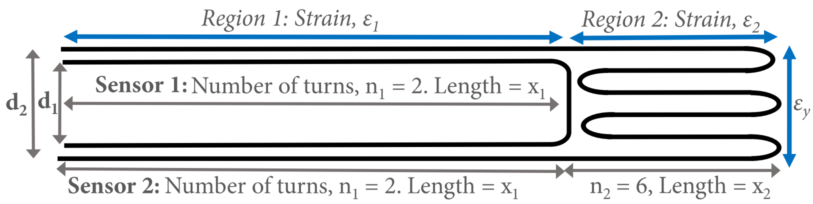

(a) 1D Differential Sensing

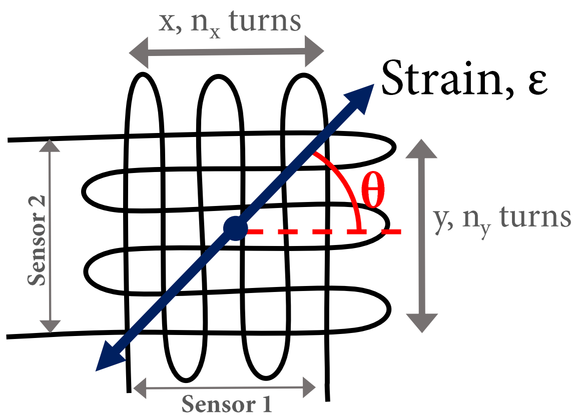

(b) Rotational Differential Sensing

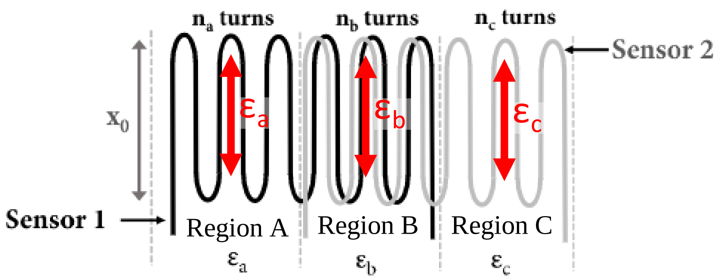

(c) Locational Differential Sensing

Figure 3.5 Morphological variations of differential sensing for different sensing objectives. (a) A pair of CTPE sensors are installed in a 1D configuration with the differential area at the tip to allow identification of the magnitude of the strain. (b) Differential configuration for rotational sensing of object. (c) Differential configuration for locational sensing.

The change in resistance for the two sensors undergoing strains in the two regions can be given as:

$$\Delta R_1 = R_1 \sigma (n_1 x_1 \varepsilon_{x1} + d_1 \varepsilon_y) \tag{3.22}$$

$$\Delta R_2 = R_2 \sigma (n_1 x_1 \varepsilon_{x1} + n_2 x_2 \varepsilon_{x2} + d_2 \varepsilon_y) \tag{3.23}$$

Assuming $d_1 = d_2$ and $R_1 = R_2 = R_0$, the strain ε_{x2} can be determined from the differential response:

$$\varepsilon_{x2} = \frac{\Delta R_2 - \Delta R_1}{R_0 \sigma n_2 x_2} \tag{3.24}$$

To maximise the sensitivity of the differential sensor to ε_{x2} the differential response should be maximised in two ways: by maximising the initial length of the sensor, which increases the change in length experienced for a given strain, or by increasing the number of sensor loops, n, for the sensor, such that the deformation in Region 2 is increased by a factor of n.

Differential Sensing for Orientation By considering the differential response from two orthogonally placed sensors (Fig. 3.5(b)), it is possible to obtain information as to the direction of strain applied. The change in resistance of the two sensors can be given as:

$$\Delta R_x = R_x \sigma n_x x \varepsilon |\cos\theta| \tag{3.25}$$

$$\Delta R_y = R_y \sigma n_y y \varepsilon |\sin\theta| \tag{3.26}$$

Therefore, assuming $R_x = R_y = R_0$, $n_y = n_x$ and $y = x$, the orientation can be estimated from differential sensor response as:

$$|\sin\theta| - |\cos\theta| = \frac{\Delta R_y - \Delta R_x}{R_0 \sigma n_x x} \tag{3.27}$$

Similar to the 1D differential sensing, the sensitivity can be amplified by the length and the number of turns of the two sensors.

Differential Sensing for Segmented Areas Using two sensors, with the same morphology, but one translated horizontally (Fig. 3.5(c)) allows identification of segmented areas of deformation. The response from the two sensors is:

$$\Delta R_1 = R_1 \sigma (n_a x_0 \varepsilon_a + n_b x_0 \varepsilon_b) \tag{3.28}$$

$$\Delta R_2 = R_2 \sigma (n_b x_0 \varepsilon_b + n_c x_0 \varepsilon_c) \tag{3.29}$$

Assuming the same number of sensor loops are used in each region, the discrete region in which the strain is applied and hence the location can be determined by considering the differential response:

$$\Delta R_2 - \Delta R_1 = \begin{cases} < 0 \text{ if } no\ strain\ in\ Region\ C \\ = 0 \text{ if } no\ strain\ in\ Region\ A\ and\ C \\ > 0 \text{ if } no\ strain\ in\ Region\ A \end{cases} \tag{3.30}$$

Additionally, the magnitude of the strain can be determined by the response from the relevant sensor.

$$\varepsilon_a = \frac{\Delta R_1}{R_1 \sigma n x_0} \text{ if } \varepsilon_b = \varepsilon_c = 0 \tag{3.31}$$

$$\varepsilon_b = \frac{\Delta R_1}{R_1 \sigma n x_0} \text{ if } \varepsilon_a = \varepsilon_c = 0 \tag{3.32}$$

$$\varepsilon_c = \frac{\Delta R_2}{R_2 \sigma n x_0} \text{ if } \varepsilon_a = \varepsilon_b = 0 \tag{3.33}$$

This principle can be expanded such that for ‘n’ translational differential sensors ‘n+1’ areas of deformation can be indicated. The greater the number of sensors the smaller the spacing between them and hence the greater the resolution of the location estimated.

3.2.3 Experimental Setup

The Universal Gripper uses the principle of particle jamming to grip objects of varying and potentially unknown shape and size. The gripper has an elastic membrane filled with a granular material, typically ground coffee, which allows it to conform to the shape of the target object. When a vacuum is applied, the granular material jams, gripping on to the object. Due to the adaptability and versatility of the gripper, it has become the subject of significant interest from research and industry [117]. As the gripper has a soft body it is difficult to incorporate soft sensing methods, other than using sensors external to the soft body to detect forces experienced.

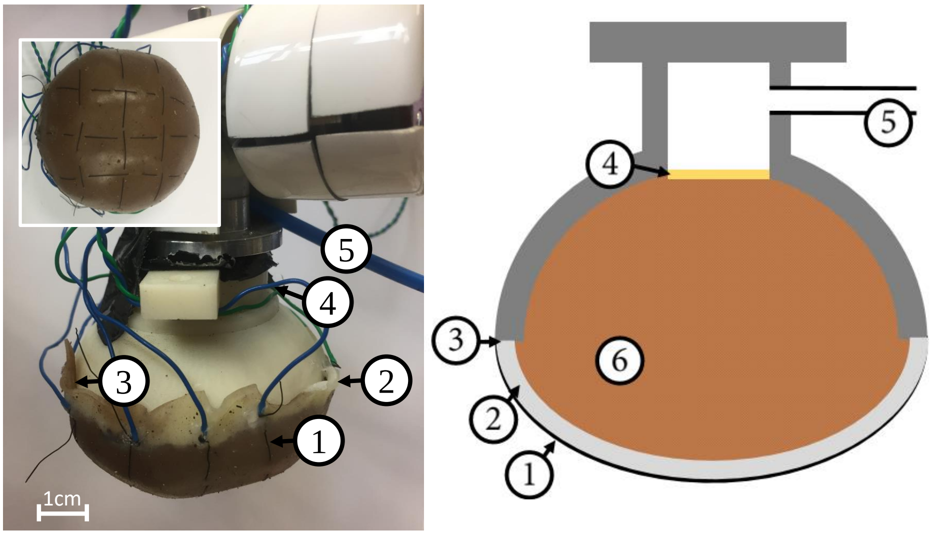

Figure 3.6 Design of Universal Gripper which allows the inclusion of CTPE sensors. 1. CTPE Sensors, 2. Outer layer of silicone, 3. Vacuum seal formed between silicone and plastic, 4. Fabric Filter, 5. Air Supply and 6. Ground Coffee.

A new design for the gripper has been developed (Fig. 3.6) using a silicone gripping surface sealed to the body of the gripper with CTPE sensors embedded within the gripper surface. The experimental setup developed use the gripper attached to a 5-DOF Robotic Arm called FireFly, as shown in Fig. 3.7(a). The gripper has been attached to a FireFly robot arm to allow position and depth control of the gripper, and the operation process is shown in the block diagram in Fig. 3.7(b). A host computer communicates with both the robotic arm and the microcontroller. The microcontroller then triggers a vacuum pump to engage the Universal Gripper, while it outputs readings from the Analog-Digital converters that are connected to electrodes attached to the CTPE sensors. The system developed allows the sensor response to be used in a feedback system to control the Universal Gripper and the vacuum pump such that the system can be automated.

3.2.4 Experimental Results

A series of experiments were undertaken with the physical robotic platform to validate the theoretical framework proposed. For the first set of experiments, four types of Universal Grippers were constructed and tested to investigate the sensing performance of the sensor grid. The specification of grippers are shown in Table 3.2. For the differential sensing experiments, an additional three set of grippers with CTPE sensors integrated were developed.

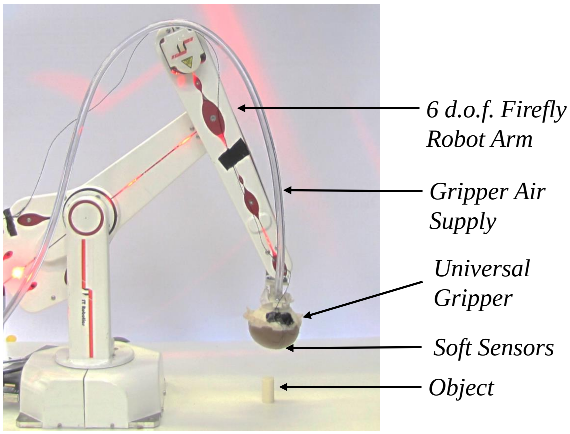

(a)

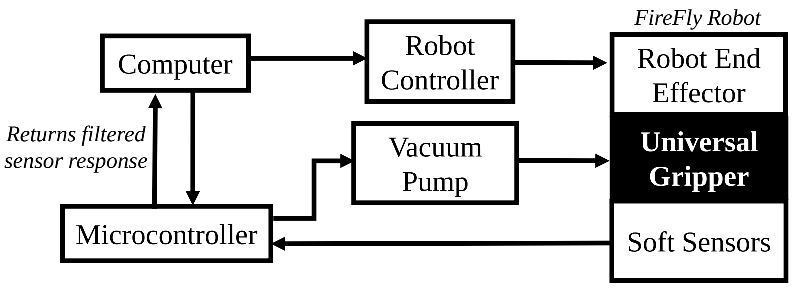

(b)

Figure 3.7 Experimental set-up of Universal Gripper attached to the Firefly robot arm. (b) Block diagram of the components in experimental system.

Table 3.2 Specifications of Universal Grippers used in the grid sensing experiments

Physical Property	Gripper 1	Gripper 2	Gripper 3	Gripper 4
Number of x sensors, N_x	1	1	3	6
Number of y sensors, N_y	0	1	3	6
Morphology	Single Sensor	Cross	Grid	Grid
Sensor Separation, s	n/a	n/a	15mm	5mm
Radius of Gripper, R	12mm	12mm	12mm	12mm

CTPE Sensor Response for 3D Objects

The initial test was performed to verify the basic sensing capabilities of CTPE applied to the Universal Gripper when interacting with various 3D-printed objects. These experiments were performed using Gripper 4 (Table 3.2) which has a grid of 6×6 sensors. Four types of 3D printed objects (Fig. 3.8(a)) were gripped. In each of these experiments, the robot arm was programmed to lower the end-effector until the object fully deformed the surface of the griper, and then the sensory data was registered. The sensory data was then used to reproduce the contour map to reconstruct the 3D shape.

In Fig. 3.8(b), it is possible to observe the different patterns of deformation corresponding to the objects in contact. For example, the contour maps of the pyramid and cube are distinguishable fairly well, whereas it is not as obvious to distinguish the pyramidal object from the hemisphere and cylinder from only the figures without some additional prior knowledge of the objects. A higher resolution of sensor grid would certainly improve object identification, implementation of more sensors could also degrade the mechanical properties of the deformable surfaces. Therefore, this work focuses on the detection of larger objects (greater than 5mm diameter) with lower resolution sensor morphologies opposed to smaller, high resolution object detection.

Single Sensor Experiments

In the next series of experiments, Gripper 1 (Table 3.2), which uses only a single sensor for detecting an object, was used. As discussed in the previous section, for this experiment it is assumed that there some prior knowledge is available, i.e. that the object is a hemisphere, and all but one of the object parameters (x_c, y_c, z_c and r) are known. The aim of object detection is to estimate one of these four parameters by using Eq. (3.12) and (3.13). Experiments were conducted with objects of different x_c, z_c, and r and repeating the experiment with each object five times. A comparison to the ground truth is plotted in Fig. 3.9. The results show that the measurement of horizontal displacement (x-direction) is most accurate with an error of less than 10% of the object size. The depth measurement (z-direction) also follows the ground truth precisely, though this is somewhat less accurate especially for smaller objects. Detection of hemisphere radius also worked reasonably well, although some deviation from the ground truth can be seen. From observation of experiments, it is proposed that these deviations from the ground truth are due to the soft surface not completely conforming to the object as a result of the material properties of the gripper.

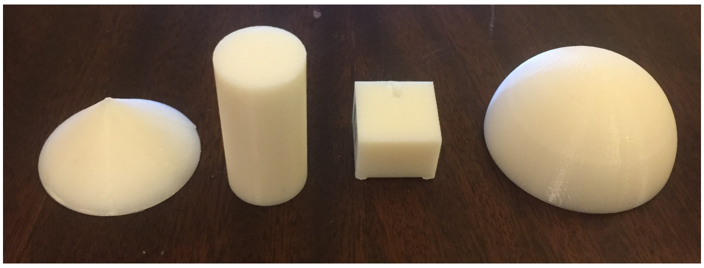

(a) Tested 3D Shapes

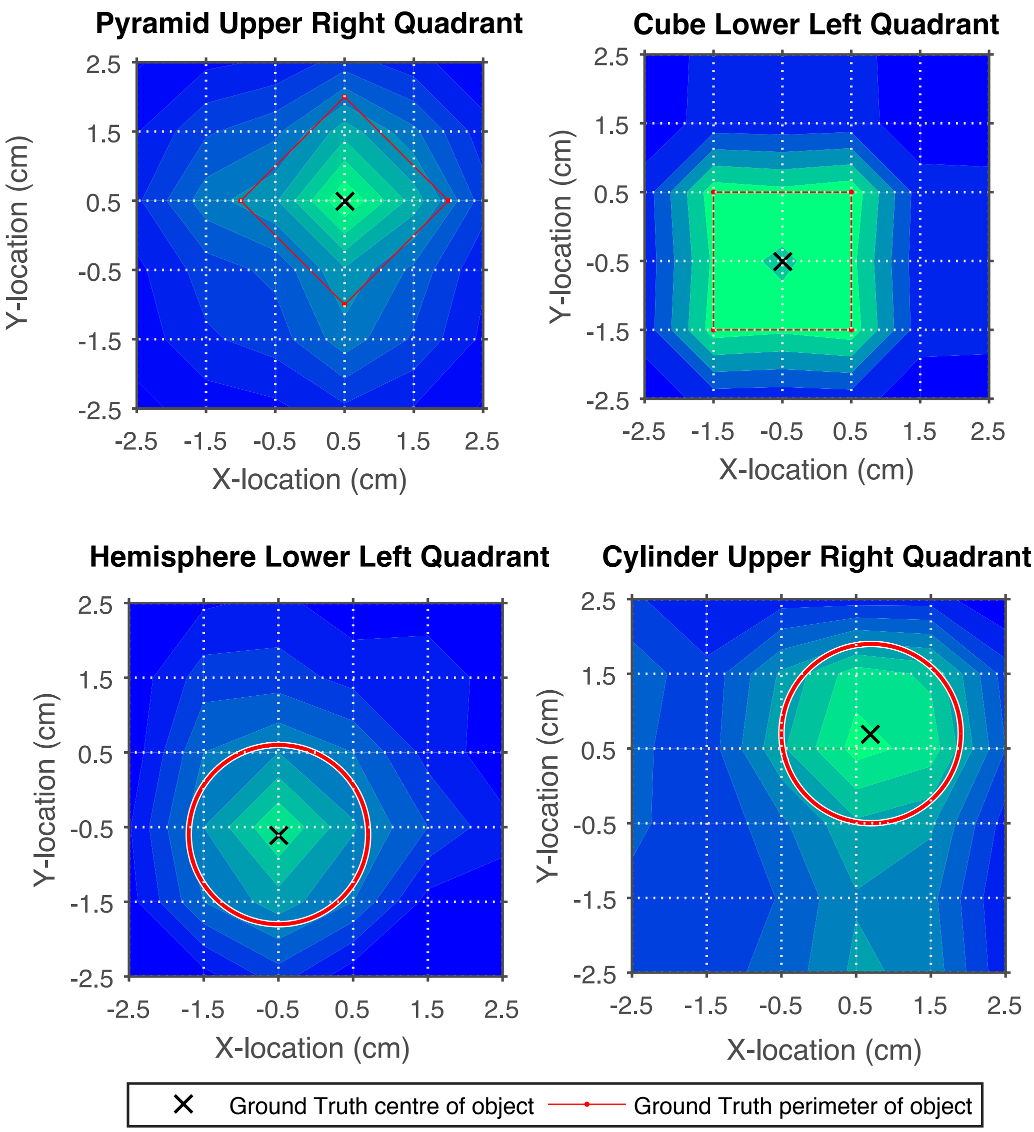

(b) Reproduced Deformations

Figure 3.8 (a) Photographs of the objects tested in the initial grasping experiments: pyramid, cylinder, cuboid, and hemisphere. (b) Visualisation of CTPE sensor response by using contour plots, along with the ground truth of objects indicated by red lines.

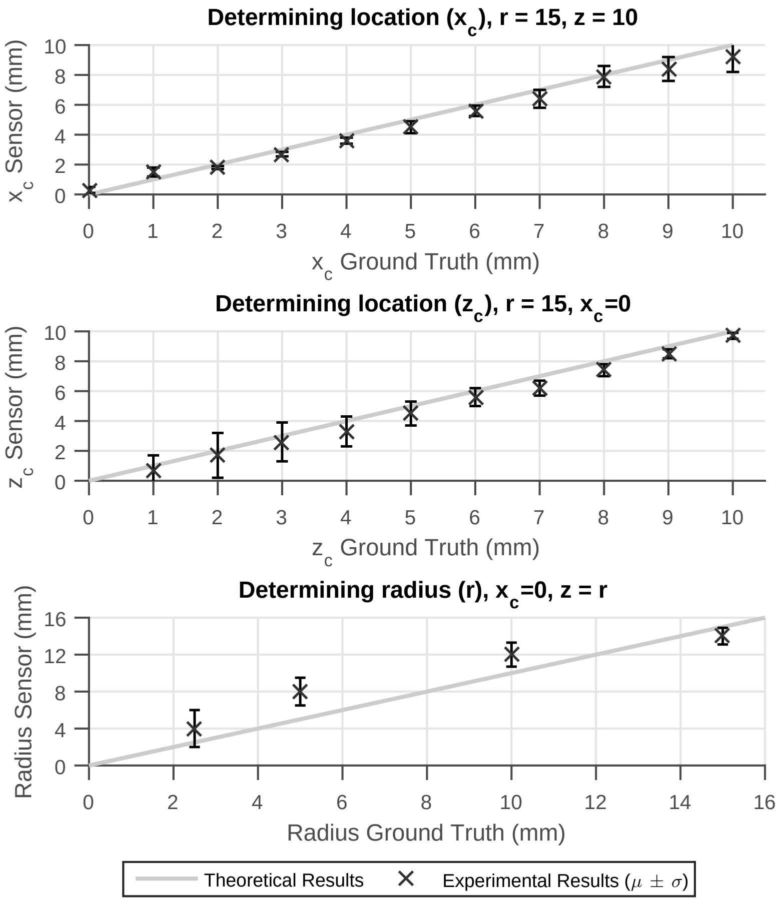

Figure 3.9 Single sensor experiments interacting with a hemisphere. (a,b) show the result of measuring location and depth of hemisphere. (c) detection experiment of different sizes of hemisphere.

Object Identification with Sensing Grid

As discussed in the theoretical framework, increasingly detailed information about the 3D object can be identified by using more sensors. To verify the theoretical framework presented in this section, the next series of experiments were conducted using a 2×2 sensor grid on the gripper which allow four parameters to be identified (x_c, y_c, z_c and r) using equations (1.19) - (1.22). This equations presented are only valid for identification of hemisphere, but the size and location can be arbitrary as long as the object gives rise to deformation on four sensors.

A series of experiments were conducted using the same robotic arm platform equipped with Gripper 3. In each experiment, one object was placed within reach of the gripper and the robotic arm was then controlled until the gripper has conformed to the shape of the object and the sensor signals have been recorded. Four sizes of hemisphere with diameters of5mm, 10mm, 15mm, and 20mm were used in this experiment. Each experiment was repeated five times and was conducted five times and for five different x-y locations and five different depth.

Fig. 3.10 shows the true position of the grasped cylinder and that determined experimentally for varying locations and varying radii of cylinder. This demonstrates that on the surface of the gripper it is possible to identify location and size of the object gripped with reasonable accuracy. With respect to the error induced in the location and size estimation, this can be partly attributed to the curvature of the gripper; there will be some variations in the accuracy towards the outer edge of the gripper. This error results from the assumption that the gripper surface is flat, which is not precisely the case for the universal gripper.

In the next set of experiments, the gripper with the 6×6 sensor grid was tested; the reduced sensor spacing should allow for object detection with a greater precision. The experiments were conducted by using Gripper 4, where three sizes of hemisphere objects were tested by placing them at different locations with respect to the gripper.

Fig. 3.11 shows the sensor response and ground truth for the detected object location in the x-y plane. In these experiments, the procedure explained in Section 3.2.2 was followed, namely to find the two largest sensor responses in each x and y direction, then, by using these two pairs of sensory information estimate the location and radius of the object. Although only three cases are tested with three types of hemisphere objects, these figures show that selection of two highest responses can be relatively easily achieved. The estimated object size and location was derived by using Eq. (3.18)-(3.21), and the results are also satisfactory in comparison to the ground truth.

Differential Sensing

The concept of differential sensing was also experimentally tested by using the robotic arm platform with another set of Universal Grippers.

1D Magntiude Differential Sensing The first differential sensing experiment was conducted for a 1D configuration as shown in Fig. 3.12a. A pair of CTPE sensors were implemented on the Universal Gripper, with one designed to have seven turns over the area to maximise the sensory information about the surface deformation on surface. As a benchmarking task the identification of disks with different diameters is used. Specifically, seven 3D printed disks with varying diameter, within the range of the differential sensor were tested.

Using the principle of differential sensing, the localised deformation on the underside of the gripper can be determined using two sensors. The sensor morphology applied to the gripper to detect the extent of the deformation when gripping a planar 2D disk is shown in

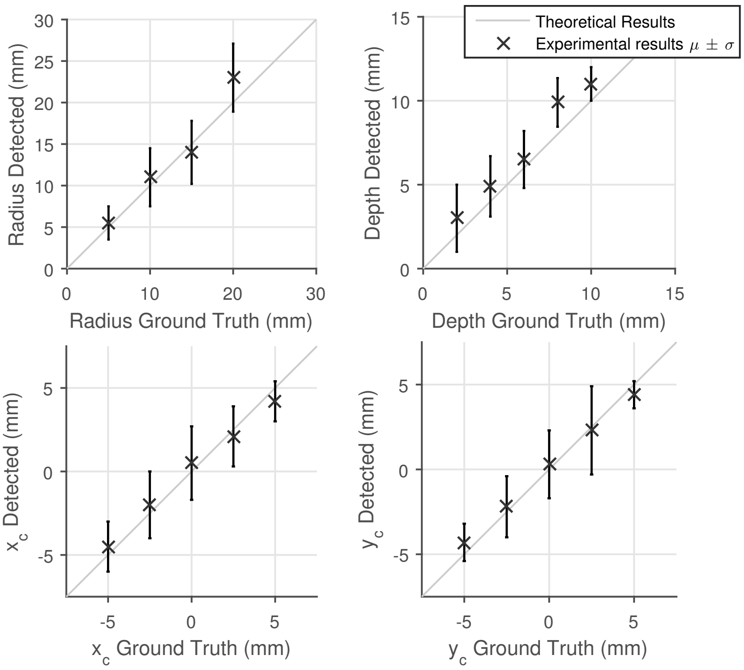

Figure 3.10 Object detection with 2×2 sensor grid. Error in the estimation of location and size of object along the y axis of the gripper with error pars showing standard deviation.

Fig. 3.12a. Theoretically, for disks of thickness h and diameter d, each sensor loop should be deformed by approximately $2h$. As such, for a sensor morphology with a separation of a between loops, strain induced by this disk on the surface should be: $\varepsilon = \frac{\Delta x}{x_0} = \frac{2z_c d}{a x_0}$, where x_0 is the natural length of Sensor 2 without deformation. From Eq. (3.24), given the sensory information ΔR_2 and ΔR_1, the diameter of the disk d can be derived by:

$$z_c = \frac{a x_0 (\Delta R_2 - \Delta R_1)}{2 d R_0 \sigma n_2 x_2} \tag{3.34}$$

Fig. 3.12(b) shows the results when disks are gripped. The grasping experiment was repeated for each disk size five times for the sensor morphology configuration. The differential sensor implemented has successfully isolated the localized strain induced by gripping the object, indicating the height of cylinder assuming the diameter is given. As expected from Eq. (3.25) the response increases linearly with strain which increases linearly with the size of disk gripped. It is also important to note that by having more loops in the differential sensing configuration in Morphology 2, it is possible to increase the precision of sensing, i.e. both deviations from the ground truth and variance of individual measurements.

Differential Sensing for Detecting Orientation and Sectional Areas In order to test the concept of differential sensing for rotational and sectional identification, two further grippers

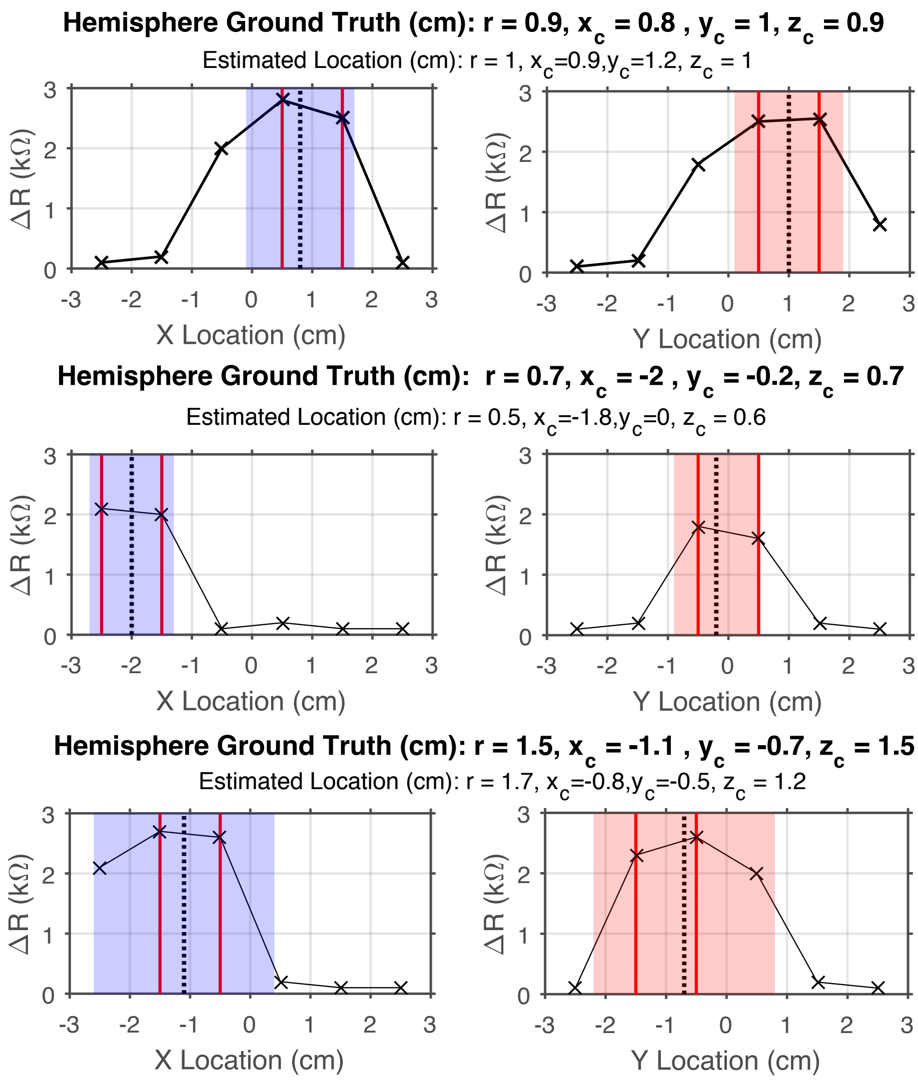

Figure 3.11 Detection experiment of hemisphere with 6×6 sensor grid. Four sizes of hemisphere were used in the experiments for detection of radius, depth and x-y location.

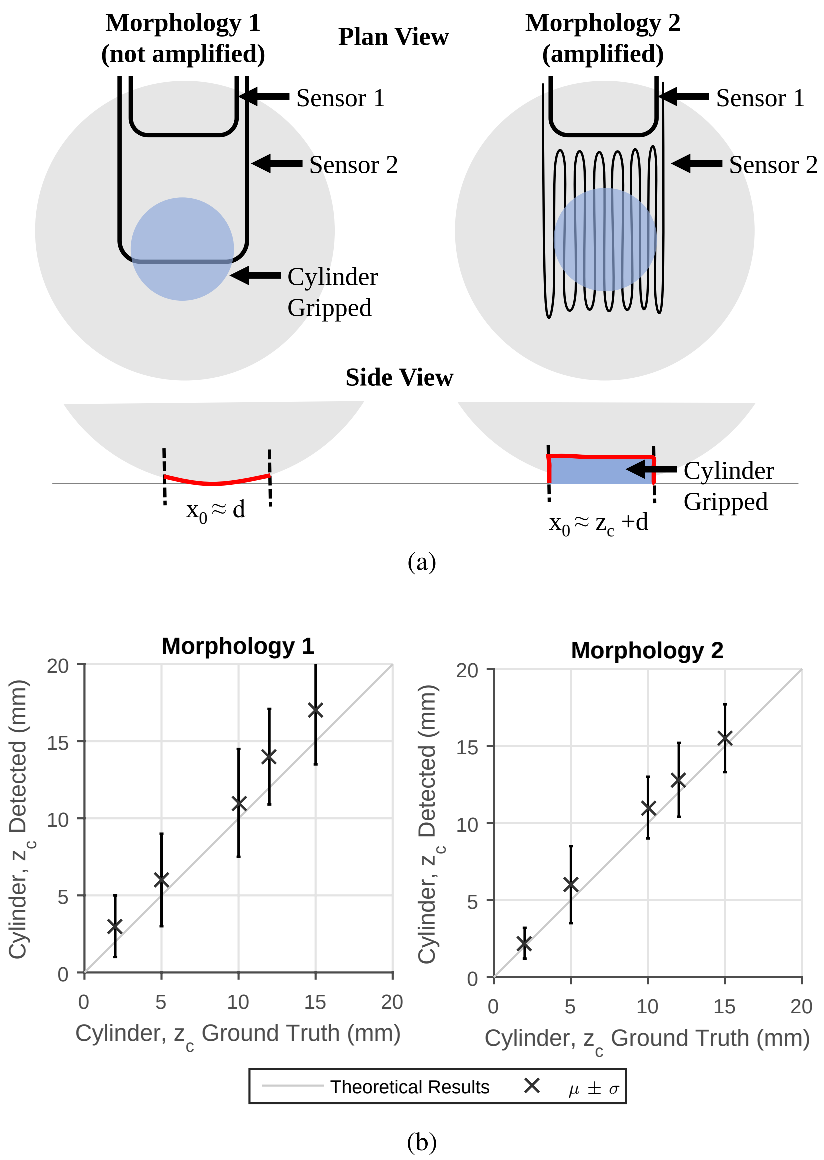

Figure 3.12 **a)** Sensor morphology used to measure the size of disk gripped and the cross sectional change in length of surface when gripping disks. **b)** Differential response when disks of increasing diameter are gripped, repeated 5 times.

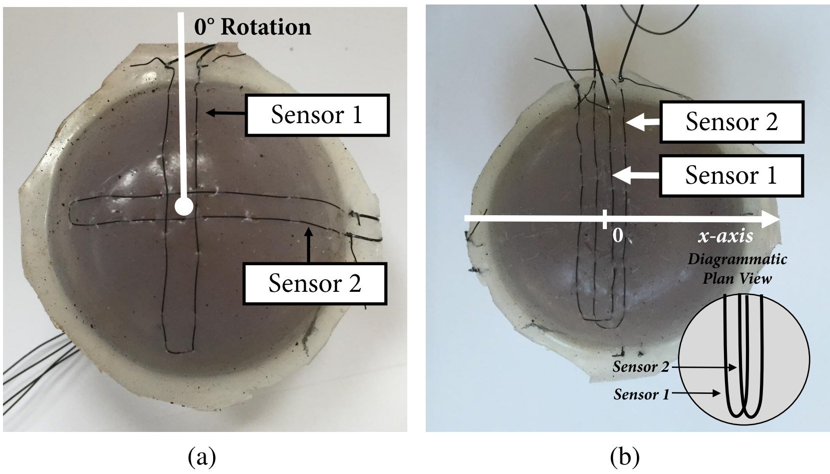

Figure 3.13 **a)** Morphology used to detect the orientation of strain caused by deformations. **b)** Sensor morphology applied to the Universal Gripper to determine x-direction location of deformation.

were developed with different sensor morphology Fig. 3.13. For detecting orientation, two orthogonal sensors are used with one loop each (with the sensor spacing of approximately 1cm), and for detecting sectional areas, a pair were implemented in parallel with translational offset of 0.8cm.

Detection of object orientation was tested by using a 3D printed cylindrical object with 1cm diameter and 7cm length. The object was placed at the middle of Universal Gripper surface, and gripped until the surface fully conforming the object. This was repeated with a rotation of the object each time followed by taking the differential sensor readings.

Fig. 3.14 shows the experimental results, indicating the sensor responses as well as the difference in response. As the object is rotated, the response from the two objects is out of phase. The sensor morphology is shown in Fig. 3.13a. The differential response follows that expected theoretically as determined in Eq.(3.28), demonstrating how object orientation can be estimated using differential sensing.

Finally, the detection of segmented areas on the gripper was tested. Here a 3D-printed hemispherical object of diameter 30mm were used, with the object pushed against the Universal Gripper surface in the middle. The experiment was also repeated by shifting the object by 3mm along the x-axis to both positive and negative directions.

Experimental results are given in Fig. 3.15 shows both the sensor responses in addition to the difference between them. As predicted theoretically in Eq. (3.32) the sign of the differential response can be used to determine the region in which deformation occurred. In addition, as the material is soft, there is some response from the sensor when the object

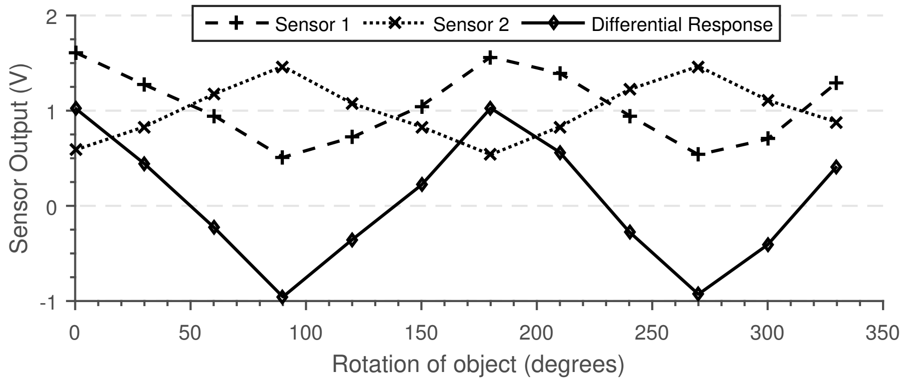

Figure 3.14 Sensor responses and differential response when a cylinder of diameter 5mm is gripped horizontally with different orientation. Sensor 1 and 2 give responses with a phase shift of 90 degrees, that can be used for differential sensing to detect rotational location of the object.

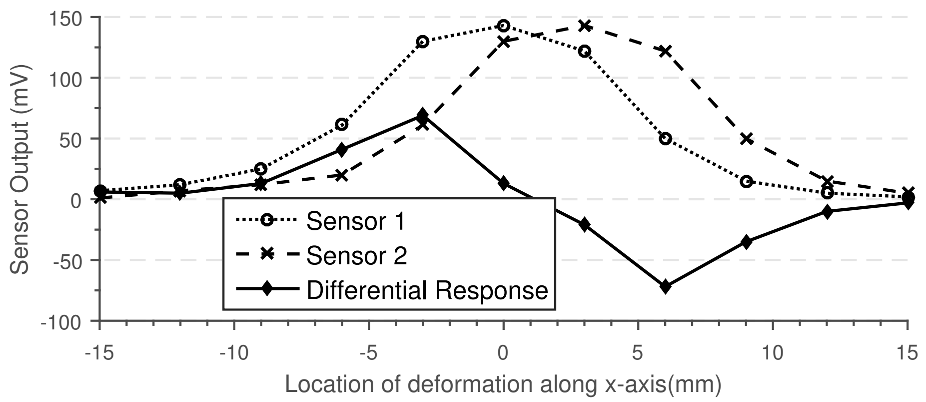

Figure 3.15 Responses of Sensor 1 and Sensor 2 with differential responses when a hemisphere of radius 5mm is gripped at different locations along the x-axis.

is gripped outside the sensing region. Therefore, the magnitude of the response can be used to determine the location over a wider area than predicted, however, there is greatest sensitivity in the region between the sensors, between -5mm to 5mm. Although this is an initial indication of how differential sensing can be used to determine location, using more sensors would allow the location to be determined with more precision.

Gripping Force Estimation

This subsection considers how to estimate the gripping force of object from the information of a single sensor applied to the gripper. In general, gripping force of object in Universal

Gripper can be estimated by the sum of static friction F_f from surface contact and vacuum suction force F_s when an airtight seal is achieved [28].

Therefore, for a gripped cylinder, the frictional force F_f and the suction force F_s can be estimated from the depth z_c of gripped object as follows:

$$F_f = 2\pi r z_c \mu \tag{3.35}$$

$$F_s = P_g A^* = \pi r^2 z_c P_g \tag{3.36}$$

where r the diameter of cylinder, μ friction coefficient, and P_g is the pressure inside the airtight seal.

As such, in summary the total gripping force of the object can be estimated as:

$$F_T = F_s + F_f = \pi r z_c (2\mu + r P_g) \tag{3.37}$$

From this equation, a linear dependency between gripping force, and the depth of grip would be expected. In addition, in general, the greater the depth of the grip z_c, the greater the gripping force F_T. This equation also implies that, if z_c can be detected by a CTPE sensor, gripping force induced can be estimated assuming that all other terms could be regarded as constant.

This basic concept was tested by using Gripper 1 (Table 3.2), together with a 3D printed cylindrical object (with radius $r = 5mm$ and length $l = 50mm$). Theoretical and experimental results are shown in Fig. 3.16. To measure the influence of the contact area between the gripper and the objects on the grasping force, the depth to which the object is grasped by the gripper was varied by 2mm, and the grasping force the grip would withstand before the object could no longer be held was measured 5 times using a force meter. Although there are some variations, this indicates that for an increasing depth of grasp and hence increase of surface area of gripper in contact with the object, there is an increase in gripping force. From Fig. 3.16 it can be concluded that the gripping forces of an object with known 3D shape can be estimated using a single sensor on the Universal Gripper. This sensory information is particularly valuable when object gripping is unsuccessful, for example, due to slipping. It has been observed in experiments that such unexpected interactions with objects can be detected by the proposed method (see next chapter).

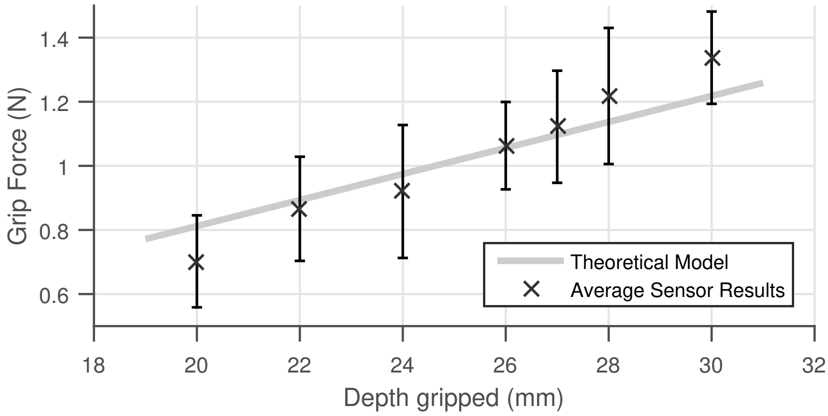

Figure 3.16 Grip force estimation base on the gripping depth sensing.

3.2.5 Framework for Deformation Sensing: Discussion & Conclusions

This research has investigated the use of the soft functional material CTPE as strain sensors applied to the Universal Gripper. The theoretical frameworks presented (grid, differential and slip sensing) use morphology to maximise the information which can be detected from a physical stimuli on a large deformable surface. The soft functional material, CTPE, employed in this project has a few unique mechanical properties including high sensitivity, minimum width, and maximum strain, in comparison to other materials with similar piezoresistive characteristics. This allows a high degree of freedom and flexibility when designing sensor morphologies. The proposed frameworks were developed in order to exploit these properties to enable high fidelity tactile sensing of soft robotics applications. These general morphologies have been exemplified in specific application scenarios such as identification of shape and location of basic objects when using the Universal Gripper for manipulation. The problem of soft body sensing is challenging because systems need to make sense of physical stimuli on continuum body (which can theoretically have infinite degrees of freedom) by using a discrete set of sensory receptors. Therefore it is necessary to develop approaches which allows the problem to be bounded.

This discussion can be more specifically applied to the differences between grid-based sensing and differential sensing. The grid based approach is a fairly general solution that could ultimately identify any shape at any location if a limitless number of sensors could be afforded. In practice, however, this approach is not always optimal as increasing the number of sensors can limit the favourable mechanical properties of soft structures. The differential sensing approach offers a conceptually different solution of soft body sensing. It does not offer a solution to gain all information about physical stimuli, however, the stimuli of interest can be obtained efficiently and accurately. Obviously these two approaches are not exclusive

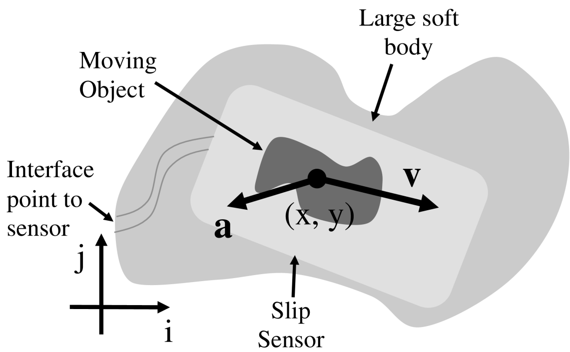

Figure 3.17 Simple model of slip with an object in contact with a soft body. The start of dynamic movement can be defined by its location and speed.

to each other, but complementary. In practical applications, optimal solutions of soft body sensing would likely be a combination of these two approaches.

3.3 Theoretical Framework for Dynamic Sensing

This same model and concept can be applied to time-varying sensor response to allow sensing of dynamic changes or movement. Movement and dynamic sensing of contact detection plays a vital role in our ability to identify and manipulate objects [70, 118]. The ability to develop soft sensors which allow movement to be detected are vital for the complex interactions and grasping between soft robots and the environment. Detecting movement between surfaces allows for stable grasping to be achieved, and for the force applied to be optimised [118, 119].

Existing work has investigated how force sensitive resistors can be used to enable movement detection to performed in one direction, and how the morphology of ridges attached to this force sensing resistor affects the performance [120]. Additional approaches uses different sensing elements to detect slipping [121]. These approaches have validated the ability to use morphology to aid movement detection but have developed sensors which are not fully soft, flexible or scaleable. This is also a sensing task where morphology and embodiment have been identified as a key methodology for achieving successful identification.

This work develops a morphology based approach to movement detection and dynamic perception of environmental interaction. The theory and framework is demonstrated with CTPE sensors.

A simple model (Fig. 3.17) of dynamic movement of a single point over a large soft body has been developed. Slippage, or the dynamic movement over a surface can be described by the location of the point of contact (or object) (x, y) and the velocity vector of the object

Table 3.3 Comparison of different slip/movement detection sensors and techniques including any morphology included to aid sensing, the output which is provided from the sensor, inherent flexibility, elasticity and also the scaling in the number of sensors with increased sensing area.

Sensing Method	**Sensing Technology**	**Morphology**	**Output Detection**	**Flexibility**	**Elasticity**	**Scalability with area**
Piezoresistive Tactile Sensors [122]	Piezoresistive MEMS sensors	Square array of sensing elements	Binary (ON/OFF) for movement	Semi-Compliant	0%	O(area)
Ridged Force Sensing [120]	Force Sensitive Resistors	Randomly separated ridges	Slip speed, distance	Semi-compliant	0%	One per area. Only 1D detection.
PVDF Tactile Sensors [123]	PVDF	Microstructure Columns	Slip and Texture detection	Flexible	0%	O(area)
Conductive Rubber Pads [124]	Conductive Rubber	Electrode patterning increasing sensitivity	Slip and Normal Force	Flexible	0%	One per area.
Force and Moment [125]	MEMS micro force and moment sensing	Layout of piezoresistive elements	Force, direction, texture	Semi-Compliant	0%	O(area)
CTPE Two-sensor Slip Sensor	**CTPE**	**Off-set two sensor**	**Movement, speed, direction and position**	**Flexible, Elastic**	**$\sim$90%**	**One per area**

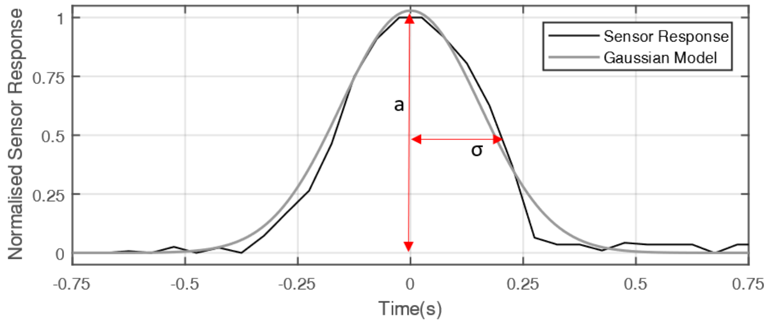

Figure 3.18 Single sensor dynamic movement sensing morphology with the peak detection response.

$\bar{v}$. This work provides a framework for the development of sensor morphologies to allow detection of movement on the surface of a soft body. The framework is scaleable, such that the number of sensors used to cover a large area is minimised.

3.3.1 Dynamic Movement Sensing Morphology

Conductive Thermoplastic elastomer (CTPE) will be used to the development of dyanmic movement sensing soft sensors. CTPE can be integrated into elastomers such as silicon by choosing a specific morphology of the CTPE 'threads', using a silicone adhesive and mechanical sticking to integrate the CTPE into one layer of CTPE before attaching an outer layer. The response of a single 'thread' of CTPE embedded in silicone (EcoFlex 00-20) to an object sliding perpendicular is shown in Fig. 3.18. As the object moves across the sensor, the sideways movement induces strain in the sensor, giving rise to the peak. The response can be modelled as a Gaussian function centred at time P.

$$p(t) = ae^{\frac{-(t-P)^2}{2\sigma^2}} \tag{3.38}$$

By detecting information about when the object is passing the single CTPE sensor thread, is is possible to develop a temporal model of an objects progress over a soft surface. The material in which the CTPE is encased determines the bandwidth of the sensor, with the soft elastomer acting as a low pass filter attenuating higher frequency components of the sensor response. The inclusion of the elastomer performs some embodied processing of the signal.

Uniform Separation Single Sensor Movement Detection

A single sensor can be constructed by using a morphology with a fixed separation, d between the sensor turns as shown in Fig.3.18. The total length of sensor perpendicular ln is signifi-

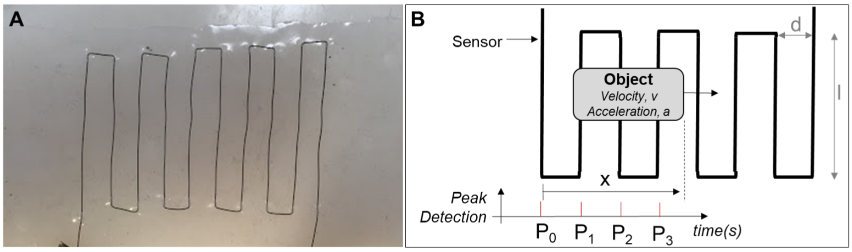

(a)

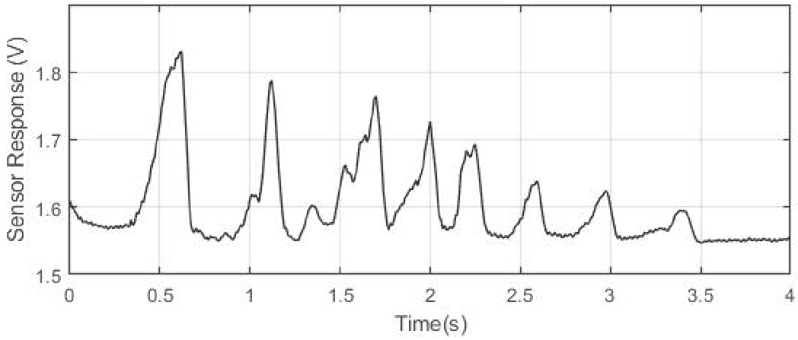

(b)

Figure 3.19 **a)** Single sensor morphology used to detect the slip, left) Picture of sensor developed, right) diagrammatic demonstration. **b)** Typical response from a single sensor.

cantly greater than that parallel, dl, such that the sensor is not sensitive to strain parallel. For a sensor with n sensor turns, the timing of the peaks detected as a response from this sensor can be given as $P_0, P_1, ..., P_n$.

Assuming the movement is purely perpendicular, using the prior knowledge of the distance between the sensor loops, once two peaks have been detected, the average velocity can be calculated using the response from the ith peak. Assuming the acceleration to be negligible, the velocity across the sensor can be determined.

$$v_{average}|_{a=0} = \frac{P_i - P_0}{di} \quad for\ i \geq 1 \tag{3.39}$$

The greater the number of peaks detected, and hence the higher the value of i, the higher the precision of the the measured velocity. The estimated distance moved by the object can also be determined:

$$\Delta x(t)|_{a=0} = id + v_{ave}(t - P_i) \tag{3.40}$$

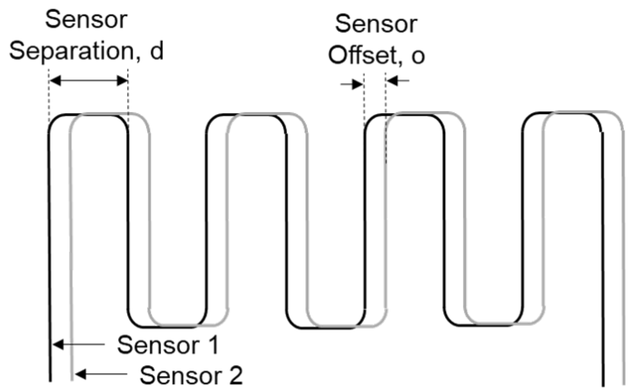

Figure 3.20 Dynamic movement sensing morphology with two sensors separated by a fixed offset to enable direction determination.

When the acceleration is non-zero, the quantitised velocity across each sensor segment can be determined:

$$v_i = \frac{P_i - P_{i-1}}{d} \quad for\, i \geq 1 \tag{3.41}$$

The value of d should be minimised to provide the greatest precision and temporal resolution. However, the combined CTPE and elastomer matrix limits the frequency range of the sensor, f_{max} due the damping effect of the elastomer. Therefore, to detect movement with a maximum velocity of v_{max}, the minimum distance between sensor lines such that the response is within bounds of the frequency response of the sensor, can be given as:

$$v_{max} < \frac{f}{d} \tag{3.42}$$

This sensor morphology does not allow absolute position to be determined, and it also not possible to determine the direction of the movement. Additionally, using a single sensor places a limit on the sensor placment distance and therefore, the resolution of the results.

Multiple Fixed Separation Sensor Movement Detection

To increase the precision of readings and increase the cut off frequency of the movement sensors, multiple sensors can be developed which have the same morphology and separation between turns, however are offset translationally by a distance o. The morphology is shown in Fig. 3.20.

Peak detection can then be performed on the signal from both the sensors, with the results stored chronologically into vectors P and Q. By setting the translation distance o such that it satisfies $o < d/2$, the direction of movement can be identified. By calculating the difference between consecutive peaks from the two sensors (P_i and Q_i) the direction can be determined:

$$|P_i - Q_i| = \begin{cases} < \frac{P_{i+1}-P_i}{2} & +vedirection \\ > \frac{P_{i+1}-P_i}{2} & -vedirection \end{cases} \tag{3.43}$$

By averaging the velocity from sensor 1 and sensor 2, the temporal resolution is increased:

$$v_i = \frac{\frac{P_i - P_0}{id} + \frac{Q_i - Q_0}{id}}{2} \quad for\, i \geq 1 \tag{3.44}$$

The precision of the response is also increased, and although the frequency cut off results in the same minimum distance between sensors, using two sensors doubles the maximum velocity which can be detected.

Sensor Morphology for 2D Movement Detection

By layering the sensor such that there are two sets of the sensor perpendicular to each other, the 2D direction of the vector can be determined. The two sensors provide the direction of velocity in the x and y axis (v_x and v_y) therefore the position, velocity and acceleration in 2D space on the surface of the sensor can be determined with reference to unit vectors **i**, **j**:

$$x = x\widehat{i} + y\widehat{j} \tag{3.45}$$

$$\overrightarrow{v} = v_x\widehat{i} + v_y\widehat{j} \tag{3.46}$$

3.3.2 Experimental Setup

A setup has been developed to test the response of different sensor morphologies to movement behaviour. The sensor is placed on a flat surface, and a UR5 arm is is used to move a ‘finger-like’ rigid probe over the surface of the sensor. This allows the velocity of the movement, the direction, and the force which applied to the probe to be varied.

For all experiments, the different trajectories are repeated five times, each time with varying force applied to the surface to test the robustness to varying force application.

3.3.3 Experimental Results

The first morphology tested in the fixed separation sensor, with two sensors offset by a fixed amount. A senor with ten turns, N=10, and a fixed off-set between sensor turns of $d = 10mm$

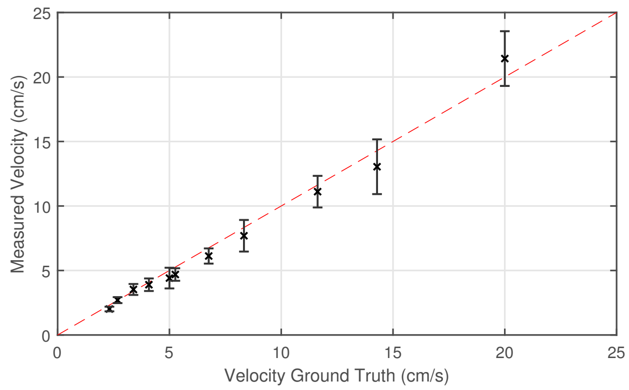

(a)

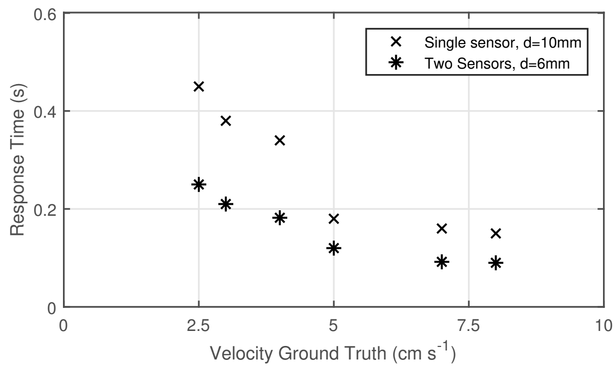

(b)

Figure 3.21 **a)** Magnitude of velocity determined experimentally and the ground truth for a two sensor with fixed separation . **b)** Response time of the movement sensor to detect movement using a single sensor and two sensors.

providing a sensor of 10 cm long. The second sensor is offset by $o = 3mm$, such $o < d/2$ the condition necessary to allow the direction of movement detection to be obtained.

The accuracy of movement detection has been tested by moving the probe over the surface perpendicular but with varying directions and speeds. The measured velocity is plotted against the ground truth of the velocity (Fig. 3.21a).

For low speeds there is a high precision and a high repeatability. As the magnitude increases to a maximum of $3ms^{-1}$, the error increases and the repeatability also decreases. This is to be expected as faster movements lead to decreased time between peaks, and any errors in peak detection become more critical.

In the second experiment, the response time of the sensor to detecting movement is investigated. The probe starts stationary off the sensor, and is then moved over the surface with a fixed velocity, with the time between the start of the slipping movement and the time movement is detected measured. The results are shown for using a single sensor in the morphology (d=10mm) and also when using both sensors (d=3-7mm). The results are shown in Fig. 3.21b. The rate of response of the sensor to movement is an important metric for robotic manipulation situations. The ability to react rapidly to movement enables grasping to be optimised.

The two sensor morphology allows for faster movement detection, however for both sensors as the slip rate increases there is a reduction in rate of decrease in the response time. This suggests there are some overheads in both the sensing material and signal processing preventing faster detection of movement.

3.3.4 Movement Detection: Discussion & Conclusions

The sensor morphology presented allows the development of large scale soft movement sensors. The morphology can be used to provide some 'embodied' encoding of information to allow the detection of additional information. This concept could be taken further by using variable distances between movement sensors to extend the information which can be encoded in the sensor.

Unlike other dynamic movement sensors, using the morphology and CTPE allows for a sensors which are flexible and also stretchable. As peak detection is used, if external strain is simultaneously applied in addition to movement, if this strain is applied at a frequency less than the the frequency of slip detected ($f_{strain} < v_{slip}/d$) filtering can be used to remove this strain frequency from the movement signal. This allows the sensor to be used in many applications where the sensor may also undergo stretch in addition to experiencing movement.

3.4 Discussion & Conclusions

This chapter has presented morphological approaches for sensing, where this provides embodied intelligence which aids the perception of different stimuli. This is a novel approach to sensing, where the focus is moved from the signal processing or sensing receptor to the sensor mechanics and environmental understanding. The essential role of the mechanics and morphology in developing a more embodied approach to perception has been demonstrated, with this research extending previous concepts of morphological aided sensing.

The differential sensing framework provides an insight into how sensor morphology can use mechanical integration to perform some of the work which would otherwise require complex signal processing. By combining this with the novel material properties of CTPE allows for exciting implementations. This also paves the way for new philosophies for embodied sensor development. In the three differential sensing case studies, despite the same number of sensors being required for each, the sensory information obtained is different depending on the relative sensor morphology. The differential sensing case studies instantiate an aspect of sensor morphology where it acts as a ‘filter and converter’ of physical stimuli [126].

Soft movement sensors are complex to develop, yet provide important perception for robotic systems. Previously, there has been limited development of fully soft, flexible and elastic movement sensors. Using morphology to identify movement has allowed for sensors which are soft, elastic and scaleable, with the embodiment enabling perception of movement. The morphology plays a key role in enabling the detection of movement, whilst the particular embodiment (combination of elastomer and spacing between the CTPE sensors) determines the localised embodied filtering effect of the sensor.

The scalability of the sensor morphologies is important due to the large area and high degrees of freedom of large robots. The frameworks presented allow the information which can be gained from a discrete number of sensors to be maximised, with the area not directly affecting the quantity of sensors required. Critically the integration methods does not impede the natural movement of the soft body, with no rigid wires required to interfere with the natural dynamics of the soft body.

The proposed theoretical frameworks are applicable more generally to deformation sensing in soft robotic manipulators; however it is necessary to continue the verification of the framework in a larger number of practical contexts. In particular, it would be interesting to extend the experiments presented in this work to more varied perception tasks, namely detecting objects with more complex geometries. By investigating such objects this will allow us to further explore the limitation and requirements in terms of sensor spacing and sensor resolution.

Chapter 4

Embodied Perception & Behaviour in Materials[1]

The integration and use of materials in soft robots has the ability to aid perception and sensing through embodiment. Developing materials which show embodied sensing and actuation capabilities has a two fold advantage. It allows the materials to contribute to environmental sensing whilst the functionalisation also allows dynamic changes of the material properties, aiding output behaviour. Under this philosophy, the role of a sensor changes; the behaviour resulting from the embodied characteristics enables the material to act as a sensor and actively contribute to the behaviour of a system.

This work addresses hypothesis two through the development of functional materials which show integrated properties aiding perception and controllable behaviours. The key novel research contribution of this work is the functionalisation of a soft material to perform sensing and aid environmental interactions enabling single point grasping.

[1]This chapter presents work developed collaboratively by myself and my supervisor F. Iida. I have initiated the problem statement, framework, undertaken the epxeriments, created the figures and written the papers. F. Iida helped with formulating and revising the paper. The peer-reviewed publication which forms the basis of this chapter is:

- Josie Hughes and Fumiya Iida. Tack and Deformation Based Sensorised Gripping Using Conductive Hot Melt Adhesive. *RoboSoft IEEE Confernce, Livirno, Italy (2018).*

A second paper, has been submitted for review:

- Josie Hughes and Fumiya Iida. Soft tactile sensing for wearable health monitoring devices.

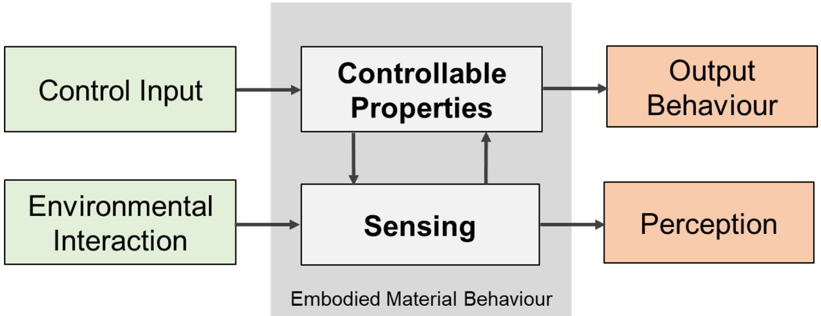

Figure 4.1 An embodied model of soft materials for use in soft robots.

4.1 Role of Embodied Materials in Soft Robotics

Materials are a key aspect of soft robotics as they provide an interface between the body and the environment. Designing and developing materials that have properties that can be altered or augmented, whilst also providing sensing capabilities provides functionality through embodiment. By having this integrated approach, separate sub-systems are not required for sensing or actuation, and sensing can be thought of as an embodied function of the entire body.

Fig. 4.1 shows a proposed model for an embodied soft material. The material has controllable properties, for example actuation, stiffness or stickiness, which can be altered with a specific control input. This input should require minimal control power, such that the technique is portable and efficient. The soft material also has inherent sensing capabilities, allowing perception of the environment. The material shows interaction between the controllable properties and sensing capabilities. By developing materials which demonstrate the capabilities of this framework, some behavioural and sensing abilities can be offloaded from the controller to materials.

In this chapter, the development of two materials which aim to utilise and demonstrate this embodied framework are presented. The first material uses temperature to control both the material properties and also the sensing capabilities. The second, a conductive silicon based sheet material shows sensing capabilities and flexibility such that the particular integration and embodiment alters the sensing capabilities.

4.2 Conductive Hot Melt Adhesive

4.2.1 Motivation

Developing a single point gripping mechanism which allows non-permanent attachment force to be achieved between two surfaces is useful for many robots, including pick and place, locomotion or climbing systems [127, 128]. The development of a single point gripper which can grasp a wide variety objects with minimal control and precision could provide a universal method of grasping. There are a variety of existing 'universal grasping' systems which utilise a variety of different mechanisms to grasp objects [129]. However, these have limitations in terms of the materials which can be lifted, the precision required and the sensing capabilities. This paper investigates how the 'tack' force, the force required to separate objects after a short period of contact, of Hot Melt Adhesive (HMA) can be used to provide embodied behaviours, allowing single point force development. The tack force of HMA is controllable by varying the temperature of the material and the force of interaction between the object and the HMA. The temperature increases the tack force and also increases the stiffness which increases the area over which the HMA is in contact with object, increasing the tack force. This variable softness is a key aspect in achieving a secure and stable grasp with minimum input force. By including conductive particles into the hot melt, the material becomes pressure sensitive. Using this embodied sensing capabilities, a feedback mechanisms can be used to optimise the grasping pressure for successful grasping of different objects. The gripping system developed and the integration of CHMA into a gripper is summarised in Fig. 4.2.

A method is proposed whereby universal grasping is achieved using the tackiness force of CHMA. By understanding the effect of temperature and force on tackiness, it is possible to control the tackiness and hence grasping force. Uniquely, this embodied grasping method has inherent pressure sensing capabilities allowing feedback to be implemented alongside force control. A grasping system can be developed which minimises both the time taken to grasp (related to the temperature of the CHMA required) and the force which must be applied, limiting the potential for damage to the object. In this work a model for the tackiness force as a function of temperature and indentation force is given. The inclusion of the material and the associated feedback system in a single point gripper has been demonstrated experimentally.

Table 4.1 summarises a number of comparable methods for single point grasping which provide alternatives to CHMA. Using suction cups is one widely adopted method in many industrial settings [130]. Although the force which can be lifted using a vacuum is significant, it can require significant suction force and can be noisy. The Universal Gripper (as discussed in Chapter 3) utilises the principle of jamming to lift a wide variety of objects [109], this is highly universal and can be used on a wide variety of materials and morphologies of

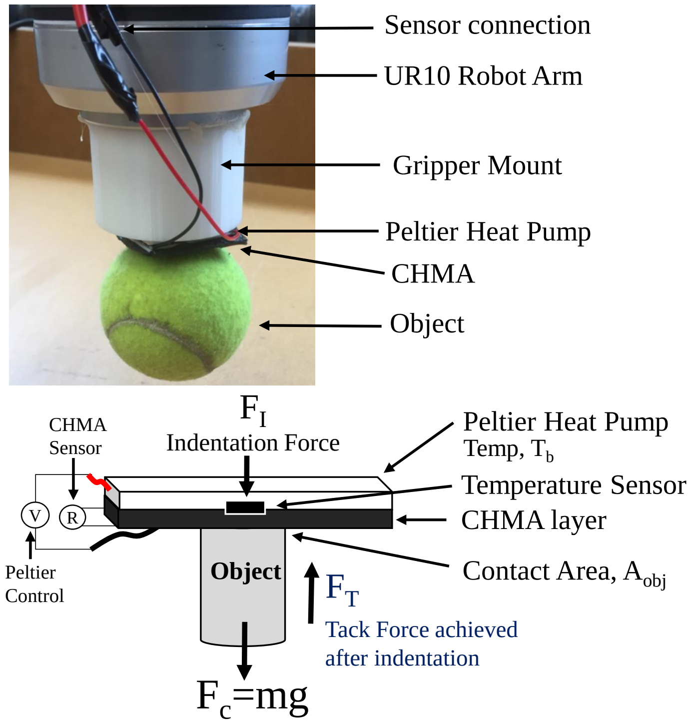

Figure 4.2 Photograph of the CHMA gripper developed (top), diagram of the gripper system (bottom).

object. However, this gripper struggles with softer or sharp materials and requires reasonable precision when grasping. The principle of using Van der Waals force, as seen in the feet of Geckos, has been highly successful for robotic applications ([131, 132]) especially for climbing robots. However, there are some materials for which this mechanism of force development will not work. Developing glue bonds is another method of non-permanent force development [127, 133], but it is time and power consuming. Low-melting point alloys provide an exiting direction for the formation of non-permanent bonds allowing ‘self-soldering’ connections but is currently not a scaleable method [134]. CHMA has a reasonable tolerance to the positioning of objects, can work for a wide variety of surfaces and materials including soft object and has inherent sensing abilities. In comparison to the other mechanisms, the embodied perception and controlable parameters allows integrated sensing and also reduces the precision and accuracy required by the controller.

Table 4.1 Comparison of different single point grasping methods summarising their key mechanisms, limitations and sensing capabilities.

Method	**Mechanism of Force**	**Force Achievable**	**Limitations**	**Release Mechanism**	**Sensing Mechanism**
Suction Cup [130]	Vacuum	High (≈100N)	• Requires flat surface • Poor for soft or sharp material	Removal of vacuum	None
Universal Gripper [109, 135]	Vacuum, Friction, Jamming	High (≈100N)	• Soft Materials • Low friction sheet material • Requires compressor	Removal of vacuum or positive pressure	None
Geckos Feet [131, 132]	Van Der Walls	Low (≈2N)	• Non-uniform surfaces • Surface material dependant • Teflon based materials	Peeling	None
Glue Bonds [127, 133]	Adhesion	High (≈100N)	• Bonding takes time • Debonding slow • Leaves residue	Melt the bond (slow)	None
CHMA	Controllable tackiness and deformation	Medium (≈50N)	• Bonding takes time • Requires some force	Shear force/melt	Inherent Pressure Sensing

4.2.2 CHMA Theory & Framework

Hot Melt Adhesive (HMA) is a thermoplastic polymer with additives which enable the material to form adhesive bonds with some flexibility to the joint [136]. The particular additives and percentage composition determine the specific material properties of a HMA. The HMA base material used is Kleiberit 779.6 Hot Melt Adhesive.

By including conductive particles within the HMA when molten, the material can be made to be conductive [25, 103]. To fabricate the material, HMA pellets is heated up such that the material becomes molten. The conductive particles (carbon black) can then be added to the melt. To ensure even distribution of the particles within the melt, the material is mixed as it cools and the viscosity increases. The CHMA can then be poured into moulds, or poured to form sheets of varying thickness. Conductive electrodes can be placed into the material when it is still soft. The material can be placed on top of a Peltier Heater element with a temperature sensor placed within the material. A diagram of the setup is shown in Fig. 4.2. The following sections discusses the three controllable properties of the material: stiffness, tackiness and conductivity.

Tackiness of HMA

When the temperature of CHMA is raised, the material becomes ‘tacky’. Hot tack describes the ability of a material for form a rapid bond, and is highly dependent on the wettability of the material [137]. In the case of CHMA the tackiness varies and is induced at temperatures above room temperature [136]. Tackiness is a result of the sum of the cohesive strength of the material in addition to its adhesive strength (the binding forces between two materials due to the interaction of surface molecules due to physical, chemical and electrostatic interactions [138]). Tack is not a fundamental material property and does not have exact mathematical correlations to other quantities. It provides an interesting embodied functionality to the material which can be exploited for grasping.

When the temperature of material rises above room temperature and the viscosity starts to decrease, the tackiness increases until a point at which the viscosity decreases and the material behaves more like a liquid and the tackiness begins to decreases. This is the point at which the cohesive strength of the material begins to reduce resulting in this decrease in tackiness. This region where the viscosity increases such that the material is 'tacky' before we have this drop in cohesive strength drops is the region of interest for this work.

The tackiness force can be modelled as a function of the temperature of bonding T_b and the initial indentation force F_I. We assume an approximately constant bonding time (5 seconds) and constant indentation speed such these parameters are constant and do not effect the tack force. To investigate the tack force of CHMA, we consider a thin layer of CHMA such that the material deformation can be ignored. The tack force is defined by the force required to release an object of surface area A_{obj} with a given applied force of interaction F_I at a given bonding temperature T_b. For the region of interest, the relationship between the temperature and the tack energy has been shown to obey the Arrhenius behaviour [139, 140]. The tack force is also dependant on the area of contact A_{obj}, and has a power law dependency on the indentation force F_I [140]. Therefore a simple model for the tackiness can be given:

$$F_T = F_I^{\mu} \sigma T_b^{1/2} exp\left(\frac{-\phi}{T_b}\right) A_{obj} \tag{4.1}$$

There are three constants, σ, ϕ and $\mu whicharedeterminedexperimentally, andareafunctionoftheexactm$ The tack force was determined by measuring the peak force required to remove the object from the CHMA. Each experiment was repeated five times. The theoretical model results are also shown for comparison.

Deformation of HMA

Previously, a thin layer of CHMA was modelled such that deformation can be assumed to be insignificant. We now consider a thicker layer of CHMA where the softness varies with temperature T_b. The area in contact with the object A_{obj} is now a function of T_b.

When HMA is above a given temperature, the viscosity of the material drops such that it can no longer be modelled as an elastic material, but as viscoelastic [141]. In this region the material exhibits behaviour which combines liquid-like and solid-like characteristics. To model this material, the Hertz elastic contact model can be combined with the Boltzmann hereditary integral to provide an approximate model for linear viscoelastic indentation [142].

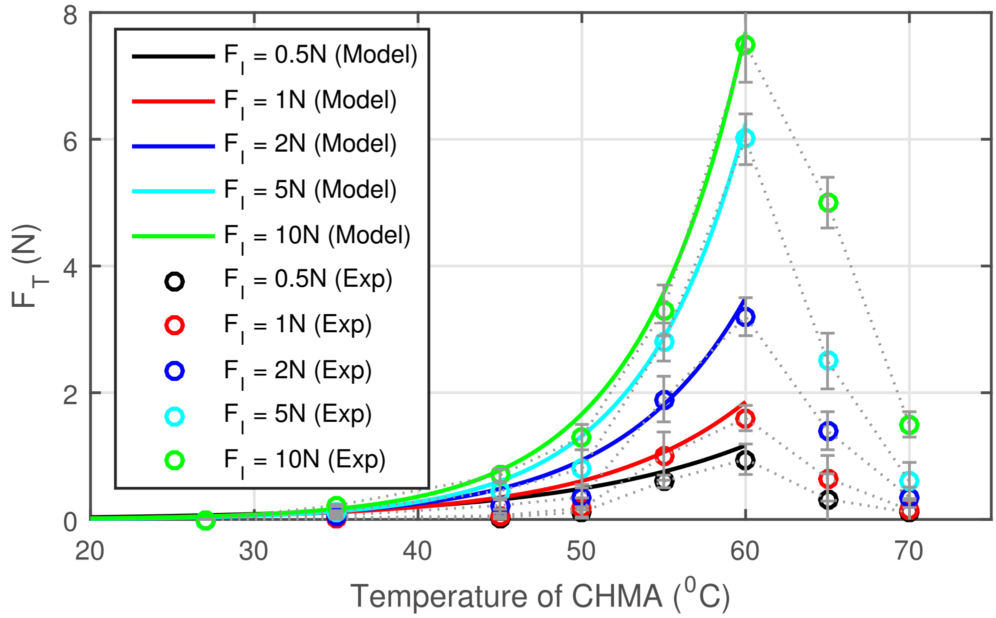

Figure 4.3 Tack force of a plastic cylinder (diameter 20mm) measured experimentally, repeated 5 times over a varying temperature range where the indentation force (F_I) applied is varied.

Treating HMA to be a linear viscoelastic material, the indentation profile can be determined with respect to the material properties and the temperature of the material. Starting with the elastic model for indentation, for an indenter pressed into a linear viscoelastic body, during the loading of the indenter, the penetration depth and the contact area grow with time [143]. Therefore the constitutive equations for viscoelastic materials can be adapted from the elastic model. Following on from the work of [142], the steady-state form for penetration depth for a constant indentation load of F_I for time t can be given as:

$$h(t) = \left(\frac{F_I t}{2C(1+\upsilon)\eta}\right)^{\frac{1}{n}} \begin{cases} C_{sphere} = \frac{4r^{0.5}}{3(1-\nu^2)} \\ C_{flat} = \frac{D}{1-\nu^2} \end{cases} \tag{4.2}$$

where C is the respective shape factor, n varies with shape (n = 1 for sphere, $3/2$ for flat) and the initial force of indentation, F_I (Fig. 4.4). The Poisson's ratio, ν, varies marginally over the temperature range of interest, and can thus be considered constant, whereas η the steady-state shear viscosity changes significantly over the temperature range, with the behaviour given on the data sheet for the material.

Assuming the material has full contact with the deformed area, the area in contact with the HMA can be given by:

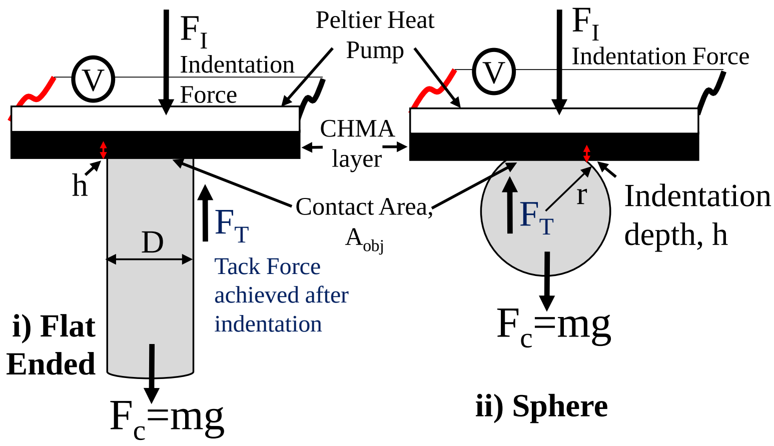

Figure 4.4 Axis symmetrical indentors interacting with a visoelastic showing the parameters which can be used to describe the indentation profile

$$A_{obj}(t,\eta) = \begin{cases} \frac{\pi D^2}{4} + \pi D h(t) : Flat \\ \pi r^2 (1 - \frac{r - h(t,T_b)}{r} : Spherical \end{cases} \tag{4.3}$$

Modelling the Poisson's ratio as approximately constant and using the values of the steady-state shear viscosity the predicted tack force can be determined and compared to the experimental results. Similarly to the experimental results above, the tack force was measured over a range of temperatures for a given indentation force with a thicker layer of CHMA. The tack force for a cylinder and sphere was determined for a fixed indentation force, and is shown in comparison to the thin film tack force results (Fig. 4.5). This shows the increase in achievable force when the thickness of the material can no longer be considered to be a thin film. This is considerable (20%), showing that the coupled ability to control the softness in addition to the tackiness has a significant effect on the ability of the material to apply force.

Deformation Sensing of CHMA

By including conductive particles, carbon black, into the HMA the polymer can be made conductive, assuming the percolation threshold is exceeded [144]. This is a principle which is utilised in many soft thermoplastic sensing applications, and thus is not the focus of this work. This provides enables a material which provides emboded perception.

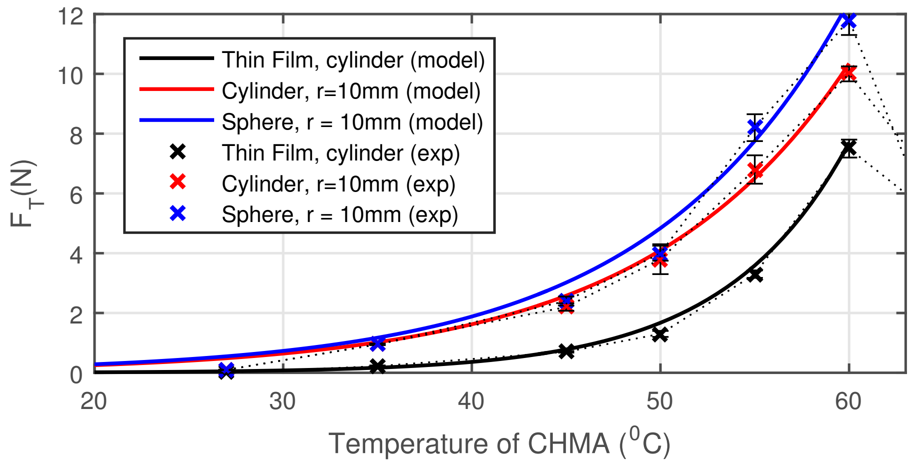

Figure 4.5 Variation of Tack force generated with a cylinder indented on thin film CHMA, and a cylinder and sphere on a 8mm of CHMA with 10N of indentation force applied. The experiments were repeated 5 times at each temperature.

The material conductivity is temperature dependant, where the bulk resistance (under no load) can be modelled by the typical temperature coefficient of resistance where [145]:

$$R(T)_{bulk} = R_0(1 + \alpha(T - T_0)) \tag{4.4}$$

Fig. 4.6 shows the varying resistance with pressure for different temperatures. The resistance decreases with a power law relationship with respect to pressure [146]; this behaviour is partly due to the relaxation behaviour of the thermoplastic and is partly controlled by the stress relaxation behaviour. This is the typical behaviour for uniaxial loading for such pressure-sensitive mechanisms [147]. This combined temperature and pressure sensitive model of bulk resistance is given by:

$$R(T, p) = R_0(1 + \alpha(T - T_0)) + \gamma p^{\frac{1}{\beta}} \tag{4.5}$$

where α, β and γ are determined from experimental results and reflect the material properties and the percentage of conductive particle inclusion into the HMA. Fig. 4.6 shows the theoretical model and the measured resistance normalised by the unloaded resistance where the resistance across the a $30mm^2$ section of CHMA is measured under varying temperature and load conditions. In this situation we are not considering unloading, only the application of pressure when the CHMA comes in contact with the object.

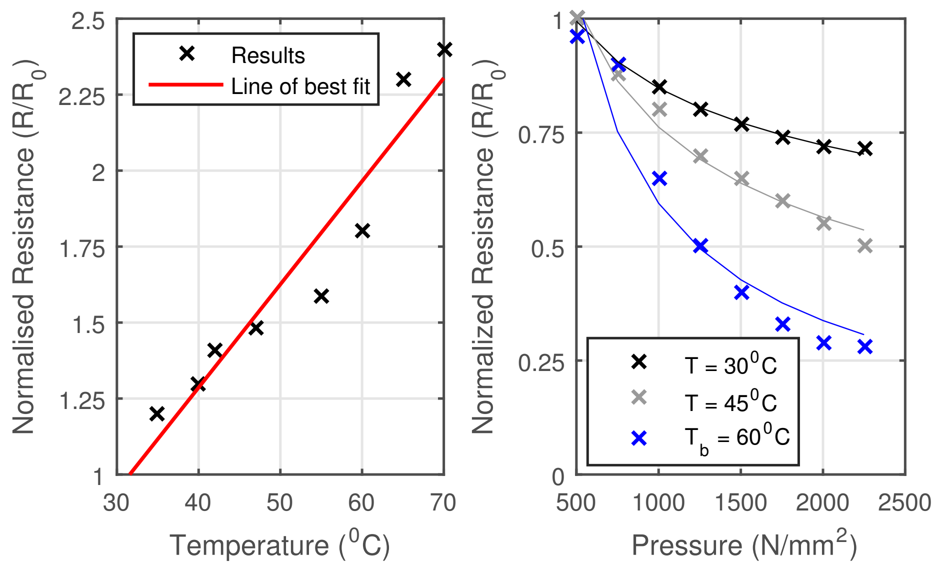

Figure 4.6 The varying base resistance (R_0) with varying temperature (left), the change in resistance with pressure applied to the material (right). For CHMA with 5%wt carbon black.

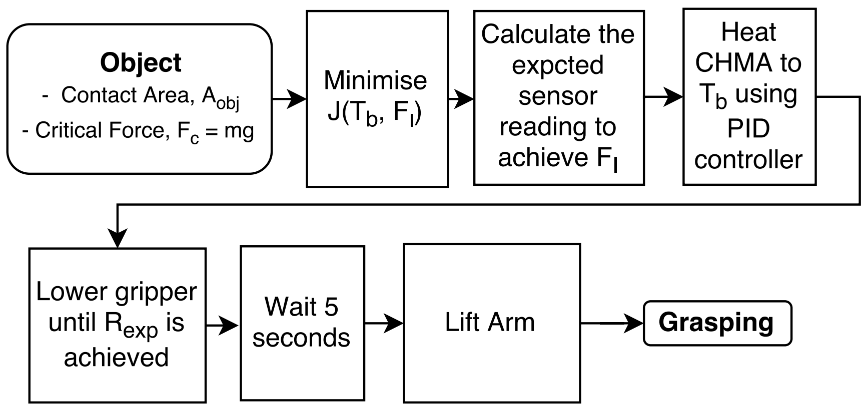

Figure 4.7 Summary of the CHMA feedback mechanism implemented for grasping.

4.2.3 Experimental Implementation

The material has been incorporated within a gripper designed to perform pick and place, exploiting the embodiment behaviours of CHMA for both perception and behavioural control. By varying the temperature, it is possible to set the softness and tackiness to pick a given object. The robot end effector can then be lowered over an object with a known mass and estimated area of contact until sufficient pressure for successful grasping is measured by the CHMA. The combined temperature and force of indentation is chosen such that for the specific item the tack force exceeds the critical force $F_T \geq F_c = m_{obj}g$.

To determined the required combination of temperature and force of indentation for a particular grasp, we want to minimise the cost function:

$$J(T_b, F_I) = \lambda(T_b - T) + \mu F_I \tag{4.6}$$

This cost function has been chosen to achieve a low temperature to minimise heating time and to minimise F_i such that the items picked are not damaged. The values of λ and μ should be chosen to represent this balance. In these experiments, the values were chosen empirically to achieve moderate speed and moderate F_I (λ = 0.3, μ = 0.7.)

For a given object, the critical force F_c is known, and the contact area can be estimated, thus the temperature and force required can be selected using (4.1), (4.2), (4.3) and to minimise (4.6). The correct temperature of the CHMA is achieved using a PID controller controlling the current to a Peltier Heater with feedback from a temperature sensor. The expected sensor results for the required force, F_i can be calculated and a simple feedback loop can be implemented whereby the robot gripper is lowered until sufficient F_i has been achieved. This is summarised in Fig. 4.7.

An object can be released by increasing the temperature and using shear force, as the shear adhesive force is less than the normal force. There can be some minimal residue left on the picked objects, however this can be reduced by using lower temperature.

4.2.4 Experimental Results

To test the capabilities of the gripper a variety of objects were gripped. In particular, items were chosen which are challenging for the other grasping methods mentioned in Table. 4.1. Table. 4.2 and Fig.4.8 showing the grasping results for these items. For each item the temperature of bonding and indentation force was determined using the mass and estimated

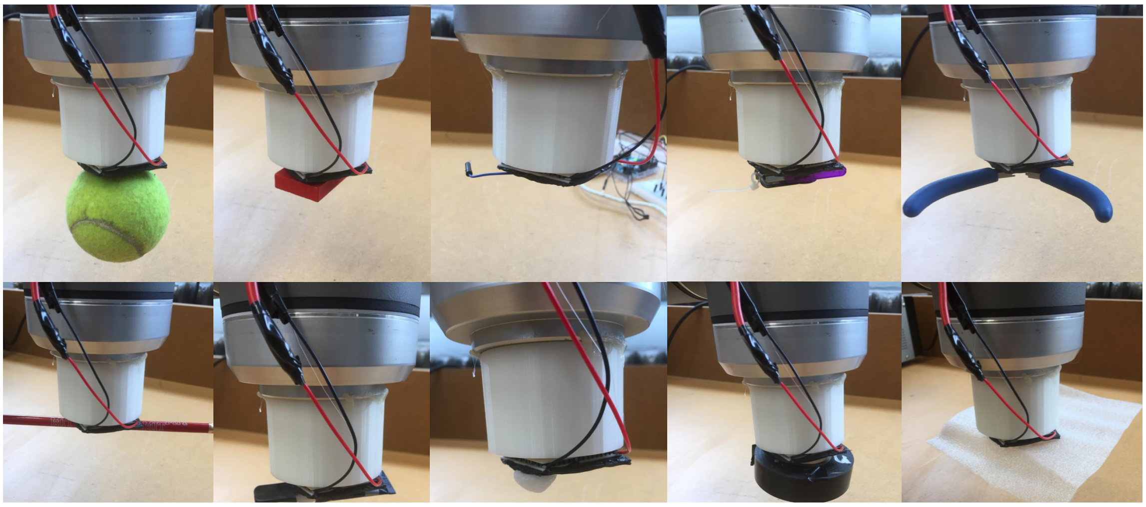

Figure 4.8 Demonstration of the successful lifting of items using the gripper. Left to Right: Ball, PTFE block, wire, memory stick, pliers, pencil, super glue, foam, tape, fabric.

contact area. Each item was gripped 10 times and the success and the tack force achieved measured using the same procedure as the previous experiments.

The average measured tack force F_T was in some cases lower than the critical force F_c, notably for the ball, pliers and tape. For the tape, the lower tack force was reflected in the picking success rate where there were some failures. In the case of the tape and ball this was significant, with the success rate dropping to 80%. These objects had more complex geometries and deformation profiles, such that the estimated contact area approximation was insufficient. Therefore the desired indentation force and temperature failed to achieve sufficient tack force. Additionally for the ball, the 'fluffy' surface of the ball reduced the effective surface area affecting the predictions of the tack model. A more comprehensive analysis and model should investigate the effects of the materials gripped.

For some of the smaller objects such as the wire, the measured tack force far exceeded that of the critical force; for the wire the tack force was three times that of the critical force. It was observed that on gripping the wire was semi-engulfed by the CHMA such that the contact area between the object and CHMA was an significant under estimate, leading to higher than required tack forces.

The standard deviation in the measured tack force is in some cases significant; the tape and pliers showed up to 0.4N of variability. Although CHMA and the feedback system developed can be used to enable grasping, the force generated can show up to 10% variation. To increase the robustness of the system, the critical force should be increased to include a safety margin which accounts for this variability.

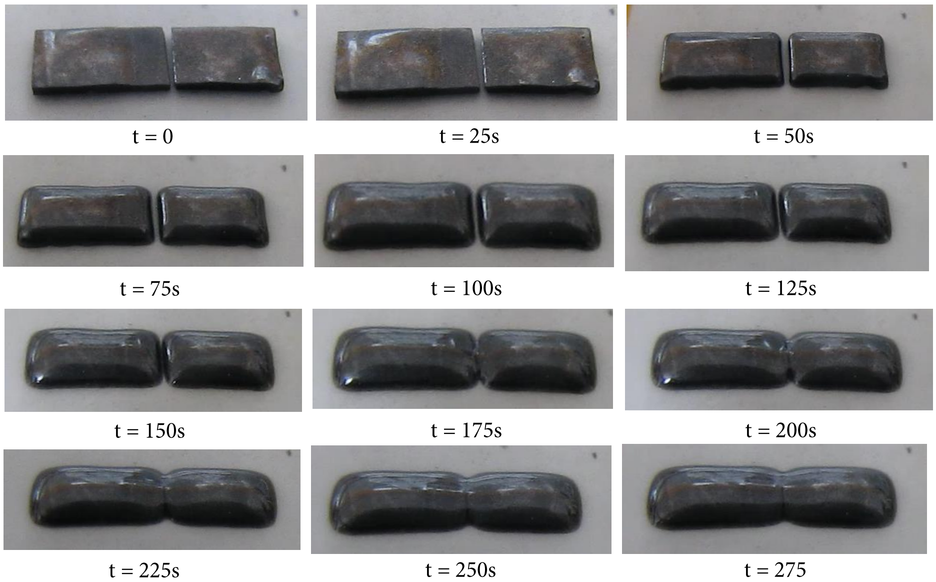

Figure 4.9 Time series showing the a broken section of CHMA as it is heated up, and reforms as a single piece, such that the sensing capabilities across the material is re-enabled.

The allowable variation in position from the centre of the gripper where objects can be successfully grasped was measured by placing the objects at increasing distances from the centre of the gripper. For all items there is some allowable variation in position. The system was particularly robust when picking up softer items with a less well defined boundary such as the fabric and foam, where up to 30mm variation in position still allows for successful gripping.

Another criteria to compare the grippers is the time to grasp. This is defined by the time to reach T_b and to lower and grasp the object. Although significant in some cases, the cost function could be further optimised to account for material properties of the object.

4.2.5 CHMA: Discussion & Conclusion

Typically, the role of material in soft robotics is provide a specific stiffness, mechanical scaffolding or compliance with the environment. In this work, the material is considered as a embodied part of the robot system, aiding and contributing to perception of the environment and the output behaviours of the system. The material becomes an integral part of the sensor. The interplay between tackiness and sensing provides an interesting embodied approach to grasping, with the parameters co-dependant.

A simple model for the tack force as a function of temperature and indentation force has been given and validated against experimental evidence. This is a simplified model, however, as shown in the experiments this provides sufficient information to be used for grasping. In

Table 4.2 Success of grasping ten items when each was grasped 10 times. Shows the object parameters, determined gripping parameters and the grasping results.

	Object Parameters		***Gripping Parameters***		***Results***			
Item	**Estimated Area, A_{obj} (mm^2)**	**Critical Force, F_c (N)**	**Indentation Force, F_I (N)**	**Bond Temperature, T_b ($^\circ C$)**	**Picking Success Rate, (%)**	**Measured Tack Force, F_t (N)**	**Allowable variation in position (mm)**	**Average time to grasp (s)**
Ball	100	2.2	8	62	80%	2.18 ± 0.2	20	50
PTFE	500	1	6.5	50	100%	1.2 ± 0.1	30	45
Wire	30	0.1	1.4	38	100%	0.3 ± 0.1	35	15
Memory Stick	450	0.5	3.2	42	100%	0.52 ± 0.15	25	20
Pliers	320	2.8	8.4	67	90%	2.6 ± 0.3	15	55
Pencil	310	0.9	1	44	100%	1.1 ± 0.2	30	20
Glue	220	1.5	3	52	100%	1.6 ± 0.2	25	25
Foam	350	0.08	0.9	39	100%	0.12 ± 0.4	30	15
Tape	420	3.9	1.5	66	80%	3.85 ± 0.4	15	55
Fabric	520	0.09	1	37	100%	$0.2 \pm 0.\ 1$	40	15

comparison to other solutions, the wide variety of materials and objects for which CHMA can be used to grip is significant, and the inherent sensing abilities of the material allow a feedback mechanism to be implemented without the addition of further sensing. This is a unique aspect of this method. Due to the deformability of the material which increase the effective area, and the flat surface (unlike the curved Universal Gripper), the gripper requires a low precision in comparison to other gripper methods, a considerable advantage. This offers an exciting and novel additional to standard gripping methods, and is especially suited for soft objects typically challenging for other gripers. This is enabled by the considerable contact area which can be achieved between the gripper and the object.

The material properties are such that by heating up the material and lowering the viscosity, the material surface can be returned to close to the initial surface geometry. This provides the ability for the sensing component to 'heal' with the addition of heat extending the life of the gripper (Fig. 4.9). This is another interesting embodied properties which should be investigated further.

Further work should investigate the trade off between time and indentation force and hence optimise the cost function when tailoring for specific applications. The sensor readings from when objects are lifted could enable the success of grasping to be identified, and could provide further information about the grasping process.

4.3 Conductive Silicone Sensor

In this section, the development of a conductive silicone sensor is presented. This is an example of how the embodiment or implementation of sensing material can be used to detect varying stimuli with different requirements and varying sensitivity. The material development is presented after which a case study of varying implementations for physiological monitoring is given.

4.3.1 Material Fabrication

A soft sensing material has been developed by including low percentages of conductive particles, Carbon Fibre (CF) and Carbon Black (CB), into a non-conductive matrix. A similar principle has been demonstrated previously, with the inclusion of conductive CB elements in thermoplastics [25]. There has been previous investigation of the integration of CB into a silicon matrix [148, 149], the inclusion of other metal-polymers [150] and the inclusion of carbon nanotubes [151]. By including two conductive elements, the amount of each conductive element required is reduced, limiting the negative effects the additives have on the mechanical properties of the material. When only CB is included into the silicone, the curing process of the silione can inhibit the conductivity of the CB particles due to their low surface area to volume ratio, such that a large percentage of CB is required. This significantly affects the material properties of the sensor. Including a small amount of CF (approximately 1% by weight) enables effective conductive pathways to remain after curing, such that lower percentages of CB (again, approximately 1% by weight) provide conductivity [152]. A number of different theories have been proposed for electron transport in conductor filled plastic or rubber systems, the most common and widely accepted is percolation in a continuous conducting network with the additional potential for tunnelling between isolated conducting particles [153, 154]. The focus of this paper is on the application and usage of the material developed.

To develop the sensing material, the CB and CF particles should be mixed with a solvent and allowed to dry, such that the particles are separated, before including into the silicone mix. In this case, EcoFlex Smooth On 00-20 silicone has been used. The particles should be mixed thoroughly to ensure an homogeneous distribution throughout the mix. The silicone sensor can then be poured into a mould, de-gassed, to remove and prevent gas bubbles forming. The silicone sensor is then left to cure after which it can be released from the mould and cut into the shape required.

The silicone sensor material has been formed into sheets by sandwiching between two thin outer layers of insulating silicone (Fig. 4.10) made in 3D printed moulds. This protects the sensor and allows the sheets to be easily cut into the shape required for the sensors. The sensors can be made fully waterproof by surrounding in a full layer of silicone.

The fabrication process takes approximately 4 hours and allows for customisation of the base resistance and the sensitivity by including varying the amounts of CB and CF. The sensor can undergo strains greater than 150%, with the conductivity varying with strain and pressure. Silver coated electrodes are placed into the sensing material and fixed with adhesive to provide an electrical contact to the sensing material.

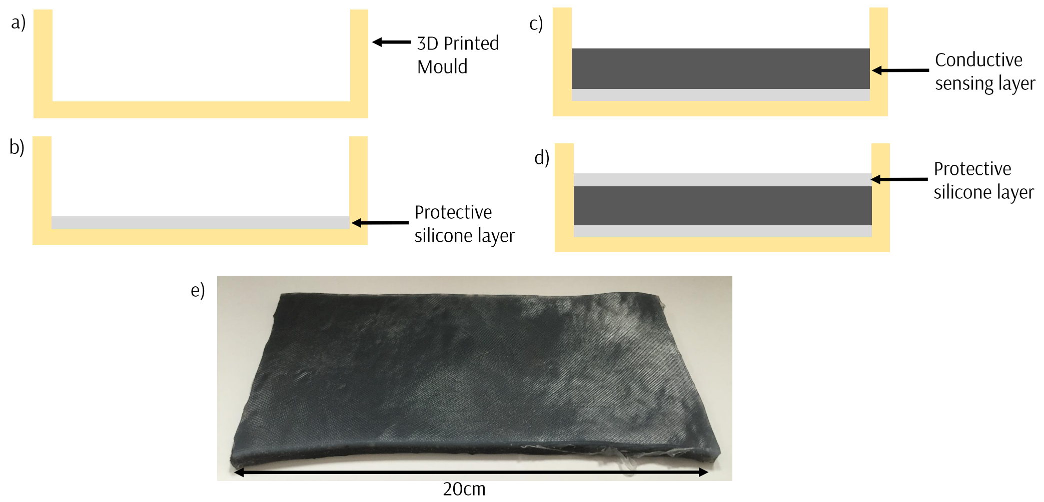

Figure 4.10 The fabrication process to develop sheets of the sensing material. a) Create a 3D printed mould for the sensor. b) Cure a thin layer of silicone in the bottom of the mould, c) Create the sensing material and pour into the mould and cure, d) add a final thin protective layer of silicone, e) The sensing sheets produced.

Sensor Characterisation

The sensing material responds to both lateral and longitudinal strain in addition to normal pressure. This is an interesting property, as allows the physical implementation of the sensor to exploit this capability, and determine the sensing mechanism required.

The characteristic response of the material to these stimuli has been obtained. The material sample tested had a composition of 1% CB percentage and 0.8% weight of CF, with the physical dimensions of of (w,h,d) 60mm x 20 mm x 4 mm. The base resistance, as measured across the width is approximately 1kΩ. To determine the strain characteristics, strains of up to 100% were applied in 10% intervals, and the resistance of the sensing material measured, with the strain cycle repeated five times. The strain resistance profile, Figure 4.11, shows that there is an approximately linear response to strain with a high repeatability. The change in resistance is significant, with the resistance increasing by a factor of 10 when the strain is increased to 100% demonstrating a high sensitivity. The sensing material is highly flexible and can continue to deform past 100% strain, to the order of 250% strain, before the tensile limit of the material is approached.

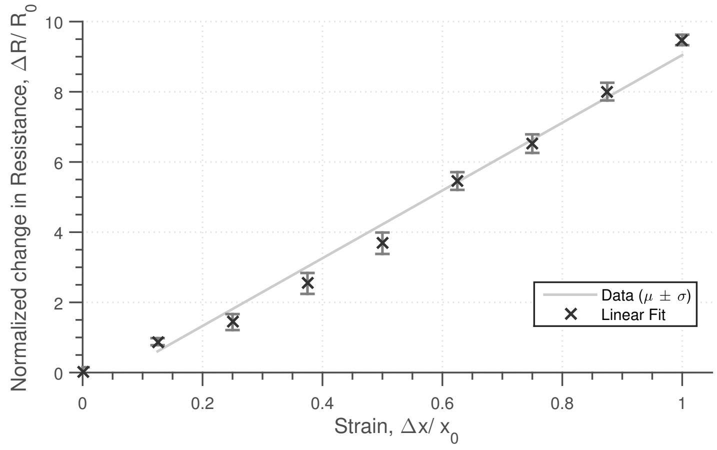

Figure 4.11 Plot of force against normal strain for the soft conductive silicon sensor showing the mean and standard deviation. Strain was applied in steps of 10%, with this cycle repeated 5 times with the average and standard deviation determined.

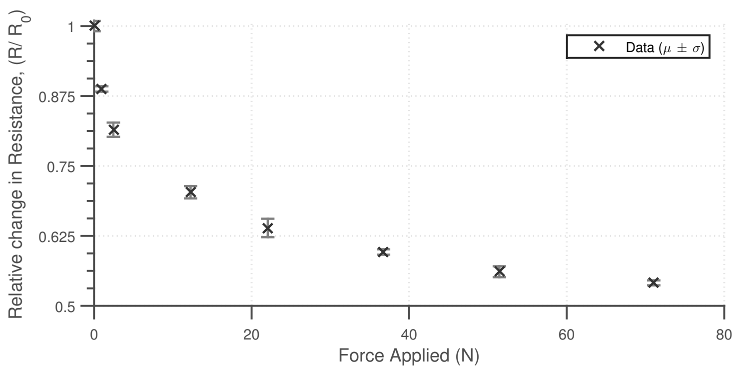

Figure 4.12 Resistance measured across the sensor (with electrodes placed at either end) when increasing loads (of base diameter 2cm) are applied to the sensor. The experiment was repeated 5 times with the average and standard deviation shown.

The sensing material is also sensitive to pressure normal to the surface. The dependence to normal force was determined by applying loads, and measuring the end to end resistance of the sensing material. The results (Fig. 4.12) show that for loads of up to 4N, there is a significant initial reduction in resistance, however, after this point, there is minimal reduction in the resistance measured. A similar response to pressure has been obtained, with other rubber or silicone based sensors with conductive elements [155]. The material compression properties contribute to the resistive properties of the material, with the rate of resistance decreasing with load as the material is increasingly compressed. The range of sensitivity can be altered by changing the physical height of the sensing material and the percentage of conductive particles included into the material.

4.3.2 Soft Silicon Sensor: Material Design Parameters

It has been shown that the sensing materials responds to both strain and normal force (pressure), but, the particular response also depends on the sensor material parameters, which can be determined externally. Thus, the embodiment and physical realisation of the sensor determine the specific characteristics. The parameters which have been found to affect the response of the sensing material include:

- **Material Composition.** This is the most significant factor influencing the sensor characteristics. The CB and CF content added to the material affect the base resistance and the sensitivity of the sensor. It also affects the mechanical properties of the sensor, which places upper limits on the amount of these conductive particles which can be included into the silicone matrix.

- **2D Dimensions & electrode placement.** Assuming the electrodes are placed at the outer ends of the sensing material, the un-deformed resistance of the sensor is dependent on the dimensions of the sensor. The dimensions also affect the force-strain response of the sensor.

- **Sensor thickness.** Assuming the conductive particles in the sensor are homogeneously distributed, the thickness of the sensor has little effect on the base resistance of the sensor. This affects the strain-force behaviour, and also the response to normal force. The greater the thickness of the sensor, the greater region of the sensitive linear region to the material to strain. This is because the material can undergo greater compression caused by the load before reaching the compression limit after which limited or no further compression can occur.

- **Silicone Matrix.** The material properties are predominantly determined by the silicone matrix used as the base material. Sensing materials have been developed with silicone of different shore hardness and elasticity, which affects the strain-force properties of the material, again mapping to a change in strain-resistance properties.The curing mechanism used to form the silicone also affects the resistance-strain properties of the sensor.

Sensor Material Parameters: Effects of Material Composition

The addition of the CB and CF provides a path of conductance to the silicone. The sensor properties vary for different composition of CB and CF. Fig. 4.13 shows the varying base

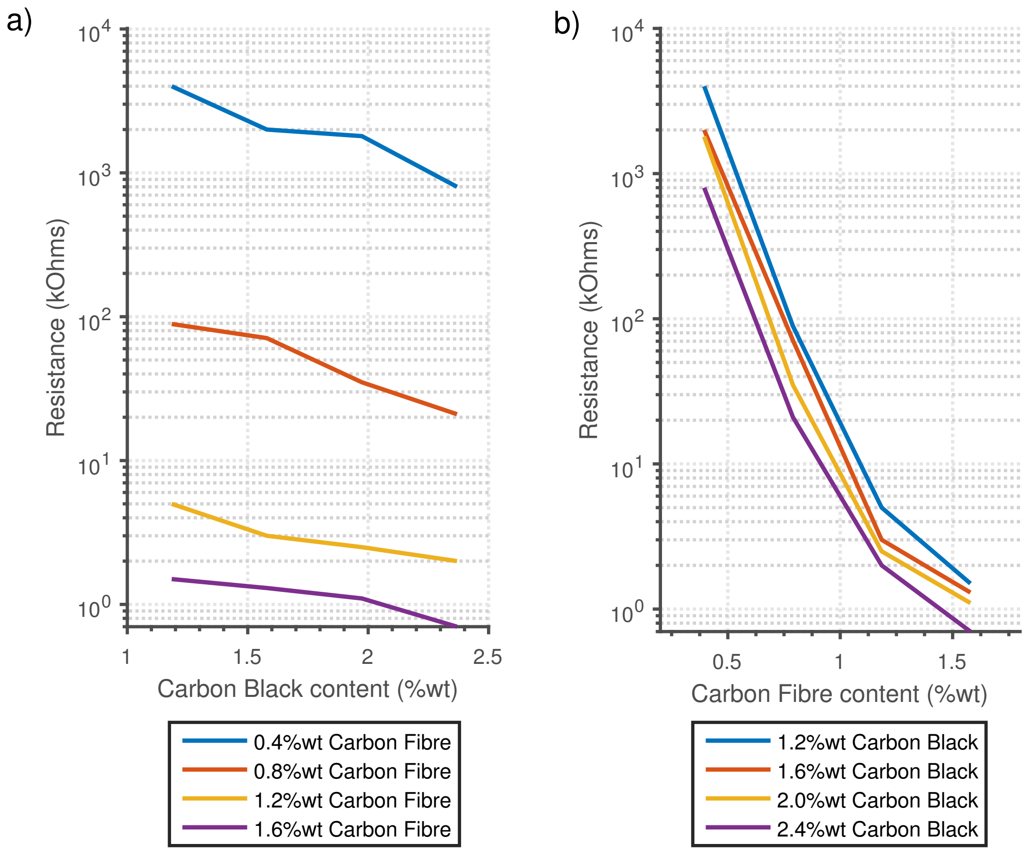

Figure 4.13 Base (un-strained) resistance of 16 different samples of the conductive silicone sensor with varying CB content (a) and CF content (b) showing how the inclusion of these conductive elements affects conductivity.

'unstrained' resistance of a sensor of a given dimensions[2]. The results show that although the CB is required to make the sensor conductive, further increase of CB does not significantly increase the conductivity of the sensor. In comparison, the addition of CF significantly increase the conductivity of the sensor. However, there is a limit on the weight percentage of CF which can be added to the silicon composite without loosing elasticity of the sensor and preventing the sensor from curing. Due to this there is a limit on the achievable conductivity of the sensor.

A key characteristic of a strain sensor is the gauge factor; the ratio of relative change in electrical resistance to the mechanical strain. The greater the gauge factor the greater the sensitivity to strain. The gauge factor of these soft silicone sensing materials is dependant on the sensitivity to strain. The gauge factor for the silicon sensors was determined experimen-

[2]Sensor dimensions: 25 mm x 10 mm x 4mm, using EcoFlex 00-20 Silicone

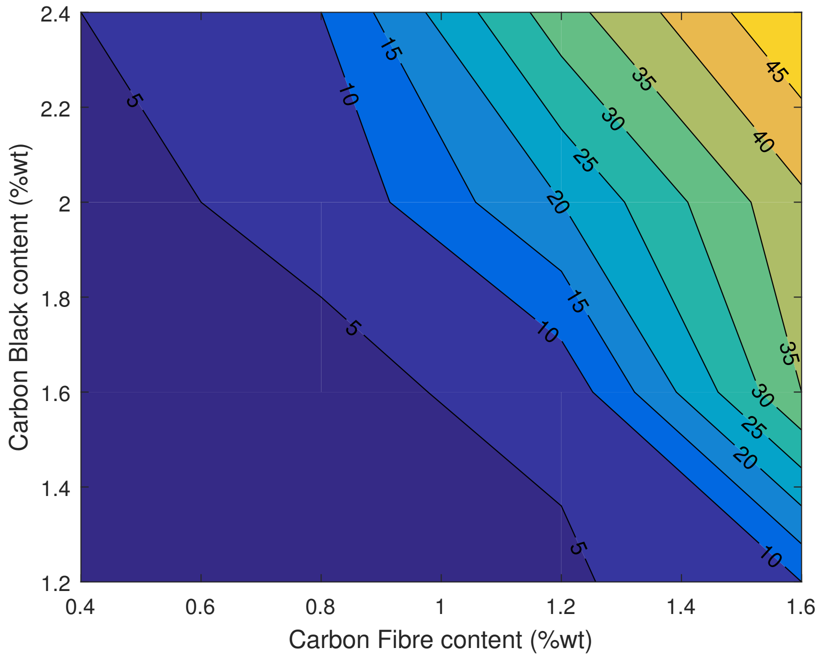

Figure 4.14 Variation in gauge factor of the conductive silicon material of sensors with varying composition of CB and CF. The gauge factor is given on the contour lines of the plot.

tally by measuring the resistance at 0% strain and also at 100% for a given volume of sensor and using the ratio between these values to determine the gauge factor. Fig. 4.14 shows the change in gauge factor with material composition. The higher the concentration of CB and CF increases the gauge factor significantly, however increasing the CF content has a more significant effect on increasing the gauge factor and hence increasing the sensitivity of the sensor.

4.3.3 Case Study: Wearable Sensor

Obtaining accurate information about a persons activity and behaviour is recognised as one of the key challenges in pervasive computing and has innumerable applications including medicine, rehabilitation, entertainment and tactical scenarios [156]. The development of wearable sensors has enabled human activity to be monitored facilitated by the use of low power, low cost wireless hardware [157]. The monitoring of physiological signals such as heart rate, respiration rate and muscle behaviour is an area in which wearable sensors can make considerable impact; these sensing devices are gaining significant attention for the scientific community and in industry [158]. To achieve this the sensors need to be able to perform physiological measurements without impeding movement or being obtrusive.

Existing sensors display problems with longevity, repeatability and rigidity. As such, there is a need for multi-functional wearable sensors which are compact, lightweight, do not restrict daily behaviour and which can detect a range of physiological stimuli [159].

Currently many wearable sensing techniques use traditional 'rigid' sensing materials and only detect one specific physiological stimuli. Many are uncomfortable for the users and restrict or affect their typical movements. Soft sensors, sensors with a mechanical impedance close to that of animal tissue, provide a significant opportunity in comparison to rigid wearable as the mechanical impedance is matched to that of the user. The sensors do not restrict natural kinematics, enabling long term comfortable monitoring of the wearer. There has been increasing development of soft sensing for wearable devices as areas such as ubiquitous computing gain increasing traction. However, many existing soft sensors lack the robustness, ease of integration (often full body suits are required) and the flexibility to be used to measure a range of different stimuli [160].

This case study presents a method of manufacturing a soft sensor material which detects deformation. This sensor can be used for on-body sensing to detect a range of different physiological stimuli. Uniquely, the sensor allows both rapid production and also the ability to easily change the sensor morphology. The sensor can be used to detect deformations of different magnitudes and profiles with minimal additional circuitry or amplification required. The sensor can undergo significant strains, over 200%, and has a low mechanical impedance so it does not impede movement, while also displaying sensitivity in the sensor output. The sensor can sense both changes in pressure and strain within the sensing material enabling it to be used to measure on body deformations of different magnitudes, frequencies and mechanisms.

To demonstrate the capability of the material, an insole pressure sensor to detect gait and the ground reaction force has been developed. This insole sensor highlights the ability of the sensor material to detect forces normal to the sensing material. A lateral strain sensing wireless wearable device has also been developed which allows the breathing rate, heart rate and also calf muscle deformation to be measured by wearing the device at different positions on the body. The results from the strain sensor enable the direction of walk and the gait types to be identified. The range of stimuli detected demonstrates the multifunctionality of the sensor. In addition the sensor provides unrestricted movement by the wearer, is waterproofed, easily fabricated and can be worn over clothes. Fig. 4.15 summarises the different wearable sensors which are developed to demonstrate the capabilities of the soft sensor developed.

Motivation for Soft Physiological Sensing

The ability to accurately and precisely measure physiological signals on the body has many applications including sports science, health care and medicine. The key physiological signals include breathing rate, heart rate, gait and muscle deformation, all of which can be detected and monitored by sensors which can detect changes in deformation.

Breathing rate sensors are used widely for medical applications, particularly the identification of heart disease [161], and sports analysis [162, 163]. Many of these sensors are bulky, highly rigid such that they can impede movement and provide low detection sensitivity [164], as such the development of a breathing rate sensor which is highly flexible, can be worn over clothes unobtrusively would increase usability.

Typically heart rate is often measured using a highly rigid finger clip which uses the absorbance of light as the blood pulses through a finger to detect heart rate [165]. It may be necessary for heart rate sensors to be worn for long extended periods of time. By developing a softer, flexible alternative this has significant potential as this could provide the user with more comfort when wearing. These has been some limited development of soft sensors for heart rate monitoring [166]. These could be particularly useful when the wearer is an infant.

Gait analysis is of interest to researchers and clinicians as it allows the identification of the gait and kinematic parameters of gait which also provide a quantitative analysis of muscular-skeletal functions [167]. Such sensors are used in sports to analyse and optimise performance [168], for rehabilitation, to monitor the healing of patients and for health diagnosis to determine muscular-skeletal problems and diseases [169]. Being able to precisely understand the force applied to specific foot locations has many applications. There are existing force sensors used to measure ground reaction forces (GRF) when walking by including sensors in an instrumented shoe. Determining muscle activity and deformation can also be used to determine gait characteristics particularly by considering the deformation of the calf muscle. Additionally, sensors could be used to detect muscle activity such as grasping or lifting [170], enabling the identification of activity recognition.

There are few sensors which allow multiple physiological signals to be measured using the same material and approach, which makes the material and approach described innovative.

Present Work on Physiological Monitoring

There are a wide variety of different methods for measuring physiological signals. The two main approaches involve measuring deformation induced by the physical changes in the body or measuring positional change using tri-axial accelerometers and gyroscope based systems [171–173]. The accelerometer based systems are typically rigid devices and multiple sensors are required to provide meaningful results. Additionally, such methods can make it difficult to determine particular muscle behaviour or to isolate physiological signals.

Some semi-flexible approaches have been developed including Magnetic Field Sensors development on films [174], flexible PCB based sensors [175] and optical sensors [176]. These are only semi-flexible and often have to be in direct contact with the skin whilst the range of magnitudes of deformation which can be measured is limited. Softer sensors developed include a graphene based strain sensors, which have a limited range of strain [177], and a nanowire based strain and pressure sensor [178]. There has been some limited initial investigation of such sensors for wearable sensing applications.

Intelligent textiles have been developed which have the capacity to measure physiological parameters of the human body such as knitted strain sensing material [179, 180]. There are a number of systems which can be integrated into textiles, to create sensing 'suits' for lower limb movement detection [181] or integrating conductive thermoplastic strain sensors into fabrics [182]. These have the advantage of being highly flexible, however they require the wearing of additional tight clothing and sense only strain. Others wearable sensors rely on the integration of electrodes in to the fabric [183] which limits the flexibility. These types of sensors do not have a range of sensitivity which would be suitable for measuring multiple physiological indicators.

In summary there are few multi-functional anisotropic strain and pressure based human wearable sensors which have sufficient sensitivity to detect a range of physiological stimuli. Additionally, there are a limited number of soft sensors which can undergo sufficient strain such that it does not restrict the movement of the wearer and can be worn over clothes. By obtaining all range of physiological information in a non-invasive manner enables the identification of a range of activities being undertaken by the wearer.

In the following section, the physical embodiment and implementation of the sensor is changed to utilise the pressure or strain sensitivity to detect a range of different stimuli.

Force Detecting Gait Sensor

The gait sensor developed is an insole for a shoe which measures the normal pressure or ground reaction force exerted on the sole of the foot. A sheet of the conductive silicone material was produced, and was then cut to the required size and shaped to form the insole. Electrodes can then be attached to the 2D sensor at any point such that the pressure applied to these sections of the sensor can be determined. In this case, the electrodes have been applied such that the pressure distribution under the toe, ball of the foot and heel can be measured, with placement of the electrodes and the three regions measured shown in Fig. 4.16.

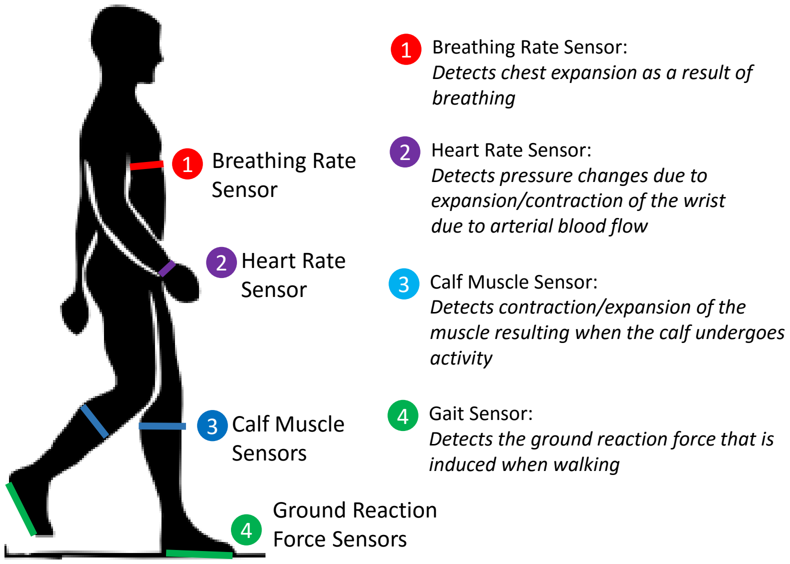

Figure 4.15 Summary of the different wearable sensors developed and the locations they should be worn to enable different stimuli to be measured.

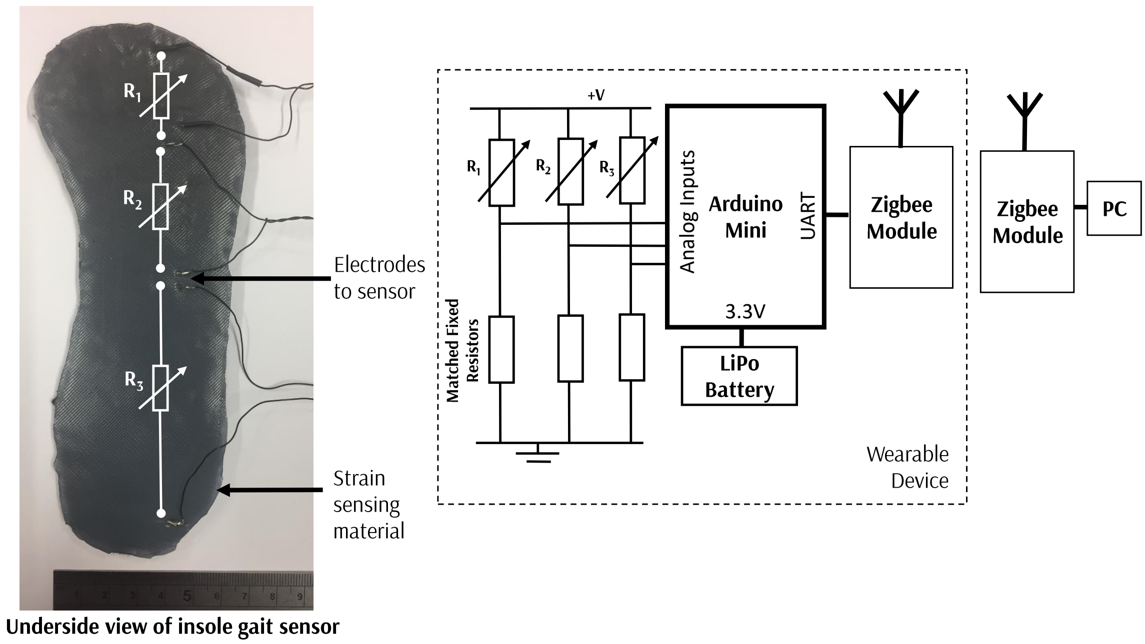

Figure 4.16 Underside of the soft silicone gait sensor developed showing the attachment to the electrodes (left) and the associated circuitry for the system, showing the interface between the sensor and the microcontroller and the wireless system (right).

The variable resistance is measured by the three pairs of electrodes with potential dividers used to provide an analogue input to the micro controller. The micro controller is powered by a Lithium Polymer battery, and a Zigbee Module is used to provide wireless communication enabling the device to be worn entirely on person. The sensors are sampled at 20Hz, with some onboard averaging performed, after which the data is transmitted to the base unit, sending packets of data in bursts with accompanying time stamps. The sensor data is averaged and filtered, with an IIR (Infinite-Impulse Response) filter implemented with a cut-off frequency of 2Hz to eliminate high frequency noise. Although Zigbee is used initially, should this be developed further, a more energy efficient wireless protocol would be used.

Strain Sensor: Breathing rate, Heart rate and Calf Sensor

A universal wearable sensor to allow the detection of breathing rate, heart rate and calf muscle behaviour has been developed using a similar system to that for the gait sensor, and is shown in Fig. 4.17. A small section of sensing material is attached to a rubber strap with electrodes added to interface with the micro controller. To detect breathing rate the wearable sensor can be worn around the chest over clothing, around the wrist to allow detection of heart rate and around the calf (again, worn over clothing) to allow the changes in profile of the calf muscle to be detected. A similar architecture to the gait sensor is used, with a wearable device developed with Zigbee wireless capability.

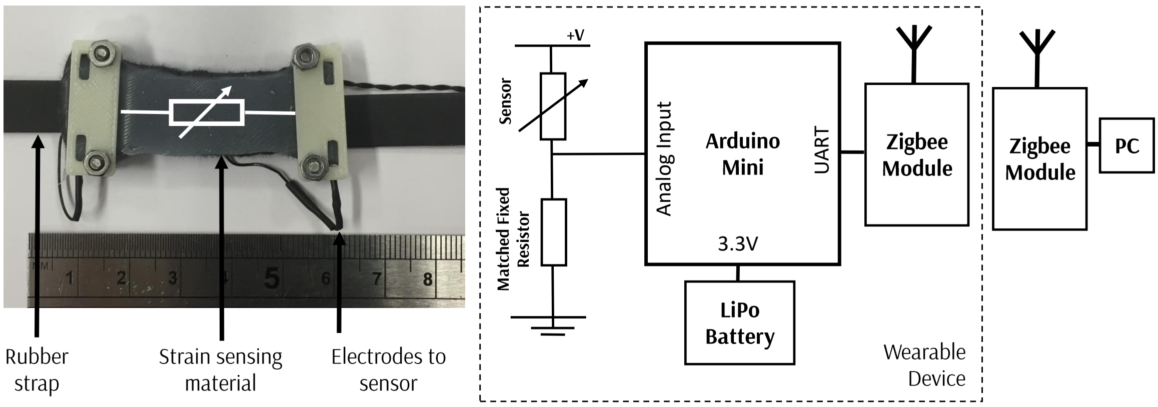

Figure 4.17 Strain sensing sensor (left) and the overview of the wearable sensing system developed showing the interface between the sensor and the microcontroller (right).

4.3.4 Results

Gait Sensor

Experimental Methods The gait sensor developed was placed inside the shoe with the wireless unit attached to the side of the shoe. Results were obtained from the sensor while two

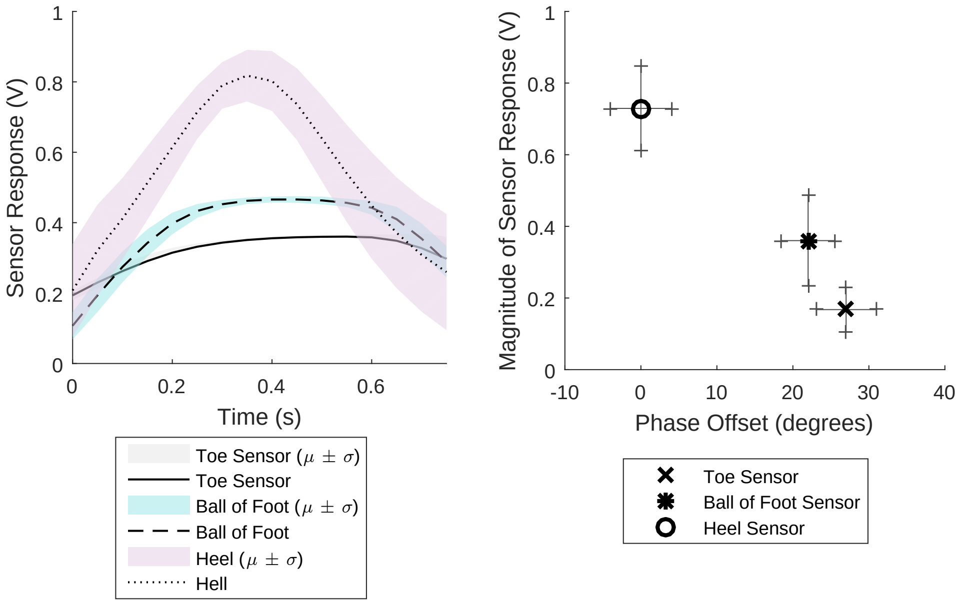

Figure 4.18 Results from the gait sensor when walking. (Left) Average response from the sensor for a single period when walking for a 5 minute period for the three sensors at constant walking rate. (Right) Plot of magnitude of response of the sensor and phase difference between the responses or a 5 minute period of walking at constant walking rate.

different users were walking each for a five minute period at a constant rate on a flat surface. In addition, the device was tested when walking, running and hopping for an approximately 5 minute period on a flat environment by one user to allow the accuracy of steps to be determined. To allow comparison to existing calibrated devices, an accelerometer based step counter device was also worn.

Experimental Results The response from the three sensors on the gait sensor when worn as an insole of a shoe is shown in Fig. 4.18 which shows the averaged results for a 2 minute period for a constant walking rate. This demonstrates that there is time delay between pressure applied to the different areas of the sensor. The pressure applied to the heel sensor is significantly larger than that of the other sensors, and the force profile is much sharper than that experienced by the toe and ball of foot sensor. This provides information as to the gait characteristics: the force profile of the step, the magnitude of the pressure on the specific location of the sensor and the time different between the pressure being applied on each part of the sensor. Fig. 4.18 b) shows the phase, magnitude relationship between the three different sensors demonstrating how the the phase and magnitude varies.

By placing electrodes in the sensor at particular positions the pressure on a particular area of the sensor can be isolated, allowing the response from different regions of the sensor

Table 4.3 Percentage error of the number of steps taken when using the soft gait sensor for different gait types.

	Percentage Error		
Number of Steps	**Walking**	**Running**	**Hopping**
200	0%	0%	0%
500	0.5%	1%	0%
750	1%	2.5%	2%

to be determined. This can be easily customised by placing the electrodes in different places on the sensing sheet. Thus to measure different areas of pressure or deformation, the sensors do not need to be altered but the electrode placement can be varied.

To determine the accuracy of the sensor to measure the number of steps taken, the percentage error when a number of steps is taken has been determined for different gaits: walking, running and hopping. Table 4.3, demonstrates that for fewer than 500 steps the accuracy is high, especially for walking gaits. The accuracy is lowest for running gaits, where the sensor response is noisier. Typical tri-axial accelerometer based step have a 5% accuracy [184, 185], therefore, this gait sensor is comparable or better than traditional 'hard' methods of sensing movement. The number of steps taken was calculated by filtering and performing peak detection across all three of the sensor streams, and requiring agreement from two of the three three sensors that the 'step' has taken place. This approach has lead to the high accuracy in step detection.

Breathing Rate Sensor

Experimental Methods To experimentally test the sensor, the device was worn around the upper chest over clothes when walking, sitting and running such that a range of different breathing rates and magnitudes of chest expansion were experienced. Over 15 minutes of data was obtained from each ofthe two users. The sensor data was windowed over a twenty second period, and the average time between peaks used to determine the breathing rate.

Experimental Results A typical sensor response is shown in Fig. 4.19, averaged over 4 minutes at constant breathing rate. This shows that there is a clear periodic signal which reflects the breathing rate; the magnitude of the response is indicative of the magnitude of the chest expansion. This response can be gained even when worn over clothing.

To test the sensing system, the results obtained experimentally have been compared to the results from a commercial breathing rate sensor (the ground truth) which has a stated accuracy of 1 breath per minute, with the results shown in Fig. 4.19. The device was tested

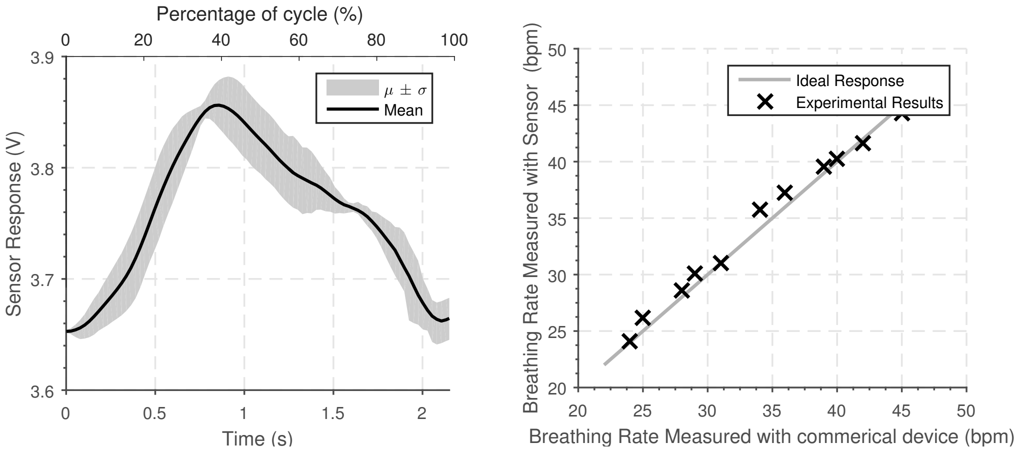

Figure 4.19 (Left) Average sensor response for the sensor when worn around the chest to measure breathing rate for a two minute period. (Right) Experimentally measured breathing rate measured over a thirty second period and the breathing rate determined by a commercial measurement system (iCare).

for eight 1 minute periods and worn when in various different situations (including walking, working and sitting) with two different users. The results demonstrate that the senor can be used to determine the breathing rate and the magnitude of the chest expansion.

Heart Rate Monitor

Experimental Methods To test the device, the device was worn on the wrist sufficiently tight such that it there is no gap between the sensor and the wrist. The sensor device was worn when sitting, walking, running such that different heart rates were experienced, and the device was used in typical conditions opposed to a closely controlled environment. Two different users were tested with the device. The rolling average time between peaks over a 20 second period was used to determine the heart beat.

Experimental Results The same sensors can be worn around the wrist to enable the heart rate to be measured. The typical sensor response when the device is worn is shown in Fig 4.20 a).

The accuracy of the heart rate measured using the device was tested by measuring heart rate over a 20 second period using both the sensing device and commercial heart rate device, with a given accuracy of 1 beat per minute. The results were taken when undergoing different activities, again including walking, sitting, working and over a range of different heart rates. The results showing the agreement between the calibrated commercial device and the wearable sensor developed are shown in Fig. 4.20 b). The heart rate determined by the

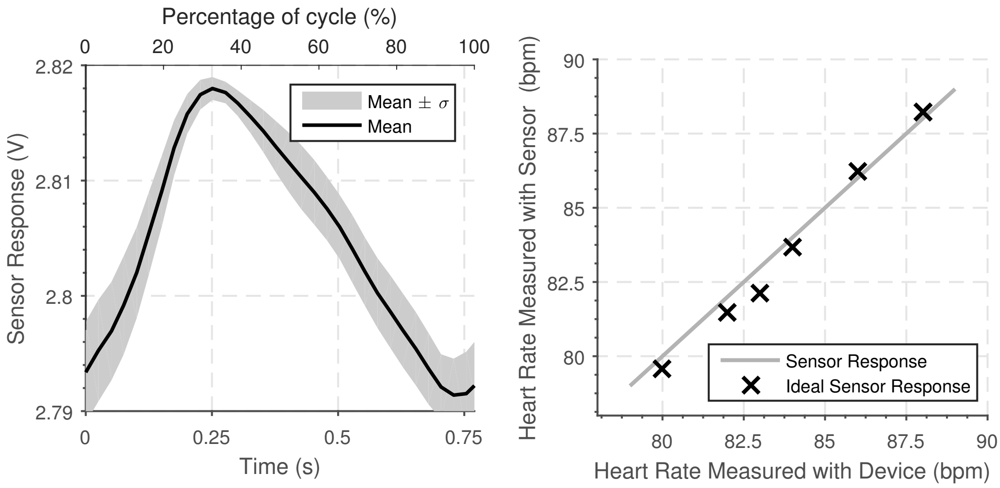

Figure 4.20 Left) Average time series of the sensor response when the sensor is worn around the wrist for one period of heart beat when measured over a two minute period. Right) Experimentally measured heart rate measured over a thirty second period and the heart rate determined by a commercial device (Polar M400).

sensing device shows a strong agreement with the commercial device, with the maximum different of 1 beat per minute.

These results indicate that is possible to use this simple method of sensor integration to measure heart rate in a non-invasive method and using a soft, non-rigid sensor.

Calf Sensors

Experimental Methods To test the calf sensor, one of the strain sensors were worn on each calf muscle, placed over the location on the calf which experiences maximum deformation. The device was tested when walking, running and hopping on flat ground for a 5 minute period. The device was also worn when walking in different direction, by recording the response when walking in a circle of constant radius. The device was tested on two users.

Experimental Results A sensor can be worn on each calf muscle to allow identification of different gait types and also to give an indication of the direction of movement. The sensor output when walking, running and hopping forwards are shown in Fig. 4.21. There is a clear increase in sensor output from the sensors on the two legs when walking and running with the two sensors response out of phase as the calf muscles in each leg alternatively engages. The frequency of response when running is much greater and the peak-to-peak magnitude of the sensor response is much larger. When hopping the two sensors response are in phase and there is far more variability in the magnitude of the response.

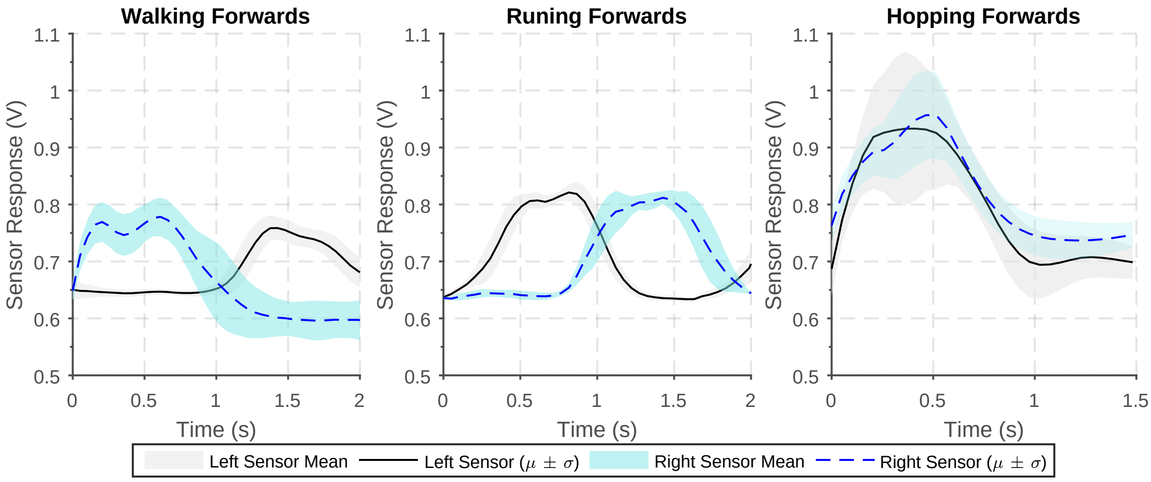

Figure 4.21 Average sensor output for a single period from two calf strain sensors worn when undertaking various gait types: a) walking forwards in a straight line, b) running forwards, c) hopping forwards.

Using these sensors to determine the peak-to-peak signal response and the frequency of the gait allows different gait types to be determined. Fig. 4.23 shows the magnitude of the response plotted against frequency of the gait for three different gait patterns. There is clear clustering between the three gait types. Walking has the lowest frequency and magnitude, running has a higher magnitude of sensor response and frequency and finally, hopping has the largest magnitude of response. If the phase difference between the two response was also considered this would also aid identification between the gait types.

By having two calf muscle sensors, it is possible to get an indication of the direction of movement as the expansion and contraction behaviour of the two calf muscles varies not walking directly forwards. The magnitude of the average of the peak-to-peak sensor response for the two sensors has been determined for 10 second periods, for 30 different cases of walking left, right and forwards. The ratio of the average magnitude between the right and the left sensor is then found. When walking forwards the sensor response is equal, such that the ratio is approximately unity. When walking right, the left calf muscle activation is greater such that the ratio is greater than one, and conversely when walking left, the right calf muscle is lower such that the ratio is less than one. These results are shown in Fig. 4.23. There is no overlap between the significant range of the sensor responses, demonstrating that using this method and the sensors it is possible to get an indication of the direction of walk.

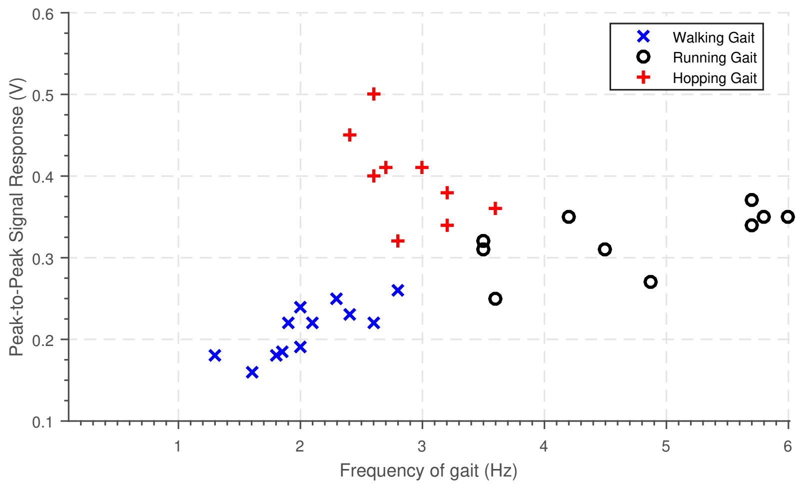

Figure 4.22 Plot of frequency of gait and the peak-to-peak magnitude of response determined from the calf sensors when undergoing various gait types.

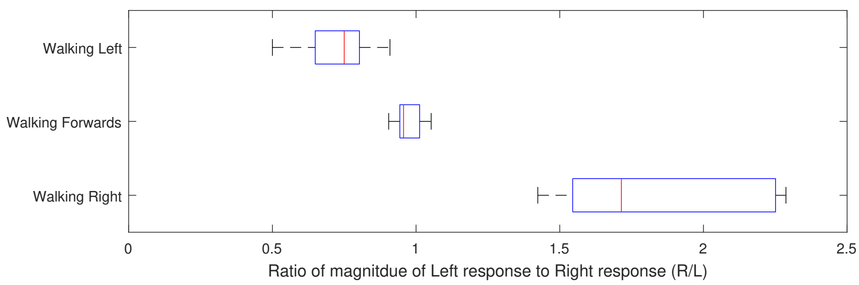

Figure 4.23 Ratio of the magntiude of the calf response for the Right calf muscle sensor to the left calf muscle sensor for different directions of walk. 20 results were recorded for each direction of movement.

4.3.5 Wearable Soft Sensors: Discussion

A sensing material have been developed by including conductive particles into a non-conductive silicone matrix. This allows the development of sensors in sheets that can be easily cut or formed into the required shape, where the embodiment determines the response. The sensitivity of the sensor is comparable to existing sensors and can be tuned by varying the carbon fibre and carbon powder content added to the silicone. The sensor is reactive to both normal pressure and strain, allowing it to be used to develop wearable sensors which detect both of these stimuli.

The normal pressure sensing capabilities of the sensing material have been demonstrated through the development of the gait sensor. This sensor provides an indication of the ground reaction force exerted at different locations on the foot to be determined. The gait sensor also enables the approximate frequency, or number of steps taken with comparable accuracy to existing methods and devices. A wearable strain sensor has been developed which can be used to measure breathing rate, heart rate and calf muscle expansion and contraction. The sensor developed is highly universal such that the same experimental setup can be used to detect these three indicators which has a range of different magnitudes and frequencies of strain to be measured by the sensor. This demonstrates the high versatility of the sensor. By using pairs of sensors on calf muscles it is possible to provide both an indication of the direction of movement and also the type of gait. Initial indications have shown how the sensors can be used to make indications of activities undergo, with gait type and direction of walking already identifiable. By combining all these physiological sensors response, it would be possible to build an overall picture of activity being undertaken. This research has aimed to extract design principles for the development of soft, wearable sensors for different applications.

In summary, three prototypes of wearable soft sensors have been developed using the same material by varying the embodiment. These are easy to fabricate and there is much flexibility in the placement of electrodes. The sensors are unobtrusive in comparison with many existing sensors. Because of the ease of integration and the potential for low cost development, this approach has the potential to be used for other strain sensing applications. There is also significant potential for soft sensors to be used for on-line health monitoring applications. In practice, there many other fields of use where similar soft sensors have the potential to make an impact, examples include automotive and aircraft control, waste water treatment plants and industrial scale distillation [13, 186].

4.4 Discussion & Conclusions

In this chapter, design approaches for developing materials have been presented. Specifically, the advantages of using an embodied approach to material development for soft robotics has been demonstrated. The overall goal of using materials where the physical properties or embodiment contributes to both the sensing and functionality requires an approach where the sensing and active components are designed in tandem. This has been demonstrated through the development of CHMA. Additionally, the case-study on wearable sensors has demonstrated how the physical embodiment or implementation changes the perception and sensitivity of the sensor.

CHMA provides integrated sensing, stiffness control and tack force control. The embodied nature provides sensing and active control of material properties, however, both these properties are dependant on the temperature of the material and thus can not be designed in isolation. Although the embodiment has enabled the material to contribute to both the perception and output behaviour, there is a trade-off in performance of the perception and behavioural capabilities. Increased temperature reduces the sensitivity of the sensor whilst increasing tack force. Thus, whilst embodiment of materials has been shown to have significant advantages, the understanding and utilisation of embodied behaviours is complex.

Chapter 5

Hybrid Mechanical Design for Behavioural Diversity[1]

The range of behavioural outputs of soft robots can be limited in terms of behavioural diversity and adaptability to the environment. To address this limitation, a concept of soft-rigid hybrid robot has been proposed where a combination of soft-rigid materials are used to develop complex mechanical systems that show anisotropic stiffness. This chapter investigates the use of mechanical design to aid and extend the behavioural range, exploiting the passive dynamics of a system. This work seeks to demonstrate Hypothesis 2, validating that environmentally adaptive behaviours can be achieved through soft-rigid hybrid systems.

The key novel research contribution of this work is the exploitation of the anisotropic stiffness of complex 3D printed soft-rigid hybrid structures. This is the demonstrated through development of a anthropomorphic skeleton hand which can show different playing styles.

5.1 Soft-Rigid Hybrid Manipulators

The ability for robots to perform complex manipulation based interactions with the environment is key for many applications as robots are increasingly required to work in complex, non-deterministic human environments [13, 187]. Soft robotic manipulators offer compliance

[1]This chapter presents work developed collaboratively work with my supervisor F. Iida. I have initiated the problem statement, framework, prepared the figures, and written the paper. F. Iida helped with formulating and revising the paper. The peer reviewed accepted paper, which was awarded the IET Innovation Award is:

- Hughes, Josie, and Fumiya Iida. "3D Printed Sensorized Soft Robotic Manipulator Design." *Conference Towards Autonomous Robotic Systems. Springer, Cham, 2017.*
- Hughes, Josie, Maiolino, Perla and Iida, Fumiya. "An anthropomorphic soft skeleton hand exploiting conditional models for piano playing." Science Robotics, 2018

and adaptability, enabling safer, softer interactions with the environment which increases the ability of the manipulator to deal with uncertainty in the environment. There are many challenges associated with the development of soft robotics, one of which is development of manipulators that are easy to manufacture, control and customise whilst still enabling reliability and repeatability in movement [42].

In this chapter, we focus on the concept of soft-rigid hybrid mechanical systems. Using combined soft and rigid structures to achieve systems with inherent stiffness and passive behaviours. This allows the system to utilise environmental interactions to achieve complex behaviours with minimal external control requirements.

In particular, this chapter contains two main focuses and implementations of hybrid manipulation systems:

- **Multi-Material 3D Printed Anthropomorphic Hand.** By utilising the inherent passive-dynamics of complex mechanical systems, significant behavioural diversity can be achieved with minimal control. A novel framework for achieving behavioural diversity by using passive dynamics of the system is proposed, which is termed 'Conditional Stiffness.' Using this approach a skeleton hand is used to achieve piano playing behaviours.

- **Hybrid 3D Printed Fingers.** Using standard 3D printing techniques, flexible joints have been created which can be controlled using simple actuation to achieve complex behaviours. Sensors are included using the differential morphology presented in Chapter 3.

In both of these systems hybrid stiffness systems are created with have joints which display anisotropic stiffness, such that the passive dynamics are leveraged to allow complex behaviours.

5.2 Anthropomorphic Soft Hand Skeleton Exploiting Conditional Stiffness

There is increasing interest in the study of nature to provide bio-inspiration for the development of robots with physical and cognitive abilities comparable to biological systems [8, 42]. Animals can perform highly complex and varied interactions with a rapidly evolving, information-rich environment [33]. Previous work on biologically inspired robotics has demonstrated that the complexity in animals' behaviour results from the reciprocal coupling between the controller (brain), the body and its interactions with the environment [11, 188].

It has been demonstrated that complex behaviour does not result from the controller or brain alone, but from a distributed complexity across the entire system including the mechanical body [189].

Mechanical design of systems plays a considerable role in the intelligent functioning of animals and machines, which can be observed in passivity-based robot control [77]. Passivity can be used to achieve a pendulum-like swing of legs for locomotion, where no explicit active control is required to achieve stable bipedal walking [78]. High functioning passively-controlled robots have achieved a range of different behaviours such as robotic swimming, flying and manipulation [79]. Smart mechanical design enables systems to show exquisite and complex behaviours that are self-stabilizing and energetically efficient at reduced computation cost [80].

Achieving functional behaviours through passivity is crucial and necessary for biological systems to survive in the natural environment, however, as a design method for robotic systems, it is known to intrinsically restrict the range of behaviour [81]. Underactuated control provides a compromise; it can expand the range of behaviours by introducing a coupling between passive mechanics and limited joint actuation [23, 24]. This creates behaviours which are highly environmentally dependant and sensitive to changes. There is limited behavioural diversity, typically with a one-to-one mapping between environment and behaviour [38, 82]. This limitation can particularly be seen in robotic manipulation and hand design where passive control and underactuated mechanical design allows only a single [83, 84], or at best, a limited number of behaviours to be achieved [85, 86]. Leveraging the intelligence of passive mechanical bodies is an exciting method for generating a range of behaviours in variable environments.

Achieving behavioural diversity in robotics while utilising passive dynamic remains a fundamental challenge. There have been several recent approaches to address this challenge, as discussed in Chapter 2. Using variable stiffness mechanics allows limited utilisation of passive behaviours in varying environments [88, 190], however leads to highly complex actuation systems [89, 191–193]. A second approach centres on the use of materials to alter or adapt the behaviour [75], the concept also introduced in Chapter 4. The increased compliance of the soft materials provides more flexibility, enabling a wider variety of mechanical dynamics. However, the inherent flexibility of soft materials can result in behaviours that are ill-defined and highly variable. Therefore, a key challenge is controlling the mechanical flexibility when using softer materials [93, 194].

Soft robots can use variable-stiffness materials to achieve a range of movements and to modulate interactions with the environment [16]. This allows the synergy between soft bodies and actuation methods to be utilised. This allows the movement of soft bodies to be

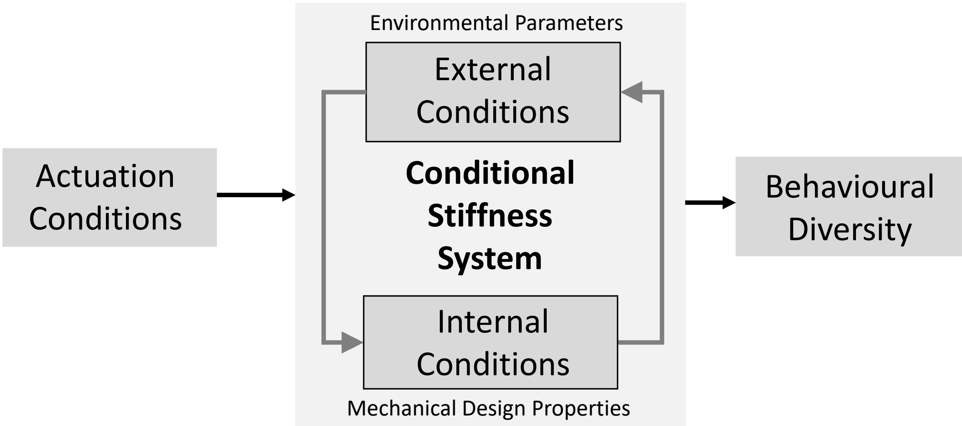

Figure 5.1 Representation of Conditional Stiffness. Actuation conditions externally trigger Conditional Stiffness which is dependent on the coupling of external conditions (environmental parameters) and the internal conditions (the mechanical design and materials). Actuation, external and internal conditions enable the creation of systems with behavioural diversity.

limited or constrained, in turn reducing the requirement for complex additional actuation sources. In particular, work on adaptive synergies [95, 97] and tendon routing [94] shows significant breakthroughs and developments with respect to robotic manipulators. Although these approaches provide methods for exploiting mechanical passive dynamics, they do not provide a framework for significantly scaling complexity and behavioural diversity.

An alternative approach, which is demonstrated in this work, is the use of hybrid soft-rigid mechanical structures, in which the stiffness of the structures can be set heterogeneously across the body. By taking advantage of state-of-the-art multi-material 3D printing techniques, complex hybrid mechanical structures can be constructed [195–197]. This heterogeneity of stiffness can be exploited to achieve a variety of mechanical dynamics necessary for different motion requirements, but this is possible only when internal and external conditions are set appropriately (Fig. 5.1). A human hand, for example, can be used in many ways, such as a strong fist hitting a rigid wall or a soft finger touching smooth surface. The variability in capabilities and task which can be performed is dependent on the mechanical design, actuation varying the mechanics and the environmental conditions.

To explore this overall concept, this work investigates the concept of Conditional Stiffness: the interactions of a single structure (i.e. an anthropomorphic robotic skeleton) showing varying passive dynamics depending on the conditions set by actuation and the environment. The mechanical complexity of structures plays the crucial roles, because, the greater the variety of mechanical dynamics of a robot, the greater the variety of Conditional Stiffness which can be determined by actuators and environment. The mechanical behaviour is bounded by the physical design and geometry of the system, for example, the joint design and the material properties. The environment and surroundings impose conditions on the complex mechanical system contributing to the behaviour [70, 96, 198]. This approach to designing and controlling a mechanical body leads to richer behavioural diversity in comparison to the previously discussed passivity-based and soft robotic approaches where the diversity of behaviour originates from the complexity of the mechanical design.

To validate the proposed approach, a case study of a dexterous robotic hand playing a piano is presented. The sound produced by the piano emerges through the coupling between the biomechanics and neuromuscular dynamic of the pianist (mechanical impedance of the finger) and the dynamics of the piano itself [199]. Piano playing thus relies on the interaction between the environment and the mechanics of the players' hand. Piano playing is a challenging task for humans, with nuanced and subtle ranges of behaviour required. Piano playing robotics research dates back to the 1980s [200], with many examples since focusing on both the mechanical and algorithm development [201–203]. Most of the robots utilise rigid finger joints with no compliance such that high accuracy of finger positioning could be achieved. Piano playing is an exacting artform which requires both highly precise rapid movements and softer more adaptive playing; this is an area which has not been explored thoroughly in previous work. Achieving expressive and varied piano playing poses a rigorous test for the Conditional Stiffness Control framework and robotics in general.

5.2.1 Designing Internal Conditions (Anthropomorphic Soft-Rigid Hybrid Skeleton Hand Skeleton)

The process of designing and building Conditional Stiffness systems to show a desired output behaviour requires a different approach to that of building conventional, actuated rigid systems. Conditional Stiffness systems exploit the complex reciprocal relationship between environment and mechanics, making the design and modelling challenging. Biological systems show a diverse range of complex joints, including highly mobile joints such as the shoulder and hand joints, which provide an excellent starting point for the exploration of Conditional Stiffness [204]. The combination of bone-bone interactions and ligaments creates complex passive behaviour [205, 206]. Unlike pin joints typically used in conventional rigid robotic systems, these structures can exhibit anisotropic behaviours depending on actuation and external conditions. For this piano playing case study, an anthropomorphic hand is developed that utilises these complex interactions. The design of internal conditions focuses on the joint design and material properties of the hand skeleton.

Fig. 5.2A shows the model of the anthropomorphic hand skeleton used which has been directly inspired by human anatomy; bones and ligaments are placed as they are in nature [207]. Every finger joint is encapsulated by ligaments constraining the movement and stiffness of the joint, allowing the two bones to move independently and interact together. Unlike many other anthropomorphic robotic hands this allows both osteokinematics, observable movement of bone shafts, and also anthrokinematics, movements at joint surfaces which cannot be directly observed and are considered to be passive [208]. By 3D printing this model (Fig. 5.2B) with varying ligament stiffness, the anisotropic properties of the finger can be varied. By giving joint ligaments with sufficient compliance, the anisotropic stiffness allows for complex behaviours influenced by external actuation and interaction with the environment.

Fig. 5.2C shows the experimentally determined stiffness of a 3D printed index finger (from the distal phalange to the metacarpus) in different directions when force is applied perpendicular to the finger-tip at varying orientations of the finger. A static force was applied to the finger-tip whilst the metacarpus was fixed, allowing the overall stiffness behaviour to be measured. Three different materials were used (Young's Modulus E_J 1, 2.5, and 50MPa) when printing with the ligaments to show a range of stiffness. Overall, due to the geometry of the bones and the interactions between the bones and the ligaments, the stiffness is greater in the ventral-dorsal direction compared to the lateral direction. In particular, lower compliance is observed in the horizontal plane where lateral movement can lead to a 'jamming' between the two bones limiting the compliance of the joint in that direction [209]. The stiffness is not completely symmetrical around the vertical axis, reflecting the asymmetric bone-bone interaction when the heads of the bones interact.

Although the stiffness deformation landscape of a single finger in only one axis is demonstrated, the finger stiffness shows similarly diverse and complex behaviours when forces in other rotational axes or translational degrees of freedom are applied. Different behaviours can be generated by exploiting the anisotropic nature of this complex structure. A similar design strategy can be applied to the other parts of the complex hand skeleton. The thumb joint is more complex and allows similar exploitation of anisotropic stiffness, with a greater number of ligaments contributing to the anisotropy and allowing a much greater range of anthrokinematic behaviour.

The ligaments in this hand CAD model are grouped into three types (Fig. 5.2): those that contribute to finger joint stiffness, span stiffness and thumb abduction/adduction stiffness. The material properties of these ligaments are denoted by E_J, E_S, and E_T respectively. These stiffness groups influence the overall behaviours of the passive hand; the material property of these ligaments controls the Conditional Stiffness of these joints. As demonstrated in

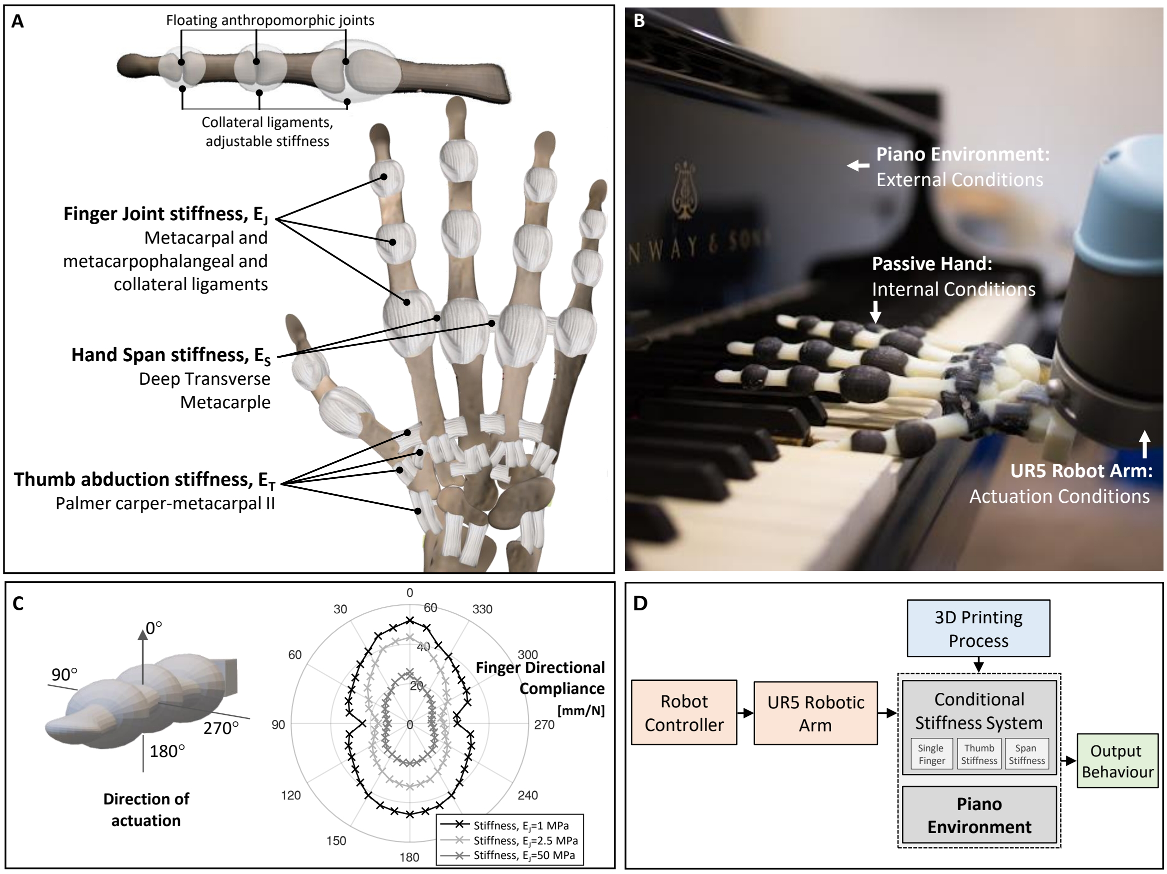

Figure 5.2 Demonstration of Conditional Stiffness. (A) Anthromorphic model of the hand used showing three groups of ligaments which influence the three behavior primatives investigated. (B) The 3D-printed hand Conditional Stiffness system attached to the UR5 robot arm which provides the external actuation and the piano environment used. (C) The directional compliance of a single fingers printed with varying ligament stiffnesses. (D) System block diagram of the method used to achieve the Conditional Stiffness system and thus achieve varying output behavior.

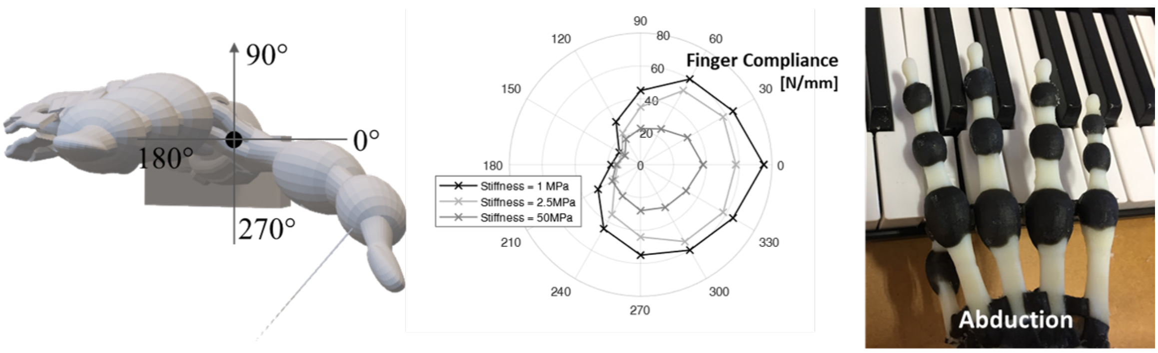

Figure 5.3 Directional compliance of the complex thumb joint printed with varying thumb ligament stiffness.

Fig. 5.2C, the collateral ligaments and other associated finger ligaments contribute to the Conditional Stiffness of the finger, which can be controlled by varying the material property E_J. The span Conditional Stiffness is controlled by the deep transverse metacarpal ligaments which is determined by the material property E_S. Finally, the Conditional Stiffness of the complex thumb joint and the range of motion is controlled by the material stiffness (E_T) of the palmer carper-metacarpal II ligaments and surrounding ligaments.

To 'engage' the Conditional Stiffness, an active component must be incorporated to provide external actuation to the passive system. In this case study a multi-degree of freedom UR5 robotic arm was used to provide wrist actuation with the passive hand attached to the arm (Fig. 5.2B and Fig. 5.2D). The wrist actuation allows for dynamic changes in hand position with respect to the environment. This promotes varying interactions and dynamic coupling between these two components allowing varying Conditional Stiffness to be observed. Fig. 5.2D (and Fig. 5.8) shows the overall architecture used to demonstrate the case study.

To experimentally determine the coupling between material properties and Conditional Stiffness experiments investigating the influence of material properties on piano playing behaviours have been undertaken. Within these experiments, the ability for actuation to trigger the varying behaviour and contribute to the reciprocal coupling between the mechanical system and the environment is investigated by introducing varying dynamic wrist actuation.

5.2.2 Results

To demonstrate the effects of varying the material properties and actuation experiments were undertaken exploring the range of behavioural diversity. To allow systematic analysis, we investigate three behaviour primitives: single finger tapping, thumb adduction/abduction, and hand span/spread behaviour. The combination of these primitives enables a wide range of playing behaviours. These three behaviour primitives map to three ligament groups for which the material properties are varied: fingers joints (E_J), thumb ligaments (E_T) and span ligaments (E_S).

Single Finger Behaviour

The complex mechanical dynamics of a single finger exhibit a wide variety of behaviours depending on the conditions provided. The first series of experiments involves a single finger playing a single note, 'tapping' one piano key while wrist actuation is only applied in the vertical plane. The control parameters of this wrist actuation include the frequency (or playing speed) and the displacement of vertical motions. For varying control parameters we observed the output frequency, rate of force applied and the maximum force at the finger-tip in contact with the surface of piano key. The focus of this analysis centred on the abilities of the internal conditions to control the overall performance of piano playing with one finger. In particular, the effect of Young's Modulus of the ligaments on the behaviour of the finger was investigated. Four single fingers were tested, each 3D-printed with joint stiffness (E_J) formed from materials with different Young's Moduli.

Fig.5.4A (left plot) shows the input-output frequency response of the finger, an important metric for achievable tempos for piano playing (63, 64). The range of output frequency in each finger was measured by moving the wrist in the vertical plane with a fixed amplitude. When increasing the input frequency, the output frequency can be considered to show no variation in comparison to the input frequency within the range of reasonable playing frequencies. As the stiffness of the ligaments is reduced, the Conditional Stiffness is such that the system shows some non-linear behaviour, with the damping effects limiting the maximum achievable frequency. Thus, lowering the stiffness limits the available range of playing frequencies, with a fully rigid finger capable of playing music with a greater range of frequencies. However, this trades off of other playing capabilities and stylistic behaviours.

Fig.5.4A (middle plot) shows the rate of force applied to piano key with respect to different frequencies (or actuation speeds). The rate of force indicates the articulation of sound, which directly influences the transition between notes ranging from slurred/legato to staccato. The lower rate of force change therefore results in smoother transition between two notes. This experiment highlights the salient differences between the rigid fingers and the softer, compliant fingers. Although rigid fingers can exhibit a larger range of force changes for a greater range of input frequencies, they struggle to achieve lower rate playing, especially at a higher frequency. These results indicate that a soft finger is necessary to play fast slurred or legato pieces, while a more rigid one should be employed for an articulated music.

Similar behaviour characteristics can be seen for the peak force when playing using a single finger, which indicates the volume of note. Fig.5.4A (right plot) shows that a rigid finger can generate a larger variety of peak forces, while the subtle control of volume is easier when a softer finger is used. The results demonstrate that the mechanical properties of the piano limit the ultimate ranges of the behaviour, however actuation can be used to trigger a given behaviour or response within these limits.

These results highlight the various trade-offs of different stiffness of finger ligaments and show how complex stiffness allows the behaviour of the finger to be mechanically altered. When combined with external actuation Conditional Stiffness can be used to achieve a range of playing behaviours. There is not one unique combination of actuation and internal

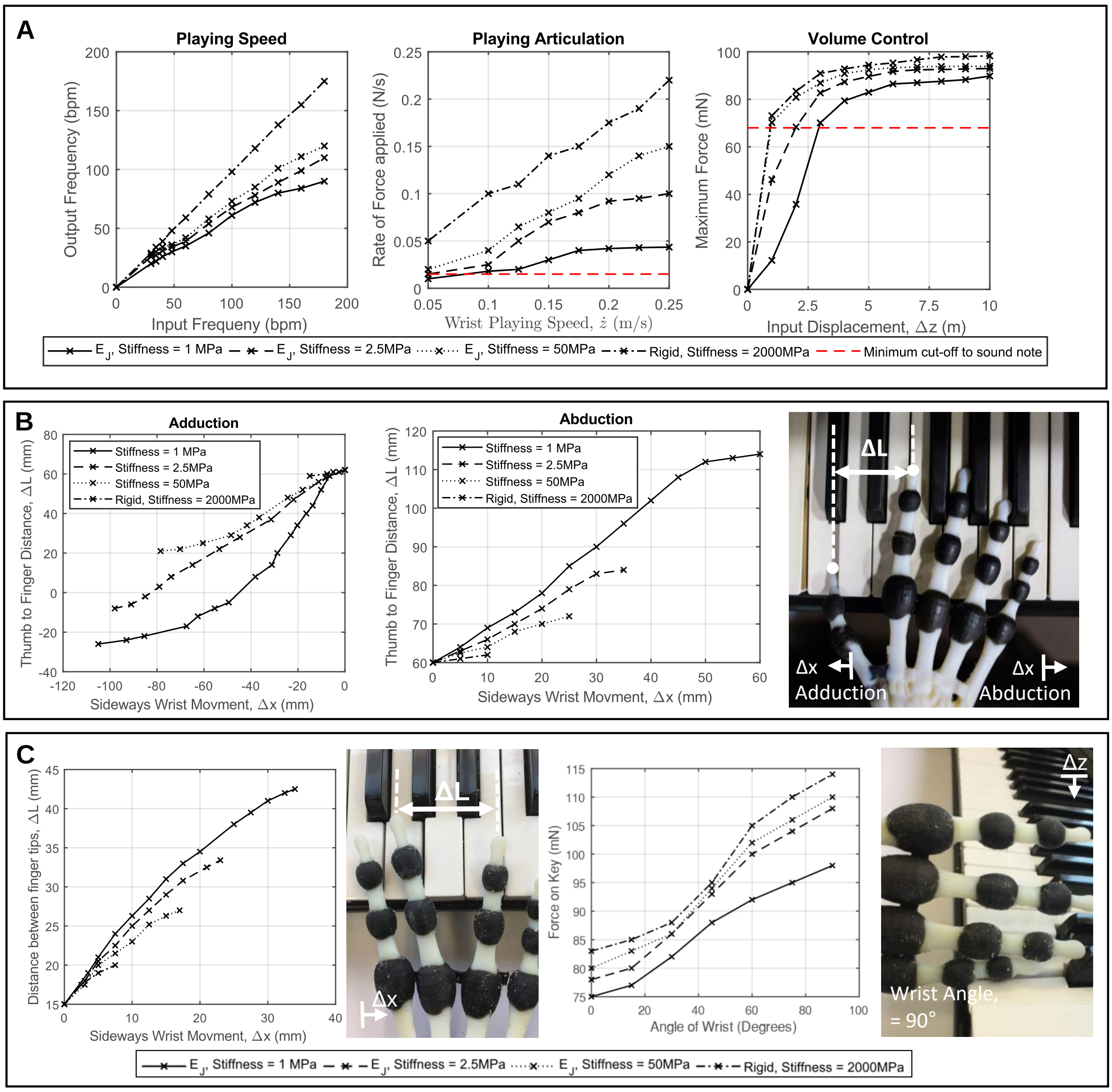

Figure 5.4 Experimental Testing of Behavioural Primatives. (A) Single Finger playing experiments with 3D printed fingers with varying material stiffness (E_J) showing the effects of varying different control parameters: frequency of playing (playing speed), rate of note playing (playing style, e.g. legato/staccato) and the maximum force detected on the finger tip (volume). The force was measure using FSR on the piano keys. (B) Abduction/Adduction distance measured between the tip of the thumb and the tip of the first finger when wrist is actuated horizontally after the thumb is moved vertically down such that it is pressing the key. Experiments were undertaken with hands with varying thumb ligament stiffness (ET). (C) Hand span stiffness demonstrated with a single finger (left) where the displacement between the second and third finger is measured with the second finger is playing a note and the wrist is actuated horizontally. Whole hand playing (right) when the wrist is actuated at varying amounts changing the stiffness and hence output force.

mechanical properties for one playing style. However, the choice of the materials and mechanical properties does limit the range of behaviours that can be achieved.

Thumb Adduction/Abduction Behaviour

The next series of experiments considered the use of multiple fingers, utilising environmental conditions to achieve complex behaviour. For these experiments we specifically focus on the thumb and index fingers as they exhibit a rich variety of motions in comparison to other human hand movements. The thumb abduction and adduction movement are particularly interesting as the range of movements and behaviour reflects the complexity of the thumb anatomy and provides a great deal of functionality for hands (65), and more specifically for piano playing.

In the following experiments, finger movement was articulated in two phases: first, the wrist was actuated downward with a certain stroke and a fixed speed such that the thumb finger-tip could press the key down all the way. Secondly, the wrist was then moved horizontal to the keys such that the index finger moved over the thumb. It is important to note that the thumb abduction behaviour is possible because the thumb finger is prevented from moving sideways by the neighbouring key during the second movement. After these wrist actions, the horizontal distance between thumb and index finger tips is measured as an indication of the adduction/abduction behaviour of the hand. This type of behaviour is used by human players to allow smooth transitions when moving sequentially over notes, for example playing scales, or performing jumps and rapid movements (66).

As in the single finger experiments, we investigated the effect of ligament material properties on the behaviour of the hand. Only the material properties of the adduction/abduction ligaments were varied, while the others were kept the same. Fig.5.4B shows the distance between the two fingers with respect to different horizontal displacement of the wrist joint for four different modulus thumb stiffness ligaments (modulus from 1 MPa to 2GPa were tested).

When rigid ligaments were used, the two fingers have a limited ability to move relative to each other when horizontal displacement is applied to the wrist. Thus, when the wrist was moved the maximum adduction distance was experimentally found to be approximately 18mm, with the thumb only able to move on the pressed key until the neighbouring key prevented further movement. In contrast, when decreasing the stiffness of the ligament, the maximum adduction distance can be significantly extended, with over 80mm adduction seen with the 1MPa ligaments. Considering the width of ordinary piano key to be 13mm, the ligament stiffness can influence the capability of playing between 5 keys with abduction. The softness of the ligament also influences the nonlinear relationship between the wrist movement and the abduction distance due to the complex bone-ligament interactions. The softer the ligaments the greater the non-linearity of the abduction behaviour of the thumb joint and the lower the horizontal displacement required to achieve a given range of abduction.

A similar behaviour is observed for thumb abduction. The rigid ligaments provide limited abduction with the distance again determined by the piano keys. The lower stiffness (1MPa) ligaments allow over 50mm of extension between the thumb and finger. The greatest non-linearity is also seen with the lower stiffness ligaments with the maximum abduction limited by the physical mechanics.

Hand Span Behaviour

The next experiments consider the ability of the hand to compress or stretch laterally allowing passive translation and rotation the fingers. This enables jumps and smooth transitions, allowing for varying lengths of jumps between notes. Additionally, the translation of fingers allows the hand to be rotated such that the fingers are playing on the side with the whole hand contributing to the note playing. Designing a passive anthropomorphic skeleton for these tasks is more challenging as a larger portion of the hand is involved in this behaviour. The finger joints, E_J, contribute to this hand behaviour; however, the deep transverse metacarpal ligaments (labelled as hand span stiffness) provide additional stretch and are the determining factor in the behaviour of this primitive.

The next experiments consider the ability of the fingers to move laterally, enabling smooth sideways transitions between notes and sideways note playing. Similarly to the previous experiments, the hand stretch behaviour is achieved by a two-phase articulation of wrist. The wrist is first actuated downwards by a given amount at a given rate so that the key is fully pressed with the second finger and such that sideways movement is limited by the keys. The wrist is then actuated horizontally, moving the finger laterally with the key kept pressed down such that the angle of the finger to the hand varies depending on the span stiffness. A series of experiments were conducted using four 3D printed hands with different span ligament stiffness (E_S): 1MPa, 2.5MPa, 50MPa and 2GPa. The horizontal displacement between the displaced second finger and the middle finger was measured. It is important to note that, for all these experiments, the finger ligament stiffness (E_J) was kept as low as possible (at 1MPa) to make the largest stretch possible. The measurement of lateral displacement for the four hands is shown in Fig.5.4C (left), where the stretch is measured at every 5mm increment of sideways movement.

The hands with the 2GPa and 50MPa hand stretch stiffness exhibit very small displacement, mostly under 10-20mm. As the stiffness is reduced the stretch range increases significantly, with a maximum recorded stretch of over 40mm. The response is initially linear, however for the lower stiffness ligaments, as the wrist movement increases the response becomes increasingly non-linear, as the material and geometric limits are reached. Varying the stretch ligament stiffness significantly affects the range of lateral movement possible with a single finger.

Span stiffness also influences whole hand playing, more specifically little finger playing where the wrist is at an angle to the piano (Fig.5.4C right picture). When playing chords with jumps whole hand playing is often used and the hand can be angled to achieve different styles. Here the span stiffness dominates the playing behaviour. The key force when the hand is lower a fixed amount (15mm) for different wrist angles was investigated. When the hand is perpendicular the force is the highest as the span stiffness is fully engaged and acting in full compression. At lower angles the stiffness is lower, often significantly so. The increase in force with angle is far greater for the stiffer span stiffness, with an increase of over 30mN. Varying the angle of interaction and span stiffness affects the force which can be applied to the piano keys.

Integration of Conditional Stiffness for Complex Piano Playing

Design and fabrication of individual Conditional Stiffness systems, as shown in the previous experiments, can exhibit behavioural diversity when actuation and environmental conditions are appropriately set. The next challenge is how to integrate these individual Conditional Stiffness mechanisms into a robot to create significantly increased range of behaviours. This integration challenge is difficult as some of the conditions necessary for certain behaviours can interfere with or are not compatible with others. The integration process is not simply the aggregation of individual mechanisms. The resultant behaviour depends on the interactions between the different sub-systems. Therefore, a consideration is to avoid conflicts of conditions while integrating the required behaviours without compromising behavioural performances. Here we demonstrate a case study in which such decoupling of conditions can be used to achieve a range of complex piano playing behaviour.

The case study considers the design problem of a skeletal hand that can play three considerably different pieces of music without changing the mechanical and material properties (Fig.5.4). The first piece is the four bars of 'Toccatta' by Scarletti. This is a fast-paced melody, where single note staccato playing is repeated, with periodic shifts in pitch. The second phrase of music was selected from 'Alligator Crawl' by Fats Waller. This requires consecutive smooth playing of notes an octave (8 notes) apart with a shift between each octave played. The final phrase of music is from 'Rhapsody in Blue' by Gershwin, the archetypal 'glissando' (rapid slide of thumb finger between consecutive notes), which requires thumb abduction smoothly and rapidly sliding over piano keys.

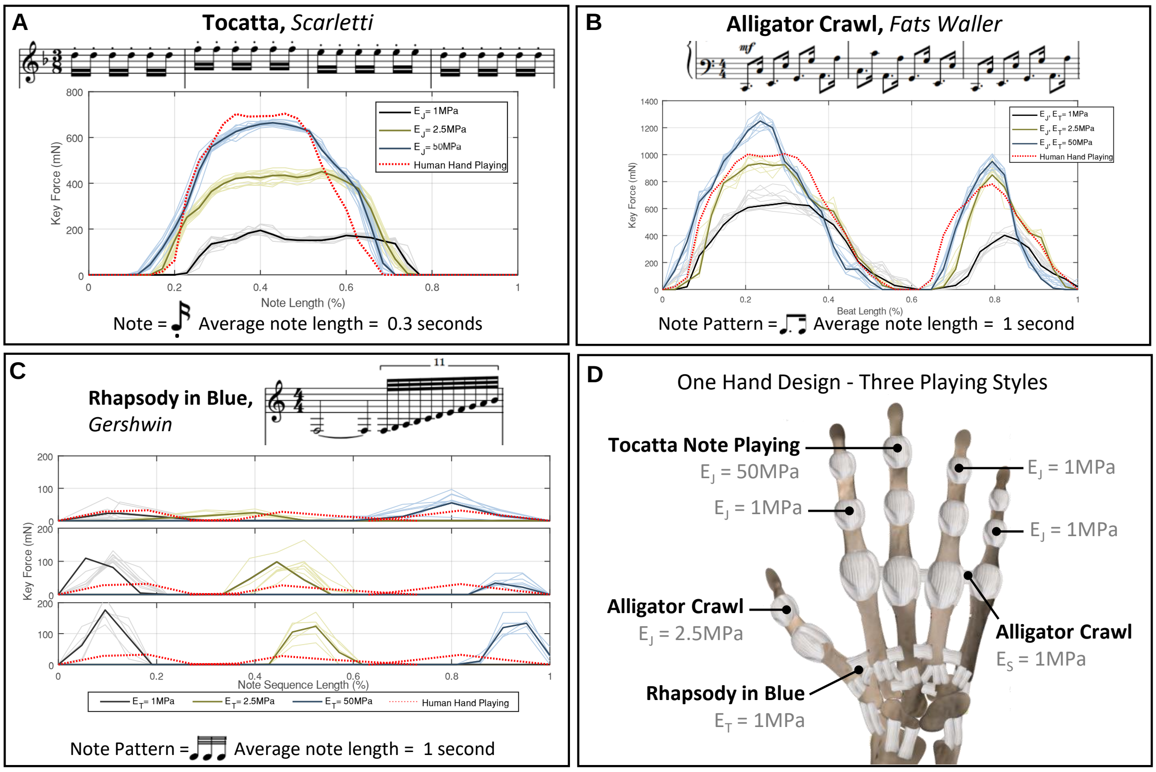

Figure 5.5 Case study demonstrating playing three musical phrases. (A) Results from playing Tocatto with a stoccato style. Shows the key force for a human playing and robot playing using the second finger with varying stiffness showing the average response (solid thick lines) and individual force profiles (thinner lines) for varying finger joint stiffness E_J of the finger joints. Shows the repeated musical pattern which forms the basis of this phrase. (B) Results from playing the two notes which form the basis of the Alligator Crawl refrain. Shows the response from the force sensors measuring the thumb force which is used to play the first note, and the little finger used to play the second note for different stiffness for all joints (E_J, E_S, E_T). (C) Force sensor results for playing the Glissando (slurred section) in the Rhapsody in Blue phrase of music. Shows the average force sensors results over three keys forming part of this slurred section played with the thumb using hands of different stiffness parameters E_T. (D) The stiffness parameters required for the various components of the hand to achieve one hand which can play all three phrases of music closest to that of human playing.

In order to play these pieces in a style similar to humans, the stiffness requirements of different parts of hand for each of these three pieces must be identified. The first piece, 'Toccatta,' requires a high frequency and high force staccato playing style, which generally requires high stiffness in the finger as lower stiffness cannot convey high-frequency strong actuation to the keys. Fig. 5.5A shows the force profiles measured through a sensor attached to a key, to compare the trajectories when the material stiffness of finger joints is varied. Compared to human performance (which is shown in the dotted red line), the stiffer finger with 50MPa ligament exhibits the performance closest to ground truth, human playing, whereas the softer fingers (2.5MPa and 1MPa) could not reach the sufficient strength and articulation with adequate temporal length. Therefore, for playing Toccatta, it is necessary to have a single finger with the higher stiffness (5MPa) material for the finger joint ligaments. To limit playing of or interaction with surrounding keys, we wish to maximise the stiffness of the playing fingers whilst lowering that of the surrounding fingers. This highlights how the environment and mechanics of the hand are coupled together, and how Conditional Stiffness can be used to achieve varying outputs.

The second phrase of music from 'Alligator Crawl' by Fats Waller requires a low hand-span stiffness to allow sideways translation of the finger to achieve the octave spread. Conversely, it is also important to keep these fingers sufficiently stiff to achieve reasonably well articulated notes, to minimize the pause between notes. To verify these requirements, we printed three hands with different thumb finger stiffness (1MPa, 2.5MPa, and 5MPa) while keeping the hand stretch stiffness at 1MPa, and measured force profiles exerted on two keys when two consequent notes were being played. Fig. 5.5B shows the experimental results compared to the force profile of human player. The lower finger stiffness with 1MPa shows poorly defined notes, leading to slurred and weak articulation. The 2.5MPa finger stiffness, in contrast, show the closest similarity to the human's, in which the height and length of both notes are similar, and there is a comparable pause in between.

The final piece, Rhapsody in Blue, requires rapid succession of playing, with a slurred transition between notes achieved by the thumb finger sliding over the string of notes. It turns out that a smooth transition similar to human's can be achieved only when the thumb abduction/adduction stiffness is set appropriately. While the wrist is moving horizontally, the thumb finger needs to interact with consecutive keys in a smooth and repetitive manner, resulting in a set of soft slurred sounds. Again three printed hands with different thumb abduction/adduction stiffness (1MPa, 2.5MPa, and 5MPa) were used in the experiment, where force profiles over three piano keys were recorded. Fig. 5.5C shows that the thumb abduction stiffness with 1MPa shows the temporal force profiles comparable to those of human player, while stiffer joints resulted in less smooth with larger articulated forces.

By combining the optimal joint material required for each of the three phrases of music, a single hand can be printed which allows all three phrases to be played (see Fig. 5.5D). The thumb must be low stiffness (1MPa) to allow abduction when playing the glissando, and a relatively low stretch stiffness should be used (2.5MPa). The finger used to play the single notes in the Tocatta (the first finger) must be high stiffness (5MPa). Additionally, the joint stiffness of the thumb and little finger must be 2.5MPa to allow sufficient articulation to play Alligator Crawl. All remaining fingers (index and fourth finger) are kept low stiffness (1MPa), such that the other fingers interact preferentially with the piano. For this case study, the three different stiffness requirements were mostly complimentary and the complex nature of the hand skeleton allows varied Conditional Stiffness to be achieved across the structure of the skeleton hand.

5.2.3 Materials and Methods

The case study presented in this work demonstrates how Conditional Stiffness can be utilised to achieve a broad range of behavioural outputs with limited control input. The production of the robotic system utilises novel 3D printing techniques to allow the printing of variable stiffness complex systems such as the anthropomorphic hand used in this case study. The mechanical design of this hand model, the enabling 3D printing methods, the integration of the full robotics system and details of the experimental methods are provided in this section.

3D Printing

Multimaterial fused deposition modelling 3D printing is an increasingly utilised technology [210, 211] which allows the rapid construction of 3D models with materials with varying mechanical properties. It enables durable 3D parts to be produced with a high accuracy and repeatability and allows different components of a model to be printed with varying Young's moduli by blending the base materials. This method allows printing of complex CAD models, such as the anthropomorphic hand, in a single print where all parts of model are fused together. Support material is required to achieve functional compliant joints and ligaments structures which must be removed in post-processing step by removing chemically. The material used for each component of the CAD model can be determined individually, allowing the material properties of the individual ligaments to be varied, thereby modulating the range and dynamic behaviour of the hand. The hand has been designed using anthropomorphic hand model, which is then adapted in the CAD software 3DS Max. The ligament design has been simplified to reduce the number of variables, with the joints modelled as

Table 5.1 3D Printer Materials used when printing the hand. Includes the ligaments of different stiffnesses, and the bones. Shows the blend of materials used to generate the materials with a given stiffness.

	Tango Black Percentage (%)	**Agile White Percentage (%)**	**Shore Hardness**	**Youngs Modulus (E)**
Ligament 1	100	0	A97	1 MPa
Ligament 2	90	10	A75	2 MPa
Ligament 3	80	20	A50	20 MPa
Ligament 4	70	30	A25	50 MPa
Bones	0	100	-	2 GPa

shells of ellipses (Fig. 5.6.) The shell thickness has been designed such that the material is sufficiently strong to prevent ripping or tearing and weakness of the joint.

A Stratasys Connex 5000 3D printer was used. Vero White, a photopolymer with high strength (tensile strength 60-70 MPa) and stiffness (flexile strength 75-110 MPa) was used to print the rigid bone structures. Vero white can be blended with other lower stiffness materials to print plastic with variable stiffness. In particular, it can be blended with Tango Black, which simulates thermoplastic elastomers with flexible, rubber-like qualities, with a Shore Hardnesss in the range of 26-28 Scale A, allowing up to 220% elongation at break. The ligaments were printed with the Tango Black Material blended with varying ratios of Vero White. The printing process takes approximately ten hours, with a further four required for effective mechanical and chemical removal of the support material. This allows rapid iteration of hand designs with minimal manual post-processing required. The hand can then be attached to a UR5 robot arm (Fig.5.2) to allow wrist actuation and control. 3D printing allows the rapid and repetitive production of hand mechanical structures where the passive dynamic behaviours can be tailored, with minimal additional construction or development work required.

5.2.4 Anthropomorphic Hand Skeleton Design

The anthropomorphic hand skeleton were adapted from a commercial 3D model[2]. The model has been used as the initial basis for the hand mechanical structure, with various modifications such as changes in material stiffness made; however changes were kept to be minimum. Starting with an anthropomorphic CAD model of the full hand and wrist including bones, ligaments, tendons and muscles, the tendon and muscles were removed to leave just the passive dynamical system which is formed from the coupling of the rigid bones and more

[2]The model was obtained from TurboSquid (https://www.turbosquid.com)

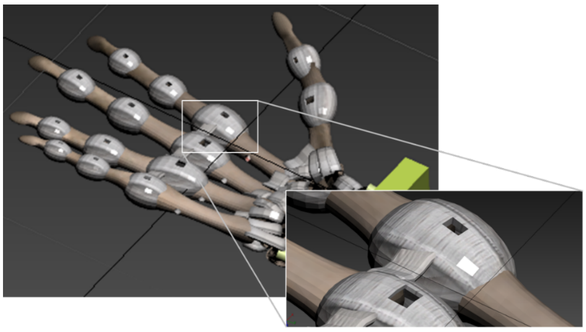

Figure 5.6 Ligament design for the CAD model of the hand showing the inclusion of the relief holes to allow the support material to be removed.

flexible ligaments. The ligaments surrounding the fingers joints (the collateral ligaments) were adapted to simplify the joints and provide increased stability and robustness to the joints. The remaining hand model was kept fully anthropomorphic to allow the mechanics of the joint interactions to be fully explored and exploited. To allow the materials of individual parts of the CAD model to be set individually, the CAD model was kept such that all parts were uniquely separable. The specific material properties of each bone and ligament can be set individually allowing control of the internal conditions of the hand.

The 3D printer prints the material in layers, with UV light used to cure the liquid material deposited. This requires a solid model to be produced, however, the model requires non-solid part in the joints where the bones must be free to move. Support material is used to produce the structure after which is it can then be removed. To remove the support material from inside the joints there must be access for the chemical solvent used, and thus small relief holes are used in the undersides of the joints (Fig. 5.6.)

Experimental Setup

For the experiments conducted in this work, the 3D printed hand skeletons were mounted directly on a UR5 robot arm. Using the arm allows precise static and dynamic control of the hand skeleton, allowing focus on the wrist kinematics without consideration for the rest of the arm. The on-board inverse kinematic of the UR5 is used, with a Python API used to allow control of the position, movement between poses and speed. The acceleration and deceleration of movement can be controlled in addition to the steady state speed allowing the dynamic and frequency response of the system to be measured. Positions corresponding to keyboard positions and fixed trajectories for chord jumps and thumb abduction movements have been collated into a database. Within this, the correct control parameters (speed, range

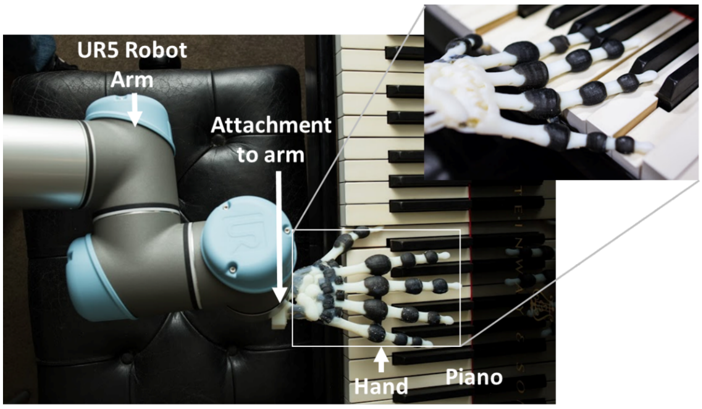

Figure 5.7 Full experimental setup showing the UR5 arm, the attachment of the hand to the am and the 3D printed hand. The UR5 arm is placed such that it is perpendicular to the environment, which is in this case the piano.

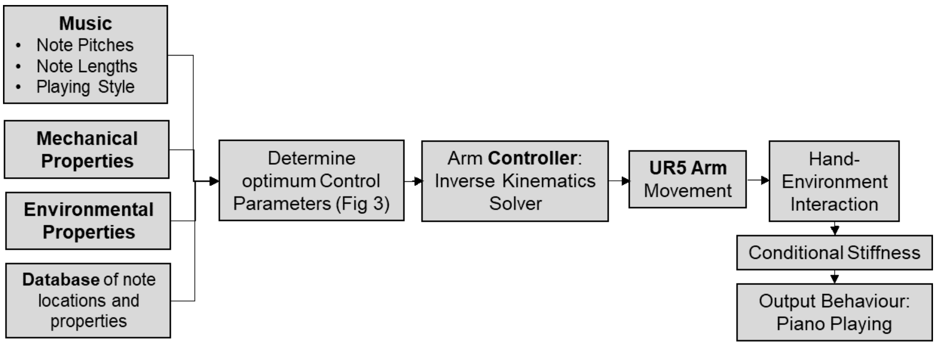

Figure 5.8 Block diagram of the system for piano playing. Showing the inputs, planning system and the overall output, piano playing.

of movement, frequency) are set to achieve the music required with the correct playing style for a specific material property required.

To measure the details of the hand skeleton behaviours, and a ground truth of human playing, the piano was sensorised with force sensing resistors (FRS). A load cell was used to perform calibration of the sensors. Analogue digital converters on an Arduino microcontroller were used to register the response from these sensors in real time, while the data was synchronised with the arm motion commands.

A block diagram of the implementation of piano playing is shown in Fig. 5.8. The inputs (music, mechanical properties, environmental properties and a database of known note locations and transitions) are input provided to a planner which determines the control parameters and required locations. The UR5 arm controller is used to determine the inverse kinematics and then control the UR5 Arm. This leads to moving the hand relative to the

Table 5.2 Summary of Arm control parameters. The dependency of wrist parameters on playing behaviour and the dependency of this on material hand properties.

Music Playing Behaviour	Wrist Parameters	Dependency on Hand Properties
Note pitch (note location)	x,y	-
Note length	t	-
Articulation (legato/staccato)	$\dot{z}$	E_J
Volume	ΔZ	E_J
Abduction/Adduction distance	Δx	E_T
Single Finger span movement	Δx	E_S
Angled Hand Playing	α	E_S

environmental, with the Conditional Stiffness giving rise to output behaviour in the form of piano playing.

Wrist Control

Inverse kinematics of the UR5 is used to allow control of the end effector in Cartesian coordinates. The considered control parameters include the position of the end effector and the corresponding velocities:

$$W = \begin{bmatrix} x & y & z \\ \alpha & \beta & \gamma \end{bmatrix} \tag{5.1}$$

$$\dot{W} = \begin{bmatrix} \dot{x} & \dot{y} & \dot{z} \\ \dot{\alpha} & \dot{\beta} & \dot{\gamma} \end{bmatrix} \tag{5.2}$$

The parameters in Table 5.2 are considered to correspond to the shown elements of piano playing. For each of the three segments of music, the wrist actuation and parameters required to determined the required playing behaviour for the material properties used. The specific wrist movement and control, is detailed in Appendix 1.

Mechanical Characterisation Experiments

To measure the compliance or stiffness of an individual finger, the finger was mounted in a fixed position horizontally. A known force was then applied to the finger-tip, and the displacement between the centre line of the finger and the displaced finger fip-measured. This method is shown in Fig. 5.9. Similarly, the method could be extended to investigating

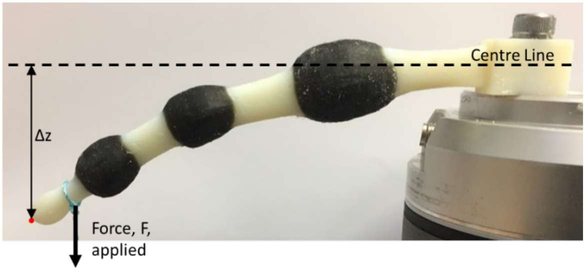

Figure 5.9 Determining the anisotropic stiffness of fingers by applying a force, F, and measuring the displacement at the tip of the finger.

the directional stiffness of the thumb joint and also the finger joints around other planes of rotation.

For the experiments investigating the single note playing behaviour primitive (Fig. 5.4), the playing of a single key which was instrumented with a force sensitive resistor was explored. The index finger was used in the experiments, with differing ligament material (E_J) for the DIP, PIP and MIP joints varied. For these experiments a single finger was used to allow the properties of the finger to be isolated from that of the rest of the hand as finger properties are determined only by E_J. The wrist control parameters (frequency, speed, displacement stroke distance) were varied for the different experiments and the response for the FSR on the key measured. The frequency of the force sensor signal was determined by measuring the average period of the output note as determined from the force sensor response, with the rate of changed used for the dynamic response. The maximum achieved force was used to indicate the achievable volume of playing. A range of frequencies, volumes and playing rates were chosen to map to typical human values and be within the capabilities of the arm providing the wrist actuation. All experiments were repeated five times with the average given.

For the thumb abduction experiments the ligament stiffness surrounding the joint (E_J) was varied with the ligaments in the rest of the hand maintained at the lowest stiffness. Although the other joints, in particular the finger joints, contribute to the measured abduction this is minimal and kept constant across all experiments. The wrist is moved such that the thumb is playing a note (middle C) with a fixed downwards displacement and angle of inflection with the piano to allow sideways movement of the fingers. The wrist is then moved horizontally such that the thumb movement is limited by the key that it is pressing, exposing the movement of the fingers relative to the thumb. Using a camera fixed above the piano, the horizontal displacement between the thumb tip and the tip of the first finger the displacement can be measured. This was repeated five times and the average distance recorded.

The final characterisation is that of the hand span behaviour primitive, with the material properties E_S varied. Similarly, the remaining joint materials were maintained at the lowest stiffness. The second finger was moved downwards such that it is pressing the middle C key. The wrist was then moved horizontally with the second finger trapped. The distance between the second and third finger was measured to provide a measurement of the compliance of the hand span. Finally, to investigate how this span stiffness affects the playing behaviour, the wrist was rotated and the little finger used to play notes with a fixed vertical displacement of 15mm, with the key force measured with a force sensitive resistor.

Piano Playing Experiments with Integrated Hand Skeleton

The three excerpts of music were chosen for the variety of playing modes as well as to demonstrate the three behaviour primitives investigated in Fig.5.4. For each phrase of music, the wrist location and movements were determined from the note requirements. For each piece of music, the optimum material properties, and control parameters to achieve the playing style were chosen from the results shown in Fig.5.4. For registering the experimental data, the same force sensitive resistors were used on the piano keys. One, two, and three sensors were installed to obtain the results given in Fig. 5.5A, B, and C, respectively.

5.2.5 Conditional Stiffness: Discussion

Despite extensive robotic manipulation research for the last half century, dexterous hand manipulation remains an unsolved research question. Many of todays advanced robots are not capable of manipulation tasks that small children perform with ease. It is hypothesised that complex passive mechanical structures can be used to address this gap in capabilities. Biological systems utilize mechanical design of bodies to achieve a wide variety of behaviours and thus this should be reflected in manipulation research. Recent advances in multi-material 3D printing technology allows systematic investigation of the complexity of passive mechanical structures. This technique allows printing of a passive anthromoporhic, providing the ability to reproduce complex human hand capabilities, e.g. various piano playing techniques, to a level that no other conventional robots can currently achieve. Piano playing has proven to be a complex and nuanced challenge, which requires a significant range of behaviour and playing styles. It is a challenge that demonstrates how the internal conditions (mechanical geometry and material properties) and external conditions (wrist actuation) can be coupled with the environment (the piano) to achieve playing of a variety of styles, with a fluidity and range of behaviours that has previously not been demonstrated in robotic piano playing work [205, 212, 213].

The introduction of soft material elements to robotic systems is particularly important when designing complex passive mechanical structures. This is exemplified by biological muscles and various internal organs; deformations of tissues provide the origins for the wide diversity of movements and functions in animals. The same principle can be applied to robotic systems and manipulators. Continuum deformable bodies have the potential to generate large varieties of behaviours, however, a new design methodology is required to unleash the potential. The inclusion of lower stiffness ligaments in the hand design has demonstrated the advantages of softer materials. Using variables stiffness ‘hybrid’ soft-rigid mechanical systems with 3D printing technologies enables the design and fabrication of structures with anisotropic stiffness properties.

The concept of Conditional Stiffness provides an insight into how such anisotropic soft-rigid hybrid structures should be systematically investigated and designed. It provides a framework that identifies the three underlying components of system, internal, external and actuation conditions. All of these must be considered to establish desired mechanical dynamics in soft-rigid hybrid structures. If these conditions are exploited adequately, a passive mechanical structure can achieve complex piano playing. This exploitation is largely dependent on the complexity of mechanical structures, which is possible due to state-of-the-art multi-material 3D printing technology.

The research presented in this work can be also inspire biological research, in which we can gain an understanding of the biological nature of dextrous manipulation by building bio-inspired robots. An obvious criticism might arise from the oversimplification of the anthropomorphic skeletal structure when compared to the biomechanics of humans when piano playing. There are a number of discrepancies in the playing mechanisms (for example, this system did not consider the roles of muscle activities and skin frictions etc.). Despite this, the proposed approach allows investigation of the underlying principles of skeletal dynamics to achieve highly challenging manipulation tasks. Previous work has stated that the sound produced by the piano emerges through the coupling between the biomechanics and neuromuscular dynamic of the pianist (mechanical impedance of the finger) and the dynamics of the piano itself [199]. Piano playing thus relies on the interaction between the mechanics of the piano keys and the players’ hand, which can be studied further by using the proposed system.

5.3 3D Printing Hybrid Structures

The previous section identified the role of passive dynamics in achieving complex and varied behaviours. In this section we consider the design and fabrication of hybrid fingers. Bio-

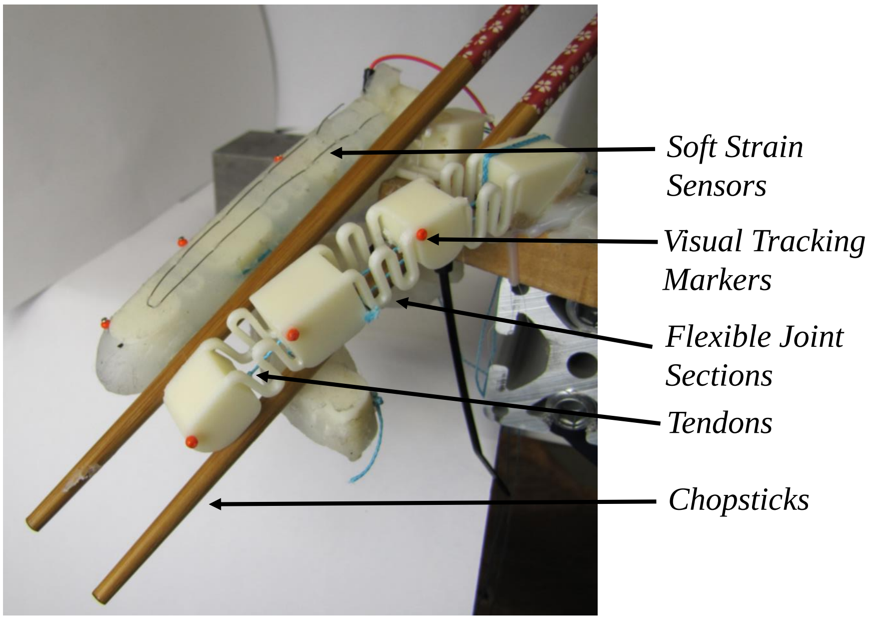

Figure 5.10 Experimental setup developed using sensorized soft-rigid hybrid finger design which enables chopsticks to be used to manipulate objects and detect size when grasped.

inspiration is used, however, simplification are made to take advantage of hybrid design. Simple tendon actuation is included to allow direct control of each finger. A soft-rigid hybrid anisotropic systems is created, where the role of hybrid design in manipulation is highlighted.

Soft-rigid hybrid manipulators use a mixture of rigid and soft components to achieve compliant systems that have sufficient rigidity to allow force to be transferred. The hand has soft-rigid hybrid stucture. A rigid bone structure which enables significant force to be applied and in-hand manipulation to be performed, but also has a soft compliant outer skin and tissues layer combined with elastic tendons and ligaments, which offers compliance and adaptability [9]. The construction of bio-inspired anthropomorphic soft manipulators can often be extremely time consuming requiring many parts and stages of construction and is often not repeatable or reliable. Manufacturing and design methods to enable rapid and easy production of manipulators are therefore required.

3D printing is a technology which has enabled robotics designs to be rapidly developed, tested and also tailored to a specific application. There has been some development of entirely 3D printed joints, however many of these are highly rigid ball and socket joints [214, 215]. This work presents a method for single material 3D printing joints and manipulators which have variable flexibility and compliance, such that a single print can be used to develop a single manipulator. The hybrid design is created from a flexible 3D printed inner structure and a silicone outer 3D structure which offers compliance and adaptability (Fig. 5.10). The 3D printed structure has joints which reflect that of a human hand and are elastic,

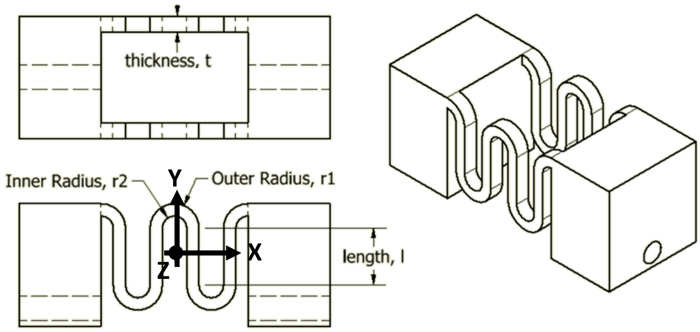

Figure 5.11 CAD drawing of the 3D printed flexible joint showing the reference system and the parameters which can be varied.

such that antagonistic pairs of tendons are not required as the passive behaviour provides the antagonistic behaviour. Soft sensors have been added to the structure to enable the deformation and position of the hybrid manipulator to be determined. The capabilities and compliant nature of this manipulator have been demonstrated by creating a robotic hand which can use chopsticks to grasp objects.

5.3.1 Materials & Methods

3D Printing Flexible Joints

The anisotropic flexible joint designed has two parallel thin rotation spring sections printed between more rigid ‘bone’ type sections (Fig. 5.11). This allows flexing in the X and Z directions as required for finger joints, whilst offering limited movement in the other degrees of freedom of the joint. The joints are 3D printed in ABS plastic, with the flexible sections printed parallel to the print bed. Unlike the design in Section 5.2 this allows for more rapid and lower cost production.

Within 3D-space the joint (Fig. 5.11) has 6 degrees of freedom and has four key tunable design characteristics: length of flexures, inner radius, outer radius and thickness. There are three degrees of freedom corresponding to movement along an axis as shown in Fig. 5.12 and the torsional moments around these axes. The joint has been simulated in Finite Element Analysis (FEA) software. Forces are applied in the X, Y, Z directions are shown in Fig. 5.12 with the relevant displacement measured. It can be seen that (Fig. 5.13) there is a close agreement with real and simulation results; in each case displacement increase linearly with the force applied. The displacement is most significant in the y-direction which is the direction in which displacement is required. In the x direction this can be considered negligible, and although present in the z-direction considerably smaller to that in the x direction. Corresponding results are observed for the three axes when moments are applied.

There are two tunable characteristics, the range of movement of the joint in the X and Z axis and also the stiffness of the joint. By understanding the effects the parameters of the joint have on the tunable characteristics, a finger can be designed with joints with the correct range for that specific joint and have a stiffness or mechanical impedance which matches that of the biological system being modelled, which itself has a stiffness resulting from the ligaments, tendons and other tissues within fingers. Critically, the stiffness in different directions can be controlled.

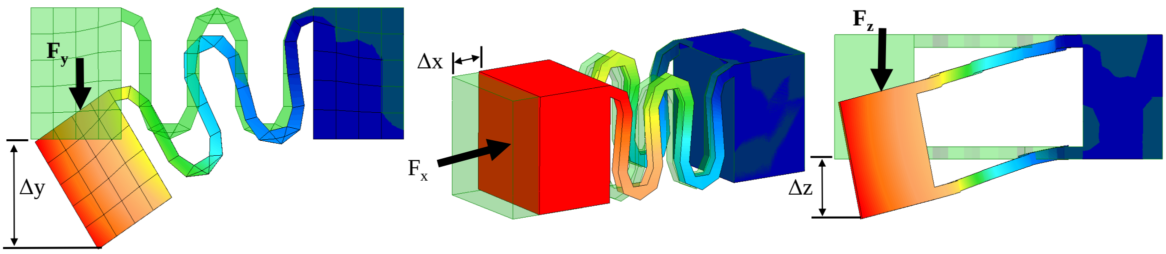

Figure 5.12 FEA simulation of the joint showing the three main degrees of freedom (DOF) (x, y, z), the forces which can be applied and the resulting displacement.

The range of movement of the joint can be determined by setting the joint parameters to physically limit the joint movement; this is predominantly determined by the joint outer radius and length of the spring section of the joint. Another characteristic that can be determined by the design parameters is the joint stiffness and compliance. The human hand has inherent mechanical impedance as a result of the structure and the ligament and tendon system. The ability to determine this stiffness or impedance allows replication of the hand mechanics. This mechanical impedance of the finger describes the relationship between externally applied force and the motion of the body; this impedance considers the damping and inertia which relates the applied force to the velocity and acceleration of the body. The passive impedance assists the human hand in dealing with changes in grasping conditions [216]. The stiffness of a finger increases linearly with the force applied, with a strong grasping requiring greater stiffness to apply a greater force [217] and is typically in the region of 50 - 200 N/mm [218].

Using FEA the effects of varying a joint parameter on the stiffness can be investigated, with theoretical and experimental displacement determined for when a 5N load is applied via the tendon (Fig. 5.14). There is a close correspondence between experimental and simulation results. Varying the length causes a linear increase in the downwards deflection and increasing the thickness of the spring sections reduces the deflection. Increasing the outer radius increases the deflection, however, the rate of increase of this displacement varies with the thickness of this section.

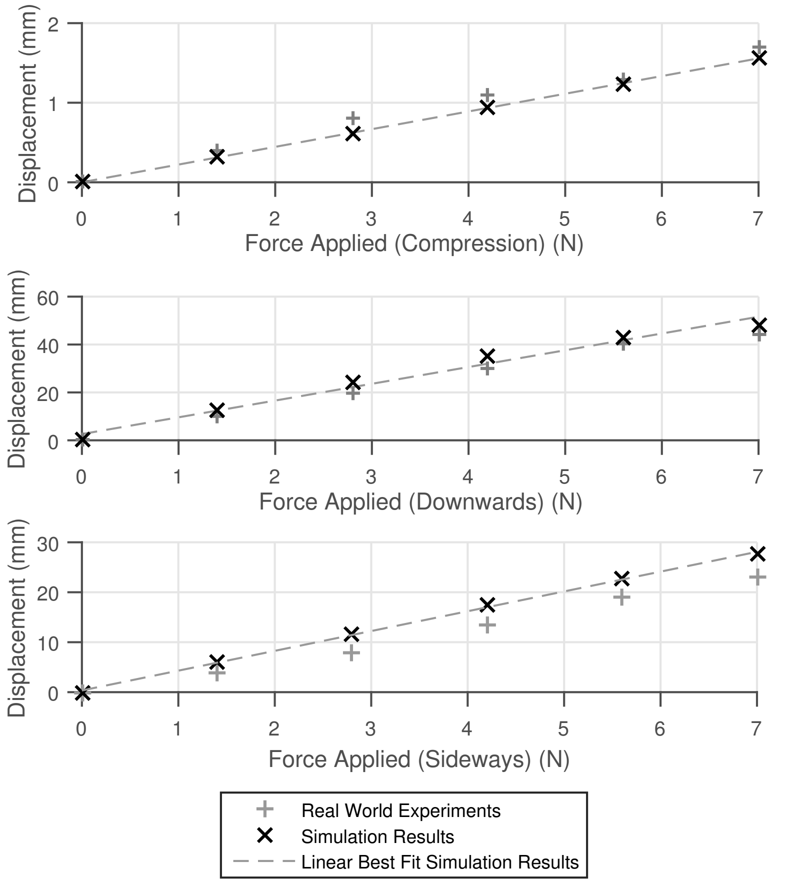

Figure 5.13 FEA simulation results and real world experiment results when force is applied to the three different DOF (in order x, y, z) with no rotational moments. Joint parameters: l = 8mm, r1 = 3mm, r2 = 5mm.

Hybrid Finger Development

The dimensions, range of movement and stiffness of the finger joints have been designed to match that of a human. To add a skin type structure to the manipulator to achieve a closer match the mechanical impedance and compliance of fingers, the 3D printed finger and tendons are cast in a finger shaped mould using EcoFlex 00-20 Silicone. To control the position of the finger, the tendons are each attached to a DC motor, which are controlled via a microcontroller using a speed controller.

Soft Sensing

To detect the 3D position of the manipulator, soft conductive thermoplastic elastomer (CTPE) sensors have been added to the finger. Conductive Thermoplastic Elastomer (CTPE) is a thermoplastic elastic matrix which is homogeneously mixed with carbon black powder under

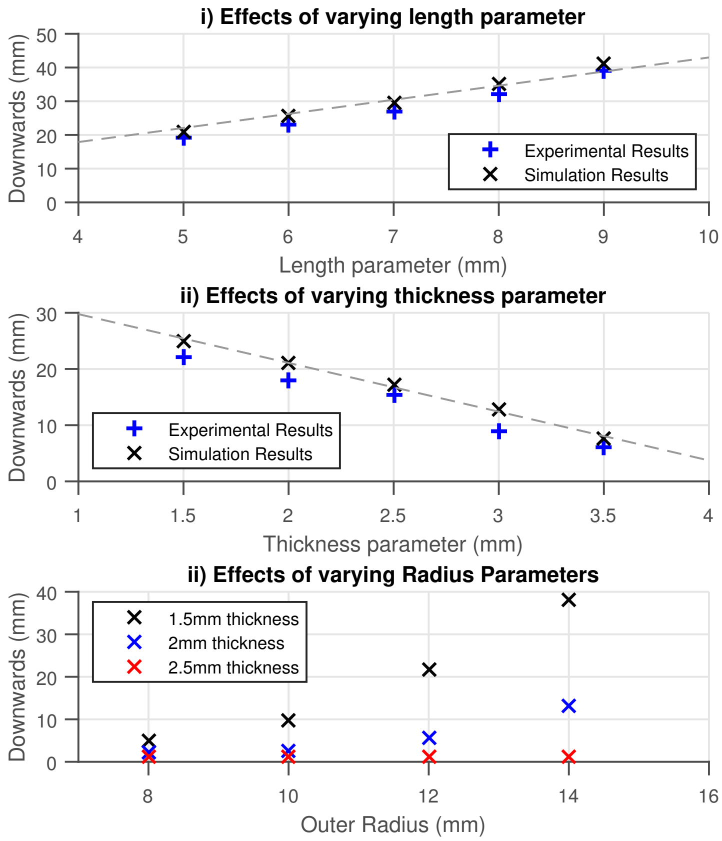

Figure 5.14 Varying deflection when a 5N load is applied for joints of varying parameters.

high pressure and temperature [25]. This process produces an electrically conductive material with a resistivity which varies linearly with the strain applied [112] and can be extruded into fibres. The sensors have previously been demonstrated in wearable applications by integrating into clothing and gloves [219]. These fibres can undergo strains of over 100% without reaching their tensile limit.

Three sensors have been attached to the silicone; one sensor placed across the top of the sensor and others on the two sides of the sensors. The sensors are connected to a potential divider to provide an analog output before being connected to a microcontroller. The top sensor are used to give an indication of the strain of the outer finger and the flex/unflex motion of the finger with the side sensors allowing sideways deflection to be determined.

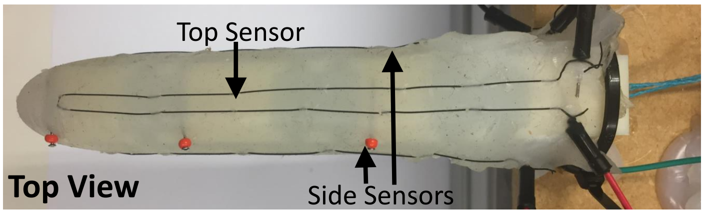

Figure 5.15 The sensorized finger showing the three integrated sensors; the top sensor to detect flexing and the two side sensors the side to side movement.

Table 5.3 Range of motion of the joints of the 3D printed finger, and that encased in silicone with comparison made to the human finger. Also the maximum perpendicular force which the finger can provide.

	Human Finger	3D Printed Finger	Silicone Encased Finger
MCP	$90°$	$98° \pm 1.5$	$78° \pm 1.5$
PIP	$80°$	$75° \pm 1$	$68° \pm 2$
DIP	$60°$	$65° \pm 1.5$	$60° \pm 2.2$
Force	12N	4N	6N

5.3.2 Results

To determine the reliability and range of movement the motion associated with each tendon has been tested by placing markers on the finger and determining the range of motion and position using vision tracking software. This has been determined for the 3D printed finger and also that cast in silicone. The horizontal force which can also be applied by the finger when a fixed force is applied to the tendon has also been determined. The results are shown in Table 5.3.

To test the sensors visual markers were placed on a sensorized finger; this allows the distance moved by the finger tip and the sensor response to be determined with respect to the sensor response. The results show a linear relationship between sensor response and distance moved; allowing the position to be determined. By considering the difference in response between the two side sensors, the side to side movement can be detected. When the finger is moving up and down the two side sensors experience the same response such that the difference between the two sensors is fixed. However, when moving side to side the sensors have the opposite responses such that the responses is doubled. (Fig. 5.16).

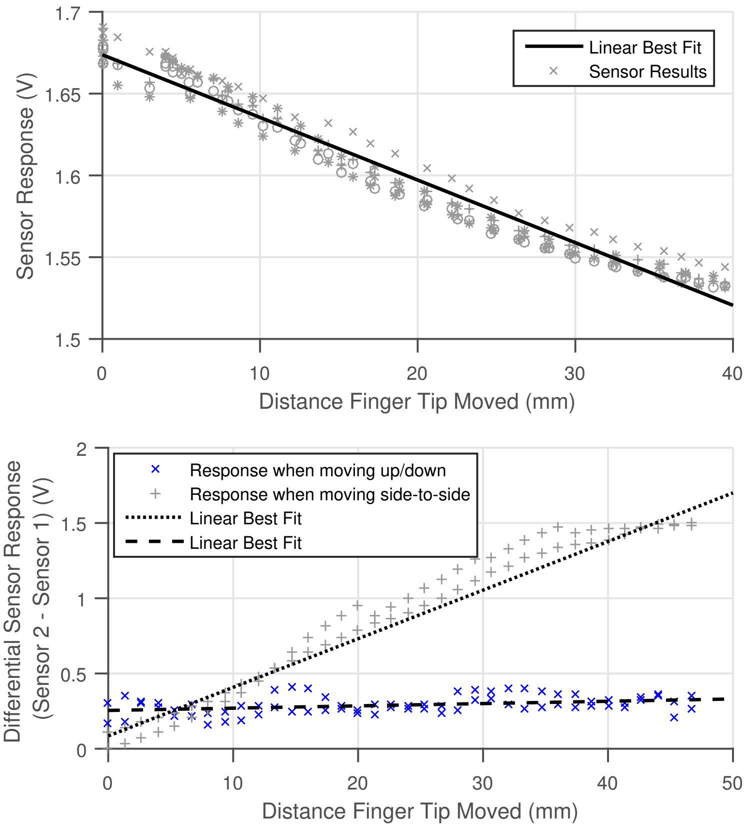

Figure 5.16 a) Varying sensors response with the distance the finger tip is moved (measured using visual markers and camera) when repeated 5 times. b) Response of the differential response (difference between the two side sensors) to side-to-side movement

Demonstration: Chopstick Gripping Results

One challenge which requires considerable dexterity and utilises compliance, anisotropic stiffness and passive behaviour of finger joints is the use of chopsticks. There has been some initial attempts to make robot hands which can use chopsticks [220], however this required the attachment of chopsticks to the hand. A three fingered hand (Fig. 5.17) which can hold and use chopsticks has been developed to show how the compliance of the fingers allows fine, dexterous control.

The top sensor on the actuated finger is used to detect when an object is gripped by when the sensor value plateaus which is the response to the chopsticks grasping objects and the fingers no longer move. By detecting the magnitude of the change of sensor response, the size of the object gripped can be estimated. The relationship between sensor response and object diameter is shown in Fig. 5.18

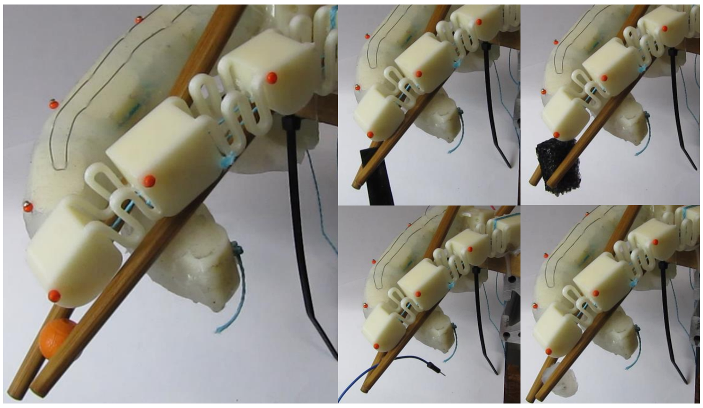

Figure 5.17 Images of different objects which can be grasped using the soft-rigid hybrid gripper.

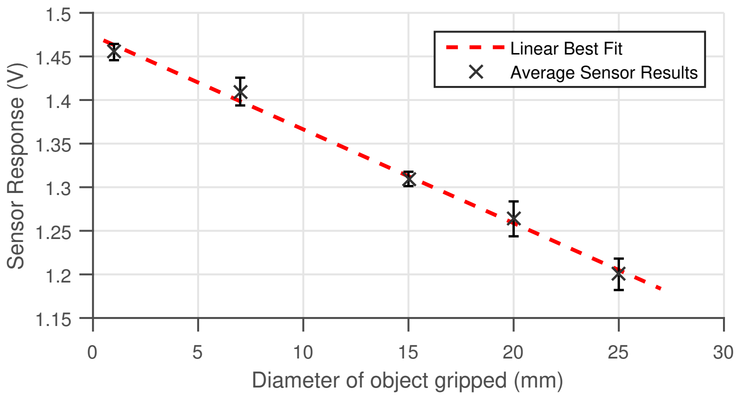

Figure 5.18 Magnitude of sensor response plotted when gripping objects of different diameter. The objects were gripped five times with the average and standard deviation of the results determined.

5.3.3 3D Printed Hybrid Joints: Discussion & Conclusions

In summary, a method by which a single 3D printed finger can be created with varying anisotropic stiffness has been presented. Joint analysis has shown how varying the parameters of the joint can affect the range of movement of the joint. The design parameters can be used to determine the mechanical impedance and range of movement of the joint so it can be designed for a given application. This allows control of the passive dyanamics, which can be used to create adaptive and complex behaviours. Rapid protoyping can be used to produce the flexible manipulator which is a fast and cost-effective allowing rapid development of manipulators.

The compliance and dexterity of the fingers has been demonstrated by developing a three fingered system which can use of chopsticks to grip objects. Soft sensors have been added which allow the position of the finger to be detected, and allows for simple control to be used to provide control.

5.4 Discussion & Conclusions

This chapter has presented a key new approach for developing soft systems which can achieve complex adaptive behaviours. Stemming from the concept of soft-rigid hybrid systems, complex systems can be developed which use soft and rigid materials to provide inherent passive dynamics to the system. Complex joints which show anisotropy can achieve varying behaviours through ‘Conditional Stiffness’. The experienced stiffness is dependant on the environment, external interaction and design of the physical system. This system leverages passive dynamics and localised embodied mechanics to achieve complex behaviours for example thumb abbduction/aduction of a human hand.

In comparison to other fully actuated manipulators, the range of movements that can be achieved is far more diverse, however, utilising passive behaviours does limit the movement of individual parts of the system which can be achieved relative to the whole system. Even with this limitation the range of behaviours which can be achieved is complex, and this behaviour can be easily modified by varying the stiffness of 3D printed joints. Understanding how to design the mechanical joints and systems for this behaviour is key.

In Section 5.3 a method of 3D printing joints with anisotropic behaviour and using only a single tendon was given. This uses both passive behaviours (for finger extension) and active control (for finger closure). This provides an simple mechanism for designing complex joints. The key advantages of soft-rigid hybrid systems is also shown by using soft-rigid hybrid joints to hold and manipulate chopsticks.

The proposed framework and concept of ‘Conditional Stiffness’ should be extended further. The internal conditions should be more thoroughly investigated to analyse the limits of what passive mechanical systems can achieve. In particular, the automation of the mechanical design process, would enable a more scalable and consistent approach. A key challenge is the integration of active stiffness control, sensory feedback, and motor learning to more closely mimic biological systems. Although these advanced motion control capabilities are important, the underlying mechanical complexity is ‘free’ and thus the exploitation of this is the most important consideration.

Chapter 6

Utilising Hybrid Body Dynamics for Perception

Animals use a range of different sensing mechanisms and methods to achieve an understanding of the environment. In additional to visual and tactile sensing methods, another inherent sensing capability is the unconscious awareness of body dynamics. This is an embodied capability that allows the detection of joint positions and hence interactions with the environment. There has been limited exploration of the use of proprioception for environmental sensing in soft robotics [72]. Using the body dynamics of soft robots for sensing exploits the inherent softness and compliant nature which enables significant environmental interaction. This Chapter focuses on exploiting the body dynamics of soft-rigid hybrid mechanical systems to maximise the information that can be gained. It brings together may of the concepts presented in the previous chapters (sensor morphology and soft-rigid hybrid design) to provide a truly embodied approach to perception through body dynamics.

6.1 Role of the body for sensing

Perception is determined not only by the sensor technologies, materials and morphologies used but also by the mechanical structure and the dynamic behaviour of the body which performs the exploration [221]. The human hand performs high fidelity perception of shape, texture, material and temperature not only due to the sensing capabilities of the hand, but also its dynamic behaviour, morphology and material properties. Proprioception, the sensing and understanding of the dynamics of a body, can therefore be an effective method of sensing and exploration. Body mechanics can be exploited by tailoring the mechanics to react to a specific stimuli and to maximise the transduction of a particular input stimuli [222].

It has been demonstrated that body dynamics can be used to provide sensing capabilities and enable an understanding of the environment in rigid systems [223, 224]. The increased compliance of soft systems enables increasingly compliant interactions with the environment, enabling greater perception through body dynamics [8]. This is a bio-inspired approach that mirrors sensing capabilities which humans use to intrinsically and unconsciously understand the world and environment. The simplest example of proprioception in animals is the understanding and perception of joint positions, which enables the spatial awareness of limbs and the sense of movement.

By unconsciously understanding joint position, an awareness of the environment can be grained from its interaction with complex bodies. For example, to detect the texture of a surface, a human would move their hand over the surface, utilising the passive dynamics of hand. In addition to the tactile information gained, the texture of the fingers causes a change in joint points and the force the hand experienced. The body mechanics and the unconscious 'sensing' properties provide environmental awareness.

Soft-rigid hybrid systems have sufficient rigidity to interact with the environment whilst their compliance allows increased environmental interaction. For this reason soft robotics have the potential to utilise this concept more than existing robotic systems. By introducing soft sensors that perform embodied unconscious proprioception sensing of the body, the response can be used to provide environmental perception.

Specifically, the mechanical design and properties of a manipulator should be designed to both:

- Transduce or amplify environmental stimuli
- Perform localised processing to reduce the requirements for complexity in perception and exploration

A model of how the interaction between the environment and the dynamic movement of a passive mechanical system can be used to aid perception is shown in Fig. 6.1. The coupling between the environment and the passive mechanical system, aided by compliance of soft-rigid hybrid systems, enables the proprioception of the mechanical system through onboard sensors to achieve perception of the environment.

Hybrid mechanical systems that display anisotropic stiffness, such as those developed in Chapter 5, allow better exploitation of the passive mechanics. Mechanical systems can be tailored to improve the response to dynamic interaction with the environment. The response is dependant on the mechanical and material properties of the environment.

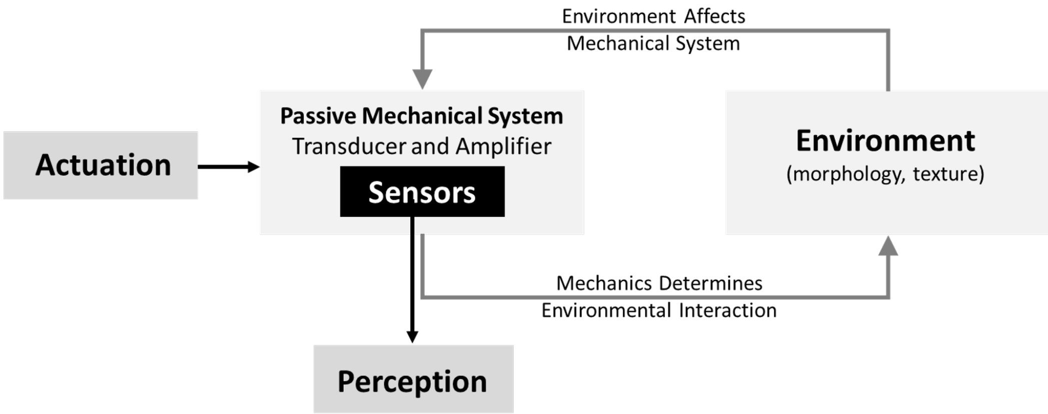

Figure 6.1 Model of how body mechanics can be used to aid perception and exploration of the environment.

This research explores how the mechanics can be designed to maximise the change experienced on interaction with the environment. It tests a number of hypotheses about how the mechanics, and material properties aid and drive perception.

6.1.1 Body Dynamics Exploitation: Hypotheses

A number of hypotheses about the relationship between perception and dynamic body mechanics are proposed:

- The passive dynamics of a soft-rigid hybrid finger can be used to aid in the **detection of objects**, including the height and size of the object. The specific passive dynamics and stiffness affects the 'filtering' effect the mechanical system has on the detection of the environment.
- The interaction between a mechanical system and the environment can be used to determine information as to the **texture and friction** of the surface.
- The passive dynamics of a manipulator and its interaction with the environment allows **detection of the stiffness of objects**.

The remainder of this chapter seeks to address these hypotheses and understand how mechanics can aid perception.

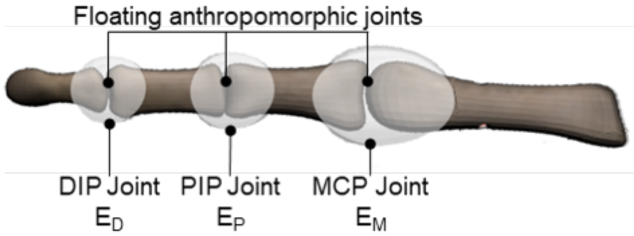

Figure 6.2 Finger used for perception experiments, showing the joints and the stiffness parameters for each joint.

6.2 Mechanical Design Parameters

To test these hypotheses we consider the mechanical structure of an anthropomorhphic finger (as developed for the hand model in Chapter 5). This shows anisotropic behaviour, and allows the stiffness of the different joints (as shown in Fig. 6.2) to be varied to investigate how it affects perception of the environment.

The finger can be manufactured using multi-material 3D printing to allow fingers of various stiffness to be developed. Similar to the Conditional Stiffness Experiments in Chapter 5, the stiffness of the material of the joints in the finger can be varied. This changes the passive dynamics of the finger and allows the directional stiffness and passive dynamics to be altered.

The complexity of the finger is such that buckling beam theories can not be applied directly. The interactions between the interacting bones and supporting soft material has a complexity which can be modelled directly as a pin-joint or equivalent. This complexity provides sensitivity and nuanced behaviour to environmental interaction beyond that of simply having a cantilever beam interacting with the environment.

6.3 Understanding Environmental Interactions

Considering a single anthropomorphic finger, the ‘Conditional Stiffness’ is dependant on the environment and also the dynamic actuation of the finger. Therefore, the posture of the finger and the force it exerts is dependant on the angle and speed of interaction in addition to environmental parameters. When the finger interacts with the environment the posture varies depending on the texture and friction of the environment. In this section we investigate how the dynamic interaction between the mechanical system and the environment changes the posture and force exerted by the finger.

6.3.1 Environmental Interaction: Surface Material Properties

The interaction and resultant posture of the fingers is dependant on the frictional interaction between the fingers and the environment [225]. To investigate this, the soft-rigid hybrid finger was brought in to contact with surfaces of different frictional coefficients and the posture measured. A finger (with joint stiffness E_J = 1 MPa, see Section 5.1) was mounted vertically downwards on the end of a UR5 robot arm and was lowered by a fixed amount on to surfaces with different coefficients of friction. A calibrated force sensitive resistor (FSR) was mounted between the finger and the arm to allow measurement of the force applied to the finger. A vision system was used to measure the joint angles of the finger throughout this process and the movement of the finger tip.

The postures of the fingers when interacting with different frictional surfaces are shown in Fig. 6.3a. The force and the movement of the finger tip along the surface is also shown in Fig. 6.3b. Different frictional surfaces result in varying postures of the finger. This is due to the frictional interaction between the finger tip and the environment, and the compliance of the finger joints. The postures can largely be classified into two main postural behaviours. In some cases, the frictional force between the finger tip and material surface is greater than the opposing force supplied by the stiffness of joints in the finger, such that the finger tip shows minimal movement along the surface of the material. This is the case for materials with a higher frictional coefficient. This also results in a high perpendicular force experienced by the finger. For materials with a lower frictional coefficient, the stiffness of the fingers overcomes the frictional interaction, resulting in greater finger tip movement.

These results show that sensing of body dynamics can be used to identify information about the material properties of the environment. By varying the material parameters of the finger joints, it would be possible to change the 'tipping point' at which the frictional interaction overcomes the force generated by the stiffness of the finger. This would increase the sensitivity of the system to identifying material properties in this frictional region. This is a similar concept to previous work [226] which used passive structures of varying morphologies to allow detection of stimuli using a camera. However, the introduction of soft-rigid hybrid systems provides far more complex environmental interactions. This allows more nuanced and complex environmental information to be gained.

6.3.2 Environment Interaction: Speed of Interaction

In addition to the environmental parameters, control parameters of the body dynamics affect the output posture or force generated. One parameter that has a significant effect on this is the speed of interaction between the finger and the environment.

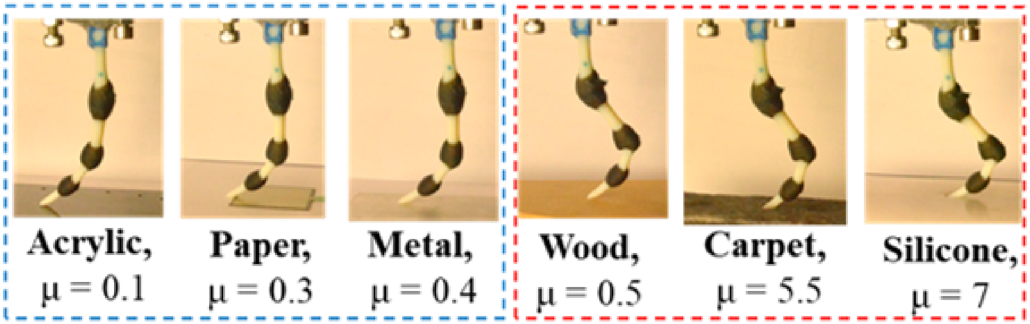

(a)

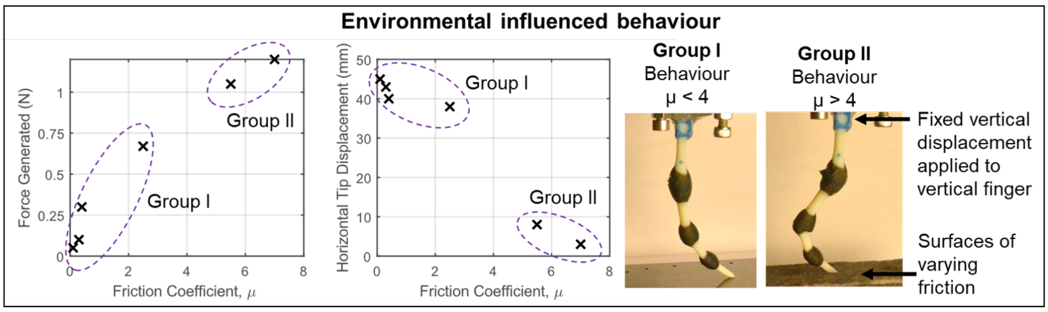

(b)

Figure 6.3 **a)** Finger postures resulting from interactions with environments of different frictional coefficients. **b)** Force generated and horizontal tip displacement for the interaction between the finger and environments of different finger stiffness.

In these experiment, the finger (mounted perpendicular to the surface) was lowered at different speeds vertically downwards on to a flat surface. It was lowered 2cm lower than the point at which the finger tip first hits the surface such that the joints undergoes deformation. The posture (joint angles and tip displacement) and peak force, measured using the FSR as in the previous experiment, was recorded for interactions of different speeds. A measure of the posture is generated by summing the changes of the angles of the three joints in the finger.

Fig. 6.4 shows the relationship between the sum of the angular displacements of the joints and the force generated for different speeds. There is an approximately linear relationship between the change in posture of the finger and the force exerted. The greater the joint displacement, the larger the force the joint provides, due to the elastic nature of the joints they provide a force proportional to the deformation, and hence the greater the force measured by the FSR. There are three main groupings which showed visibly distinct postures.

The relationship between the speed of interaction and posture of the finger is highly complex. The increased velocity gives rise to an increased angular displacement. Due to the soft-rigid hybrid nature of the fingers and the complex geometry, under faster interaction speeds, the joints have less time to respond to the impact force. Thus, the joints rigid bone-bone interaction dominates the behaviours such that the stiffness of the ligaments is overcome, and the joints deforms without letting the finger tip move. The normal force that is generated is higher and hence the frictional force is greater, preventing the tip of the finger from moving across the surface (Fig. 6.4b). This leads to a a greater change in the sum of the angular displacement of the joints. In comparison, at slower speeds the impact force is lower and more distributed over time such that the ligaments stiffness determines the behaviour, with smaller changes in joint position resulting in finger tip movement. This is a highly complex interaction and is highly depend on the design of the soft-rigid hybrid system.

To maximise the change of joint angle of the system, a faster interaction is required. Additionally, changing the material properties changes the response. This could allow for optimisation of the mechanics for different speeds of environmental interaction.

6.3.3 Environmental Interaction: Angle of Interaction

A second dynamic property that affects the response of the finger is the angle of interaction. This is defined by the angle α between the normal of the environment and the central axis of the finger, such that when the finger is perpendicular to flat environment and approaching from above α is 180^0. The posture of the finger was measured as the angle of interaction (α) is changed when the finger is in contact with the environment.

The finger is again mounted on the UR5 perpendicular to the environment. The finger was then lowered vertical downwards by 2cm lower than when the tip of the finger first

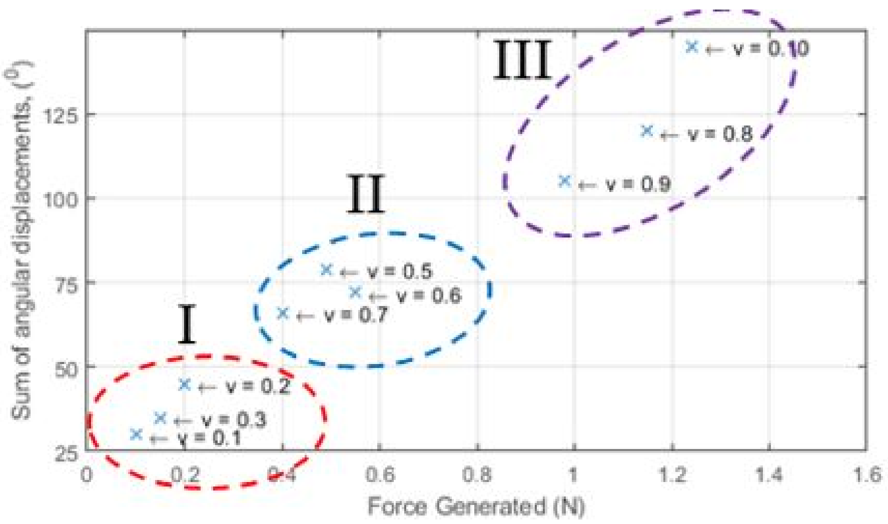

(a)

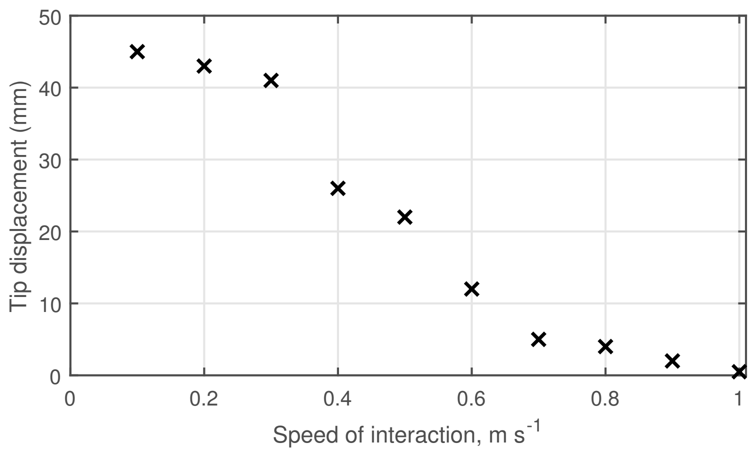

(b)

Figure 6.4 **a)**Varying joint displacement and force generated for interactions with the environment of different speeds. **b)** Varying finger tip displacement for interactions of different speeds.

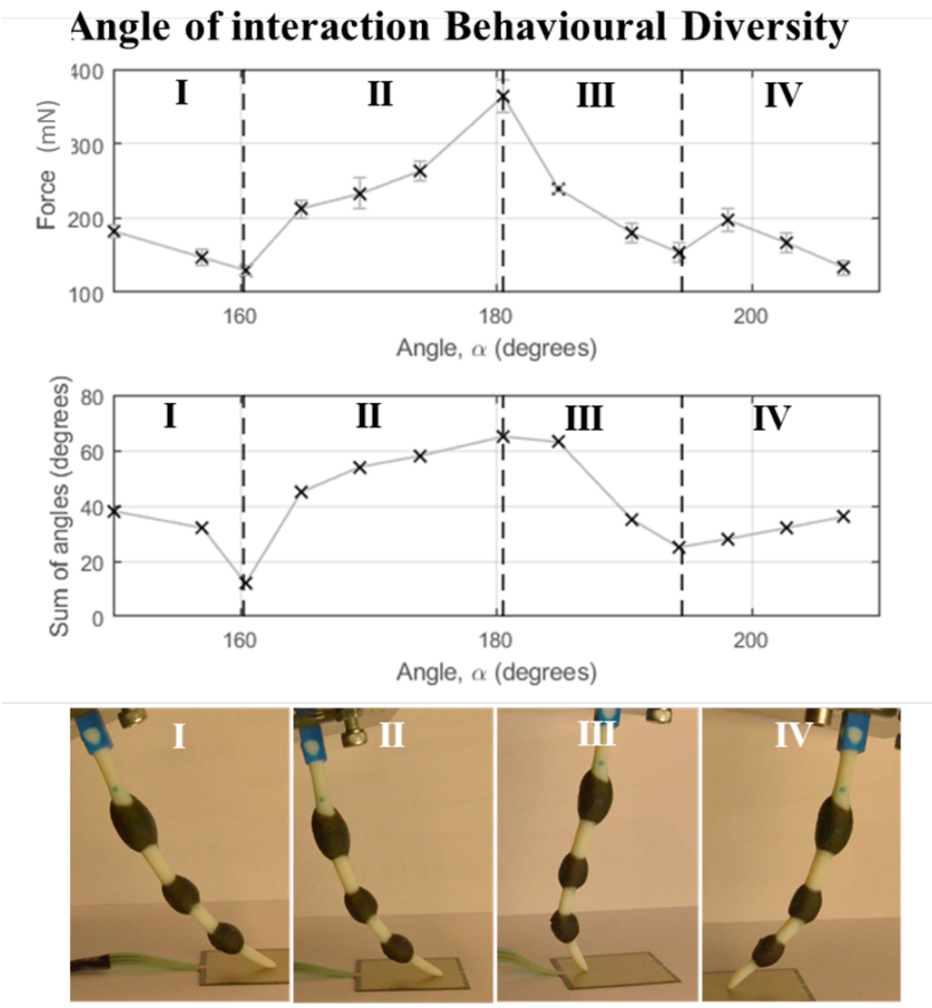

Figure 6.5 Varying behaviour with different angular interactions with the environment.

interacts with the environment. The angle of interaction is then changed (Fig. 6.5) with the vertical height above the environment kept constant. The sum of displacements of the joints is measured using vision, and the force between the finger tip and the surface measured using a force sensitive resistor on the surface. The results are shown in Fig. 6.5. This shows the range of behaviours that can be achieved depends on the environment and the angle of interaction. This response changes with different material properties of the joints.

By varying the angle of interaction with a surface, or dynamically changing the angle when in contact with the surface, the change in posture and hence sensitivity to environmental stimuli can be maximised.

6.4 Results: Environmental Proprioception

The previous section identified that joint position can be used to provide an indication of the environment. It has also been demonstrated how the dynamics of the interaction can be optimised to maximise the change in joint position and hence provide maximum sensitivity to environmental changes. In the following section we explore how this can be exploited to enable perception of the objects by integrating simple posture sensing.

6.4.1 Object Parameter Detection

Rigid objects can be explored using the body dynamics of single finger by moving the finger over objects. An indication of the objects height profile can be gained by using temporal posture information. For more rigid fingers the system can be thought of as a cantilever beam interacting with the environment, however for the softer fingers the interactions are more complex.

FSR and CTPE Sensors are used to provide information as to the force response of the finger to the environment and CTPE is used to provide information as to the postural information of the finger. There is significant scope for investigation into the optimum morphology of the CTPE to detect the posture of fingers. However, for these experiments the sensor was placed along the upper surface of the finger, in a loop. This simple morphology provides a single measurement of the posture of the finger, and has been placed along the direction which experienced maximum strain when the finger deforms. Fingers with different joint stiffness were printed (E_J of 1MPa, 2.5MPa, 5MPa and 50MPa), to allow investigation of how changing the stiffness affects the response of the system. A diagram showing the experimental setup used and the location of the FSR and the CTPE sensors integrated into the system is shown in Fig. 6.6.

The finger was mounted on the end of a UR5 arm (Fig. 6.6B), and the finger moved over rigid objects which have a rectangular cross section with varying height and width. The response of the sensors embedded in the finger is recorded over time.

A typical response of the sensors is shown in Fig. 6.7. For both sensors there is an approximately step change from the base level sensing reading. It is proposed that the length of the square wave provides information as to the width of the object and the magnitude of the response provides information as to the height of the object.

By detecting the step increase as the finger is moved in contact with the object, the length of time the sensor is above this reading (t_{step}) can be used to provide an indication of the objects width by knowing the speed, (v), the finger is moving at ($w_{est} = vt_{step}$).

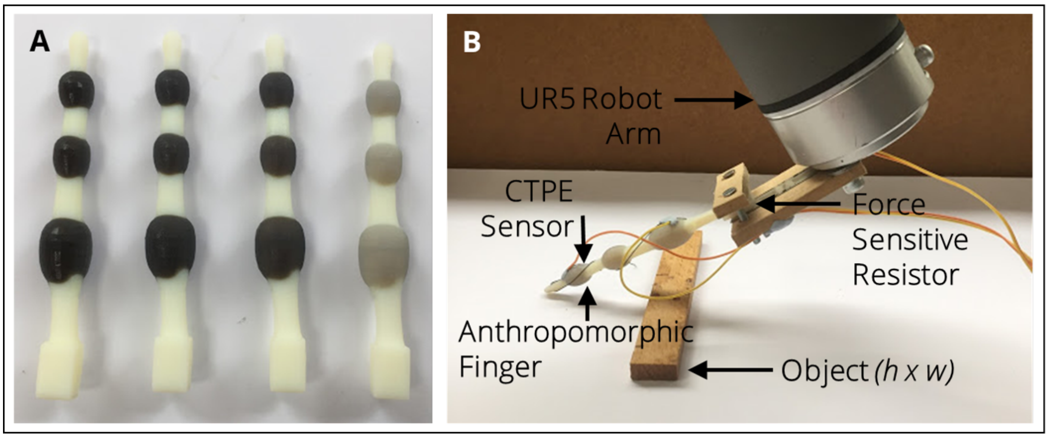

Figure 6.6 Setup using the UR5 robot arm, finger and the FSR and CTPE sensor attached.

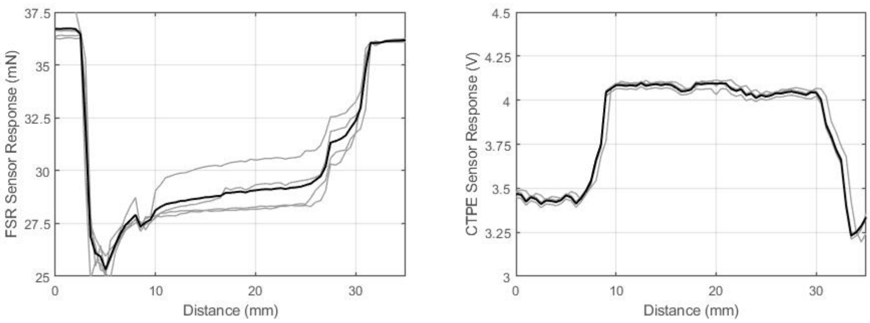

Figure 6.7 Typical response from FSR and CTPE sensor when the finger is moved over an object. Showing multiple responses of the same object in grey and the average response in the thicker black line.

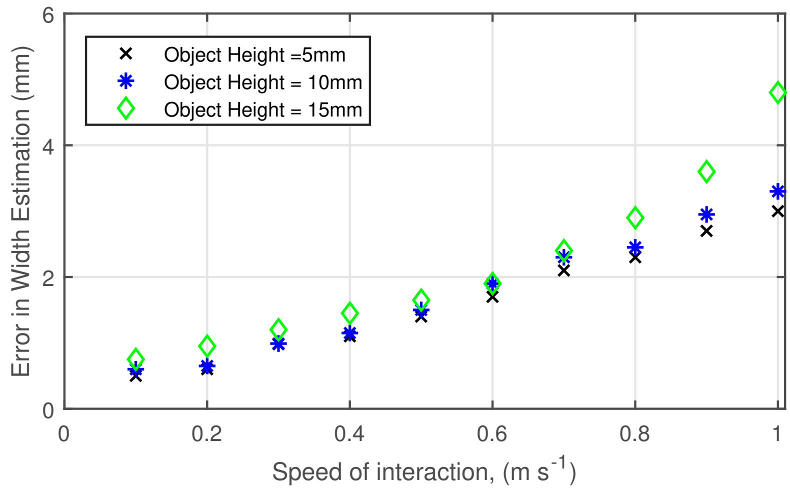

Figure 6.8 Error when using a finger of stiffness E_J =1 MPa to detect the width of objects of different heights, where the width if fixed (20mm).

Firstly the effect of the speed of interaction was investigated. A finger with a fixed stiffness (E_J = 1MPa) was used. The error in the estimation of width was recorded for different speeds of interaction. The results are shown in Fig. 6.8 for objects with different heights but a fixed width (20mm).

The slower the interaction the lower the error. Additionally, the greater the height the object the larger the error in width detection. Although the error reduces with speed, after a certain reduction is speed there is minimal additional increase in precision.

The next set of experiment investigate how the material properties and stiffness of the fingers affects object detection. Fingers of different stiffness are used to explore objects of different widths to understand how varying stiffness can be used to aid perception.

Fig. 6.9 shows the error in width detection for objects of varying width. The postural information (i.e. CTPE sensor results) gained from the lower stiffness finger provides more accurate detection of width. As the object width increase, the error also increases. The fingers which are more compliant are most adaptive to the environment and provide this greater accuracy. The stiffer fingers respond too early to the object, with the higher part of the finger interacting with the surface of the object, before the finger tip detect the edge of the object. The stiffer fingers respond to any stimuli, opposed to the desired stimuli, the edge of the object, resulting in this higher error.

Conversely, for the force sensitive resistor results, the higher stiffness fingers provided the lowest error when detecting the width of the objects. The force detection is most responsive for stiffer fingers, and despite the posture of the finger changing too early, the force is not

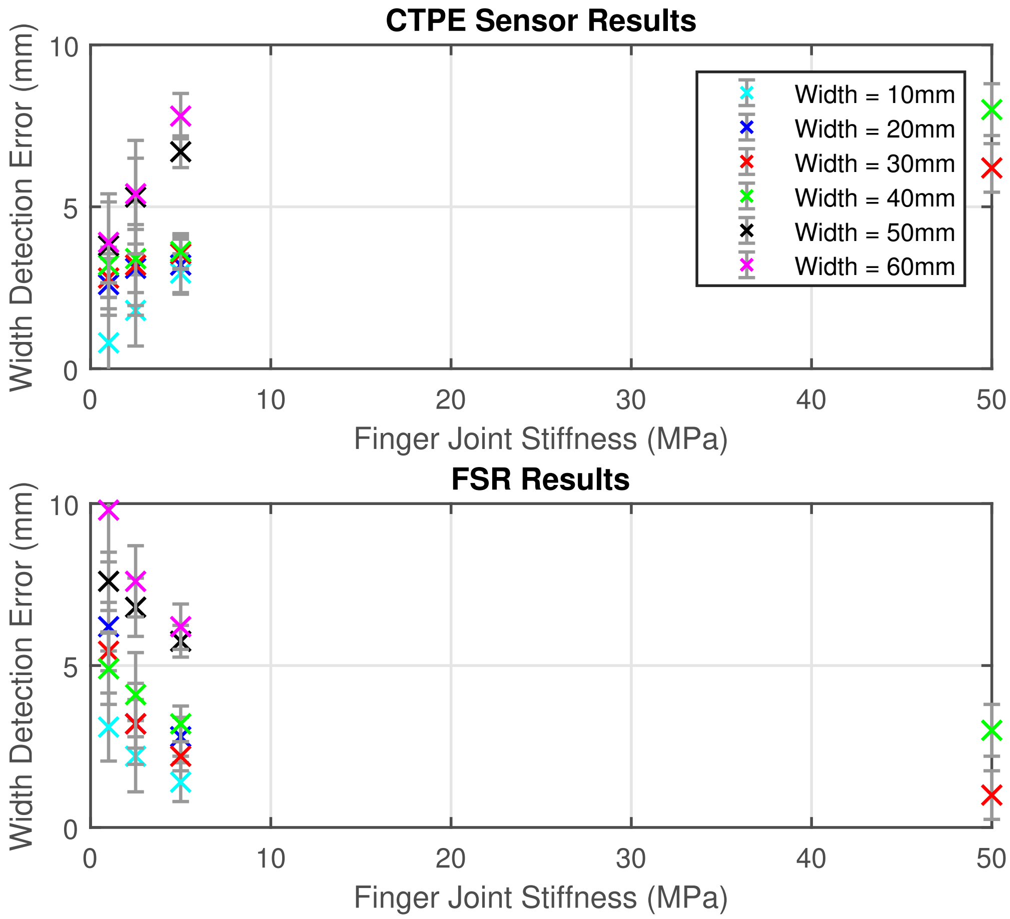

Figure 6.9 Errors in width detection for fingers of different stiffness for objects of different widths. Each experiment was repeated 5 times. The stiffest finger (50MPa) was insufficiently compliant to detect the higher and larger objects

measured until the finger truly detects the object. The difference in error between the different fingers is less significant for the FSR in comparison to the CTPE results.

6.4.2 Detection of Material Stiffness

In this section the response of fingers of different stiffness to objects of different stiffness is investigated. The postural response when the fingers interact with materials of different properties was recorded. A finger was mounted onto the end of the UR5 parallel to the surface. Fingers of different joint stiffness were lowered onto cubes of varying stiffness (but with the same surface friction) to identify which finger stiffness provides the greatest ability to identify between different materials. They are lowered down 1cm below the point

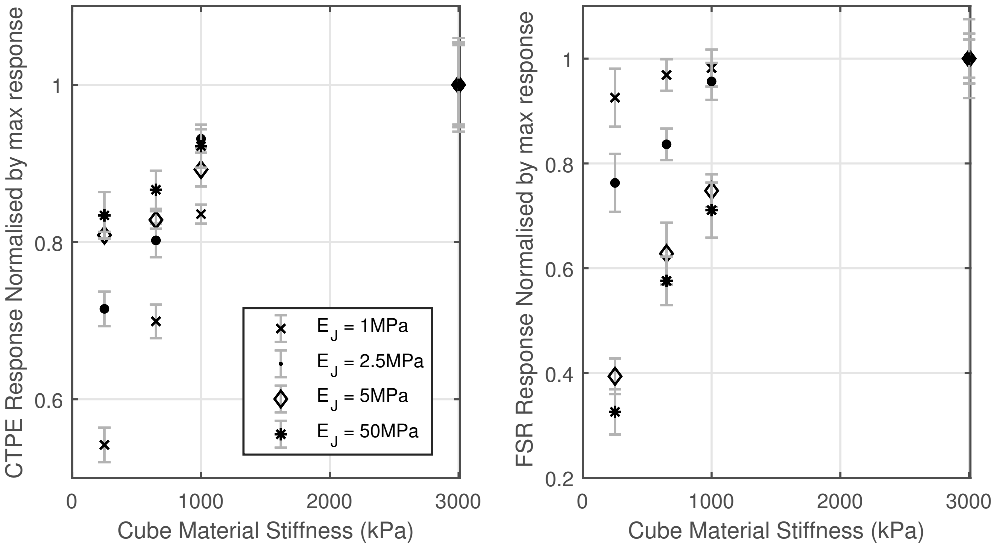

Figure 6.10 Response of the FSR and CTPE sensor (normalised against the largest response) when interacting with objects of different stiffness but same size and friction by tapping.

at which the finger first touches the cube surface such that the fingers undergo deformation. This is repeated 10 times for each cube and finger combination. The responses from the FSR and CTPE, mounted as in the previous experiment, was recorded. The results are shown in Fig. 6.10. The response from both sensors is normalised against the highest change in response for each finger to allow direct comparison between fingers and sensors as the physical integration changes the base resistance.

The largest changes in posture and hence CTPE response are seen for the lowest stiffness finger. However, for the lower stiffness fingers, the biggest change in sensor reading is observed for the softest materials which are most compliance and hence can undergo the greatest change in posture. However, if the stiffness was further reduced, the fingers could become too compliant such that there is no variation in the response to different materials. The fingers that are stiffer also show the greatest change for lowest stiffness materials, however with a lower magnitude change. In comparison, the FSR results show a much greater change in response to different objects. However, the stiffest fingers shows the greatest change in force. There is a trade-off in terms of range, sensitivity and precision. The lower stiffness fingers are most suited when using posture to detect body dynamics, providing the largest range of response but this limits the sensitivity when using force to detect stiffness.

6.5 Discussion & Conclusion

In this section it was investigated how body dynamics can be used to understand the environment. It has been demonstrated how the resultant mechanics of complex soft-rigid hybrid systems varies depending on both the environment and the dynamic control of the system. The 'soft' component of hybrid robots provides a compliance that allows for greater exploitation of proprioception than typical rigid robotic systems. Further work optimising the dynamics and mechanical properties should be investigated.

By introducing sensors that allow the identification of posture and force applied, it is possible to achieve some awareness of the environmental morphology and material properties. Further work to understand how the sensor morphology can best aid proprioception (incorporating work from Chapter 3) and provide the greatest understanding about the environment is required to further extend this concept.

The optimisation of mechanical systems to transduce or amplify the environmental stimuli has been introduced by investigating fingers with different stiffness. This has shown mechanical properties vastly affect the abilities of sensing through body dynamics. Extending this work to investigate how the physical dynamics and anisotropic stiffness of systems can be used to maximise the perception should be pursued.

Looking further forward to where this concept could be applied, there are many potential application. This concept could be extended such that in addition to the mechanics aiding perception, the mechanics could 'guide' or aid exploration. For example, the physical mechanical system could be used to identify depressions in a surface. Examples of where this principle could be used include medical palpation and examination. This is a currently a task which makes use of the mechanics and proprioception of the human hand.

Chapter 7

Discussion & Conclusions

This thesis proposes an approach to the development of soft robots utilising distributed intelligence from embodiment. Within this model, the integration of materials and morphology contribute towards both sensing and perception and enable complex environmental interactions. A number of case studies are given in Chapters 3-6 which demonstrate the strength of this embodied approach and provide new design methodologies and frameworks for the design and manufacture of soft robots.

Key to the design philosophy for embodied soft robotics is the integrated approach, where it is understood that materials, morphology and mechanical design contribute to the adaptive behaviours. Chapter 3 focuses on the development of morphologies for soft sensors to aid the perception of varying stimuli for large area soft sensing. The morphology allows localised processing of the deformation of the soft body such that the embodied intelligence aids perception. Following on from this, Chapter 4 discusses the direct embodiment of materials to achieve both sensing and active behaviours. The role of embodiment to extend the range of behavioural output is analysed in Chapter 5, with soft-rigid hybrid design approaches proposed. Finally, in Chapter 6, the use of body mechanics of soft-rigid hybrid systems for environmental perception is explored. This exploits the complex environmental interactions which can be achieved with soft-rigid hybrid systems.

The work presented in this thesis is only a small step towards using an embodied approach to achieve soft robotics with rich, varied and nuanced behaviour which is enabled by high sensitivity perception. This chapter aims to relate the findings presented in the different chapters to the larger research area and discusses future work. The next section discusses the achievements in the context of the hypotheses and contributions stated in Chapter 1.

7.1 Summary of Research Contributions

The research contributions made in this thesis address the two main hypotheses. This section provides a summary of the research contributions and their relevance to these hypotheses.

7.1.1 Hypothesis 1: Soft-Rigid Hybrid Design Enables Increasingly Adaptive Behaviours

The design and fabrication of soft-rigid hybrid robots can enable increasingly environmentally adaptive behaviours. This hypothesis has been demonstrated by the following research contributions:

- In Chapter 5 it was shown how nuanced and complex adaptive behaviours can be achieved from passive dynamics. The anisotropic stiffness of soft rigid hybrid structures allows complex passive dynamics to be achieved. Such systems can be manufactured using multi-material 3D printing. This has enabled the development of a soft-rigid hybrid anthropomorphic skeleton hand that can perform piano playing in various styles. This hand exhibits complex thumb abduction and adduction behaviour that is typically hard to achieve in robotic systems.

- The ability of materials to change their properties and thereby contribute to environmentally adaptive behaviours was shown in Chapter 4. The material developed, CHMA, allowed the stiffness and 'tack' force to be modified to allow grasping.

7.1.2 Hypothesis 2: Sensing materials and morphology can provide intelligence through embodiment which assists perception.

This hypothesis has been demonstrated by the following research contributions:

- Chapter 3 introduced sensor morphologies for soft sensing. Sensor morphology specifically applied to soft sensing showed the importance of morphology for soft systems through a number of case studies (object recognition, reconstruction and motion detection). Development of the 'differential sensing' morphology demonstrated how morphology can be used to provide embodied processing or intelligence. This morphology was applied to the Universal Gripper to allow sensing of the deformable surface. This is believed to be one of the first implementations of soft sensing on the surface of the Universal Gripper.

- The role of materials in sensing and funtionalisation was shown in Chapter 4. This work showed the functionalisation of a soft material (CHMA) to provide integrated sensing and change in material properties.
- Chapter 6 demonstrated how materials and the mechanical design of soft-rigid hybrid systems can aid perception through body dynamics. Soft sensors were integrated to provide postural sensing. The postural information allowed body dynamics to be used to provide environmental awareness.

7.2 Impact and Utility of Contributions

The exploration of sensor morphologies for addressing the challenge of large area soft sensing has demonstrated that this embodied approach can be used to assist with perception. The work in Chapter 3 extends the concept of sensor morphology for perception beyond existing approaches [35]. Analysis of a simple grid morphology outlines the abilities and role of morphology in deformation sensing, and has been extended to allow object identification. The development of the 'Differential Sensing' framework provides a new approach to sensing, where the morphology is used to directly change what the sensor perceives. Through embodiment the morphology performs local processing of the strain experienced allowing detection of the magnitude, location and direction of the applied strain. This is a new method of approaching sensor morphology, which could be extended to allow identification of more generalised parameters such as specific objects or shapes.

This embodied approach of using sensor morphology to enable sensing of complex deformable bodies has been exemplified by applying the morphologies to the Universal Gripper. Believed to be on the first implementation of directly sensing the deformable area, this provides the ability to detect objects when grasping. This could enable perception of the environment and allow for adaptive control when grasping objects. Many of the challenges surrounding sensing for soft robotics are addressed in this approach [194]. The scalability and ease of integration significantly aids the potential impact of this approach.

The role of embodiment of the sensor has been considered, however the material itself can also be used to contribute to the perception and behaviour of a system. Developing materials with embedded sensing capabilities allows the contribution of the materials to be extended to influence the overall behaviour [75]. By extending the embodied properties further, such that the material properties can be also controlled, the utility of the sensor is further increased. The embodied properties provide integrated multi-functionality. This provides a new approach for material development, where the required sensing and functional changes should be considered when choosing the materials required. Using this concept

CHMA (Conductive Hot Melt Adhesive) was developed. The material allows both sensing and functional change such that it could be used to perform single-point grasping.

Alongside the sensing capabilities, the development of complex behaviours is a second area where embodiment can be utilised. The concept of soft-rigid hybrid systems allows the design and development of systems that can show complex behaviours. A method for utilising the inherent passive dynamics of systems to achieve complexity is provided through the development of the 'Conditional Stiffness' framework. Passivity is an interesting concept as the resultant behaviours require no additional actuation or control; however the challenge remains in the design and manufacture. Multi-material 3D printing enables the printing of complex mechanical structures with varying materials [211]. Using this technique soft-rigid hybrid systems with isotropic stiffness can be developed. This allows for complex passive systems to be developed. An anthropomorphic hand utilising this concept was developed to show complex and varied behaviours. Passivity does allow for nuanced and complex behaviours which are hard to achieve using typical robotic paradigms. However, the extent to which passivity inspired approaches can be used to address many complex applications remains a question.

Although sensing in robotics is typically performed using integrated sensing technology, biological systems use a wider variety of sensing approach [224]. One of which is using the body dynamics to provide sensory information based on environmental interactions. Soft-rigid hybrid robotic systems provide increase compliance, whilst also having sufficient rigidity to allow the body mechanics to be directly used to understand the environment. It has been show how environmental parameters affect the interaction between robotic systems and the environment. By integrating soft sensors into hybrid systems to provide postural awareness, body dynamics can be used to obtain information about the environment, such as the morphology or material properties. An extension of previous approaches to this area, it has been demonstrated how the mechanics of the mechanical body can be altered to maximise the ability to distinguish and detect particular stimuli.

7.2.1 Related Work

In addition to the work presented in this thesis, there are number of other research projects which have leveraged or have augmented the presented work and led to peer reviewed research publications[1]. These project are briefly summarised, with more details given in Appendix B.

[1]The work published or accepted in peer reviewed journals is denoted with a *, with submitted work under review marked with an $^{+}$.

- **Automated Robotic Lettuce Harvester.** Iceberg lettuce is a crop which is challenging to automatically harvest as it is easily damaged so is harvested manually which is labour intensive. This research focused on the development of a soft-rigid hybrid manipulator for iceberg lettuce harvesting. This was then integrated into an automated harvesting system and tested in the field.

- **Lettuce leaf removal*.** After lettuce harvesting (manual or automated) some outer leaves often remain which must be removed to achieve ‘supermarket-ready’ lettuce. An automated novel vision pipeline and manipulation system utilising hybrid concepts has been developed.

- **Data Synthesis for Classification in Autonomous Robotic Grasping System**.** Although only tactile sensing has been considered in this work, combining this with vision would enable greater environmental awareness. This research examines how limited data sets of product images of ‘off the shelf’ items can be used to generate a synthetic data set that can be used to train a neural network which allows classification, segmentation and grasping of the item. This was then tested in an object grasping scenario.

- **Flexible Assembly of Structures Using Autonomous Robotic Systems^{+}.** Another area where manipulation can be utilised for significant impact is in construction. In this research, a framework for flexible re-assembly is developed and a robotic platform is developed to implement and test this framework with simple Lego bricks.

7.3 Is the future of soft robotics embodied?

Soft robotics has a key role in enabling ubiquitous robotics with the capabilities and utility to improve quality of life and solve many of the challenges in the 21st Century [5, 21]. However, to extend impact and utility, its capabilities must be extended. The work presented has been designed not only to demonstrate the technologies, frameworks and approaches for embodied soft robotics, but also to understand the fundamental limits of embodiment applied to soft robotics.

This thesis started with a design approach for soft robotics that leverages embodied intelligence (Fig. 1.1). The presented research examined how this approach can be used to aid perception and the adaptive behaviours of soft systems. Chapters 3-4 focused on the roles of material and morphology to aid perception, with Chapters 5-6 focusing on the development of adaptive soft rigid hybrid systems. The question now remains: is embodiment critical and how far can this approach take soft robotics? As highlighted in this work, most notably in Chapter 5 with the development of the anthropomorphic skeleton hand, bio-inspired solutions show embodied behaviours, which enable the entire body to contribute towards the 'intelligence' of the system. This is also seen in Chapter 6 with use of body dynamics aiding perception. This concept has been proposed as an explanation for complexity in behaviours and perception that are seen in biological systems [11]. This has been demonstrated through the use of sensor morphology (Chapter 3) to provide intelligent understanding of deformation. Additionally, passive mechanical systems can provide behaviours, for example complex thumb abduction or adduction of an anthromophoric hand. Using this approach, embodiment has shown how local processing can be used to aid perception and behaviours. It could be argued that similar behaviour could be achieved using signal processing in place of sensor morphology, or using highly complex actuation and control systems. However, these methods are computationally and mechanically inefficient in that the mechanics and control are focusing on low level tasks. This prevents large scale systems from achieving behaviours or perception coming close to that of animals. However, is extrapolating the work and concept presented here sufficient to achieve the complexity of systems required?

The embodied approach makes design and development more complex. The whole system must be developed in an integrated manner, where sensing, actuation, perception and intelligence are considered at every stage and for every system of the robot. This design complexity is rewarded in the resultant behaviours. The final piece in this jigsaw of soft robotic development to make embodiment truly powerful is the link from embodiment in the physical system through to learning. This would address how material, mechanics and morphology could be used to allow systems to learn faster or become more intelligent than they would other. The approach could be extended to encompass the link between embodied in the physical systems which aids and contributes towards the learning of the system.

This would extend the embodiment concept to include body-awareness and unconscious behaviours which the system can produce without direct control or 'thought'. Designing embodiment to enable systems which show more complex intelligence unconscious behaviours furthers extends the range of behaviours and responsiveness of soft systems. This behaviour could example mirror the unconscious understanding of body dynamics and movement, or the unconscious reaction of an biological system to pain or heat.

7.4 Future Work

The framework and technologies developed have demonstrated the potential of localised computation and embodiment. To extend this work towards achieving soft robotics with the required capabilities, a number of directions for further exploration are proposed.

The sensing morphologies developed provided novel methods for achieving large area soft sensing. The elastomer in which the sensors are embedded provides a key role. Developing further understanding of the potential filtering effects could allow the embodied behaviour to be increased. Can material be used to limit or dictate the response that can be gained from the sensor morphology? The integration of material properties and sensor morphology further extends and tests the approach of utilising embodied intelligence in soft robots.

To take the approach of embodiment further, the influence that embodiment has on the learning abilities of a system should be understood. Specifically understanding how sensor morphology can be used to reduce the time a system takes to learn, or how it can be used to aid unsupervised learning. Additionally, investigating how learning can be applied to the sensory-actuation system to allow learning to exploit 'Conditional Stiffness' would allow automated exploitation of this physical phenomena.

Exploiting passivity to create systems that can achieve nuanced and complex movements has shown how complex hybrid systems can be used to maximise environmental interactions. Passivity is 'intelligence' which can be leveraged at no additional cost to the system. Understanding the optimum point at which additional control or actuation aids output behaviour at a reasonable additional computation and power costs would enable an ideal trade-off between passivity and actuation to be reached.

The development of hybrid joint systems which can be used to achieve conditional stiffness was demonstrated with single joint systems. Extending this to include interactions between multiple joints and formulating the required design rules would aid development. This could allow the development of large systems with increasingly complex and interesting dynamics to be investigated. Understanding the mapping between isotropic stiffness and behaviours would allow this to be exploited and would allow more formal design approaches to be developed.

The research focused on the use of body dynamics for perception considered only the passive behaviours of mechanical systems. Understanding the links between the design of these systems and the environmental perception that can be achieved would allow manipulators to be designed to maximise 'body awareness' of the environment. Additionally, this approach could be applied to actively controlled hybrid systems, where the effects of actuation must also be considered.

Using proprioception to guide exploration could also provide further embodied behaviours. For example, the mechanics of a hand which shows complex conditional stiffness behaviours could enable physical detection of more rigid or solid bodies in soft organisms.

In summary, this thesis has demonstrated how an intelligence provided through mechanical, morphological and material design can aid perception and environmentally adaptive behaviours. This research opens up many exiting directions for future research which questions our understanding of models of robotics systems, embedded cognition and intelligence.

Bibliography

[1] H. Lee, J. Choi, and S. Kwak, "Can human jobs be taken by robots?: The appropriate match between robot types and task types," *Archives of Design Research*, vol. 28, no. 3, pp. 49–59, 2015.

[2] H.-D. Burkhard, D. Duhaut, M. Fujita, P. Lima, R. Murphy, and R. Rojas, "The road to robocup 2050," *IEEE Robotics & Automation Magazine*, vol. 9, no. 2, pp. 31–38, 2002.

[3] S. Schaal, "The new robotics—towards human-centered machines," *HFSP journal*, vol. 1, no. 2, pp. 115–126, 2007.

[4] C. Laschi and M. Cianchetti, "Soft robotics: new perspectives for robot bodyware and control," *Frontiers in bioengineering and biotechnology*, vol. 2, p. 3, 2014.

[5] A. Edsinger and C. C. Kemp, "Manipulation in human environments," in *2006 6th IEEE-RAS International Conference on Humanoid Robots*. IEEE, 2006, pp. 102–109.

[6] H. Yousef, M. Boukallel, and K. Althoefer, "Tactile sensing for dexterous in-hand manipulation in robotics—a review," *Sensors and Actuators A: physical*, vol. 167, no. 2, pp. 171–187, 2011.

[7] G.-Z. Yang, J. Bellingham, P. E. Dupont, P. Fischer, L. Floridi, R. Full, N. Jacobstein, V. Kumar, M. McNutt, R. Merrifield *et al.*, "The grand challenges of science robotics," *Science Robotics*, vol. 3, no. 14, p. eaar7650, 2018.

[8] S. Kim, C. Laschi, and B. Trimmer, "Soft robotics: a bioinspired evolution in robotics," *Trends in biotechnology*, vol. 31, no. 5, pp. 287–294, 2013.

[9] F. Ilievski, A. D. Mazzeo, R. F. Shepherd, X. Chen, and G. M. Whitesides, "Soft robotics for chemists," *Angewandte Chemie International Edition*, vol. 50, no. 8, pp. 1890–1895, 2011.

[10] C. Laschi and M. Cianchetti, "Soft robotics: new perspectives for robot bodyware and control," *Frontiers in bioengineering and biotechnology*, vol. 2, p. 3, 2014.

[11] R. Pfeifer, M. Lungarella, and F. Iida, "Self-organization, embodiment, and biologically inspired robotics," *science*, vol. 318, no. 5853, pp. 1088–1093, 2007.

[12] S. Bauer, S. Bauer-Gogonea, I. Graz, M. Kaltenbrunner, C. Keplinger, and R. Schwödiauer, "25th anniversary article: a soft future: from robots and sensor skin to energy harvesters," *Advanced Materials*, vol. 26, no. 1, pp. 149–162, 2014.

[13] C. Majidi, “Soft robotics: a perspective—current trends and prospects for the future,” *Soft Robotics*, vol. 1, no. 1, pp. 5–11, 2014.

[14] S. Kim, C. Laschi, and B. Trimmer, “Soft robotics: a bioinspired evolution in robotics,” *Trends in biotechnology*, vol. 31, no. 5, pp. 287–294, 2013.

[15] M. Cianchetti, T. Ranzani, G. Gerboni, I. De Falco, C. Laschi, and A. Menciassi, “Stiff-flop surgical manipulator: mechanical design and experimental characterization of the single module,” in *IEEE/RSJ International Conference on Intelligent Robots and Systems*. IEEE, 2013, pp. 3576–3581.

[16] G. Tonietti, R. Schiavi, and A. Bicchi, “Design and control of a variable stiffness actuator for safe and fast physical human/robot interaction,” in *Proceedings of the 2005 IEEE International Conference on Robotics and Automation*. IEEE, 2005, pp. 526–531.

[17] X. Broquere, D. Sidobre, and I. Herrera-Aguilar, “Soft motion trajectory planner for service manipulator robot,” in *2008 IEEE/RSJ International Conference on Intelligent Robots and Systems*. IEEE, 2008, pp. 2808–2813.

[18] ——, “Soft motion trajectory planner for service manipulator robot,” in *2008 IEEE/RSJ International Conference on Intelligent Robots and Systems*. IEEE, 2008, pp. 2808–2813.

[19] M. Wehner, B. Quinlivan, P. M. Aubin, E. Martinez-Villalpando, M. Baumann, L. Stirling, K. Holt, R. Wood, and C. Walsh, “A lightweight soft exosuit for gait assistance,” in *Robotics and Automation (ICRA), 2013 IEEE International Conference on*. IEEE, 2013, pp. 3362–3369.

[20] P. Polygerinos, Z. Wang, K. C. Galloway, R. J. Wood, and C. J. Walsh, “Soft robotic glove for combined assistance and at-home rehabilitation,” *Robotics and Autonomous Systems*, vol. 73, pp. 135–143, 2015.

[21] R. Pfeifer, M. Lungarella, and F. Iida, “The challenges ahead for bio-inspired’soft’robotics,” *Communications of the ACM*, vol. 55, no. 11, pp. 76–87, 2012.

[22] H. Lipson, “Challenges and opportunities for design, simulation, and fabrication of soft robots,” *Soft Robotics*, vol. 1, no. 1, pp. 21–27, 2014.

[23] F. L. Hammond, J. Weisz, A. Andrés, P. K. Allen, and R. D. Howe, “Towards a design optimization method for reducing the mechanical complexity of underactuated robotic hands,” in *Robotics and Automation (ICRA), 2012 IEEE International Conference on*. IEEE, 2012, pp. 2843–2850.

[24] L. U. Odhner, R. R. Ma, and A. M. Dollar, “Open-loop precision grasping with underactuated hands inspired by a human manipulation strategy,” *IEEE Transactions on Automation Science and Engineering*, vol. 10, no. 3, pp. 625–633, 2013.

[25] C. Mattmann, F. Clemens, and G. Tröster, “Sensor for measuring strain in textile,” *Sensors*, vol. 8, no. 6, pp. 3719–3732, 2008.

[26] J.-B. Chossat, Y.-L. Park, R. J. Wood, and V. Duchaine, "A soft strain sensor based on ionic and metal liquids," *IEEE Sensors Journal*, vol. 13, no. 9, pp. 3405–3414, 2013.

[27] E. Guglielmino, L. Zullo, M. Cianchetti, M. Follador, D. Branson, and D. G. Caldwell, "The application of embodiment theory to the design and control of an octopus-like robotic arm," in *Robotics and Automation (ICRA), 2012 IEEE International Conference on*. IEEE, 2012, pp. 5277–5282.

[28] E. Brown, N. Rodenberg, J. Amend, A. Mozeika, E. Steltz, M. R. Zakin, H. Lipson, and H. M. Jaeger, "Universal robotic gripper based on the jamming of granular material," *Proceedings of the National Academy of Sciences*, vol. 107, no. 44, pp. 18 809–18 814, 2010.

[29] J. J. Craig, *Introduction to robotics: mechanics and control*. Pearson/Prentice Hall Upper Saddle River, NJ, USA:, 2005, vol. 3.

[30] C. Duriez, "Control of elastic soft robots based on real-time finite element method," in *Robotics and Automation (ICRA), 2013 IEEE International Conference on*. IEEE, 2013, pp. 3982–3987.

[31] C. Laschi, B. Mazzolai, V. Mattoli, M. Cianchetti, and P. Dario, "Design of a biomimetic robotic octopus arm," *Bioinspiration and Biomimetics*, vol. 4, no. 1, p. 015006, 2009.

[32] M. Calisti, A. Arienti, F. Renda, G. Levy, B. Hochner, B. Mazzolai, P. Dario, and C. Laschi, "Design and development of a soft robot with crawling and grasping capabilities," in *Robotics and Automation (ICRA), 2012 IEEE International Conference on*, May 2012, pp. 4950–4955.

[33] M. Calisti, M. Giorelli, G. Levy, B. Mazzolai, B. Hochner, C. Laschi, and P. Dario, "An octopus-bioinspired solution to movement and manipulation for soft robots," *Bioinspiration & biomimetics*, vol. 6, no. 3, p. 036002, 2011.

[34] B. A. Trimmer, A. E. Takesian, B. M. Sweet, C. B. Rogers, D. C. Hake, and D. J. Rogers, "Caterpillar locomotion: a new model for soft-bodied climbing and burrowing robots," in *7th International Symposium on Technology and the Mine Problem*, vol. 1. Mine Warfare Association Monterey, CA, 2006, pp. 1–10.

[35] R. Pfeifer and G. Gómez, "Morphological computation–connecting brain, body, and environment," in *Creating brain-like intelligence*. Springer, 2009, pp. 66–83.

[36] M. G. Catalano, G. Grioli, A. Serio, E. Farnioli, C. Piazza, and A. Bicchi, "Adaptive synergies for a humanoid robot hand," in *Humanoid Robots (Humanoids), 2012 12th IEEE-RAS International Conference on*. IEEE, 2012, pp. 7–14.

[37] A. Bicchi, M. Gabiccini, and M. Santello, "Modelling natural and artificial hands with synergies," *Phil. Trans. R. Soc. B*, vol. 366, no. 1581, pp. 3153–3161, 2011.

[38] I. Poulakakis, E. Papadopoulos, and M. Buehler, "On the stability of the passive dynamics of quadrupedal running with a bounding gait," *The International Journal of Robotics Research*, vol. 25, no. 7, pp. 669–687, 2006.

[39] M. D. Grissom, V. Chitrakaran, D. Dienno, M. Csencits, M. Pritts, B. Jones, W. McMahan, D. Dawson, C. Rahn, and I. Walker, "Design and experimental testing of the octarm soft robot manipulator," in *Defense and Security Symposium*. International Society for Optics and Photonics, 2006, pp. 62 301F–62 301F.

[40] B. S. Homberg, R. K. Katzschmann, M. R. Dogar, and D. Rus, "Haptic identification of objects using a modular soft robotic gripper," in *Intelligent Robots and Systems (IROS), 2015 IEEE/RSJ International Conference on*, Sept 2015, pp. 1698–1705.

[41] U. Culha and F. Iida, "Enhancement of finger motion range with compliant anthropomorphic joint design," *Bioinspiration and Biomimetics*, vol. 11, no. 2, p. 026001, 2016.

[42] F. Iida and C. Laschi, "Soft robotics: Challenges and perspectives," *Procedia Computer Science*, vol. 7, pp. 99–102, 2011.

[43] Y.-L. Park, B.-R. Chen, and R. J. Wood, "Design and fabrication of soft artificial skin using embedded microchannels and liquid conductors," *IEEE Sensors Journal*, vol. 12, no. 8, pp. 2711–2718, 2012.

[44] Y.-L. Park, C. Majidi, R. Kramer, P. Bérard, and R. J. Wood, "Hyperelastic pressure sensing with a liquid-embedded elastomer," *Journal of Micromechanics and Microengineering*, vol. 20, no. 12, p. 125029, 2010.

[45] D. M. Vogt, Y.-L. Park, and R. J. Wood, "Design and characterization of a soft multi-axis force sensor using embedded microfluidic channels," *IEEE Sensors Journal*, vol. 13, no. 10, pp. 4056–4064, 2013.

[46] G. Schwartz, B. C.-K. Tee, J. Mei, A. L. Appleton, D. H. Kim, H. Wang, and Z. Bao, "Flexible polymer transistors with high pressure sensitivity for application in electronic skin and health monitoring," *Nature communications*, vol. 4, p. 1859, 2013.

[47] T. Someya, T. Sekitani, S. Iba, Y. Kato, H. Kawaguchi, and T. Sakurai, "A large-area, flexible pressure sensor matrix with organic field-effect transistors for artificial skin applications," *Proceedings of the National Academy of Sciences of the United States of America*, vol. 101, no. 27, pp. 9966–9970, 2004.

[48] S. C. Mannsfeld, B. C. Tee, R. M. Stoltenberg, C. V. H. Chen, S. Barman, B. V. Muir, A. N. Sokolov, C. Reese, and Z. Bao, "Highly sensitive flexible pressure sensors with microstructured rubber dielectric layers," *Nature materials*, vol. 9, no. 10, pp. 859–864, 2010.

[49] Y. Noguchi, T. Sekitani, and T. Someya, "Organic-transistor-based flexible pressure sensors using ink-jet-printed electrodes and gate dielectric layers," *Applied physics letters*, vol. 89, no. 25, p. 3507, 2006.

[50] S. Park, M. Vosguerichian, and Z. Bao, "A review of fabrication and applications of carbon nanotube film-based flexible electronics," *Nanoscale*, vol. 5, no. 5, pp. 1727–1752, 2013.

[51] D. J. Lipomi, M. Vosgueritchian, B. C. Tee, S. L. Hellstrom, J. A. Lee, C. H. Fox, and Z. Bao, "Skin-like pressure and strain sensors based on transparent elastic films of carbon nanotubes," *Nature nanotechnology*, vol. 6, no. 12, pp. 788–792, 2011.

[52] J. Zhou, Y. Gu, P. Fei, W. Mai, Y. Gao, R. Yang, G. Bao, and Z. L. Wang, "Flexible piezotronic strain sensor," *Nano letters*, vol. 8, no. 9, pp. 3035–3040, 2008.

[53] Q. Liao, M. Mohr, X. Zhang, Z. Zhang, Y. Zhang, and H.-J. Fecht, "Carbon fiber–zno nanowire hybrid structures for flexible and adaptable strain sensors," *Nanoscale*, vol. 5, no. 24, pp. 12 350–12 355, 2013.

[54] H. Gullapalli, V. S. Vemuru, A. Kumar, A. Botello-Mendez, R. Vajtai, M. Terrones, S. Nagarajaiah, and P. M. Ajayan, "Flexible piezoelectric zno–paper nanocomposite strain sensor," *small*, vol. 6, no. 15, pp. 1641–1646, 2010.

[55] A. Frutiger, J. T. Muth, D. M. Vogt, Y. Mengüç, A. Campo, A. D. Valentine, C. J. Walsh, and J. A. Lewis, "Capacitive soft strain sensors via multicore–shell fiber printing," *Advanced Materials*, vol. 27, no. 15, pp. 2440–2446, 2015.

[56] L. Cai, L. Song, P. Luan, Q. Zhang, N. Zhang, Q. Gao, D. Zhao, X. Zhang, M. Tu, F. Yang *et al.*, "Super-stretchable, transparent carbon nanotube-based capacitive strain sensors for human motion detection," *Scientific reports*, vol. 3, 2013.

[57] G. T. Pham, Y.-B. Park, Z. Liang, C. Zhang, and B. Wang, "Processing and modeling of conductive thermoplastic/carbon nanotube films for strain sensing," *Composites Part B: Engineering*, vol. 39, no. 1, pp. 209–216, 2008.

[58] W. Luheng, D. Tianhuai, and W. Peng, "Influence of carbon black concentration on piezoresistivity for carbon-black-filled silicone rubber composite," *Carbon*, vol. 47, no. 14, pp. 3151–3157, 2009.

[59] C. Mattmann, O. Amft, H. Harms, G. Troster, and F. Clemens, "Recognizing upper body postures using textile strain sensors," in *2007 11th IEEE International Symposium on Wearable Computers*. IEEE, 2007, pp. 29–36.

[60] C. Cochrane, V. Koncar, M. Lewandowski, and C. Dufour, "Design and development of a flexible strain sensor for textile structures based on a conductive polymer composite," *Sensors*, vol. 7, no. 4, pp. 473–492, 2007.

[61] P. Calvert, D. Duggal, P. Patra, A. Agrawal, and A. Sawhney, "Conducting polymer and conducting composite strain sensors on textiles," *Molecular Crystals and Liquid Crystals*, vol. 484, no. 1, pp. 291–657, 2008.

[62] T. Yamada, Y. Hayamizu, Y. Yamamoto, Y. Yomogida, A. Izadi-Najafabadi, D. N. Futaba, and K. Hata, "A stretchable carbon nanotube strain sensor for human-motion detection," *Nature nanotechnology*, vol. 6, no. 5, pp. 296–301, 2011.

[63] B. Winstone, G. Griffiths, C. Melhuish, T. Pipe, and J. Rossiter, "Tactip—tactile fingertip device, challenges in reduction of size to ready for robot hand integration," in *Robotics and Biomimetics (ROBIO), 2012 IEEE International Conference on*. IEEE, 2012, pp. 160–166.

[64] B. Winstone, G. Griffiths, T. Pipe, C. Melhuish, and J. Rossiter, “Tactip-tactile fingertip device, texture analysis through optical tracking of skin features,” in *Conference on Biomimetic and Biohybrid Systems*. Springer, 2013, pp. 323–334.

[65] P. Puangmali, K. Althoefer, L. D. Seneviratne, D. Murphy, and P. Dasgupta, “State-of-the-art in force and tactile sensing for minimally invasive surgery,” *IEEE Sensors Journal*, vol. 8, no. 4, pp. 371–381, 2008.

[66] Y.-L. Park, K. Chau, R. J. Black, and M. R. Cutkosky, “Force sensing robot fingers using embedded fiber bragg grating sensors and shape deposition manufacturing,” in *Proceedings 2007 IEEE International Conference on Robotics and Automation*. IEEE, 2007, pp. 1510–1516.

[67] D. M. Vogt, Y.-L. Park, and R. J. Wood, “Design and characterization of a soft multi-axis force sensor using embedded microfluidic channels,” *IEEE sensors Journal*, vol. 13, no. 10, pp. 4056–4064, 2013.

[68] H. Yamashita, K. Shibuya, Z. Wang, S. Hirai, J. Nagase, K. Tsutsumi *et al.*, “Function-selectable tactile sensing system with morphological change,” in *System Integration (SII), 2016 IEEE/SICE International Symposium on*. IEEE, 2016, pp. 415–420.

[69] H. Yamashita, Z. Wang, S. Hirai, K. Shibuya *et al.*, “Morphological computation in tactile sensing: The role of wrinkle,” in *Robotics and Automation (ICRA), 2017 IEEE International Conference on*. IEEE, 2017, pp. 4977–4984.

[70] R. D. Howe and M. R. Cutkosky, “Sensing skin acceleration for slip and texture perception,” in *Robotics and Automation, 1989. Proceedings., 1989 IEEE International Conference on*. IEEE, 1989, pp. 145–150.

[71] G. Paviglianiti, F. Pierri, F. Caccavale, and M. Mattei, “Robust fault detection and isolation for proprioceptive sensors of robot manipulators,” *Mechatronics*, vol. 20, no. 1, pp. 162–170, 2010.

[72] R. K. Kramer, C. Majidi, R. Sahai, and R. J. Wood, “Soft curvature sensors for joint angle proprioception,” in *Intelligent Robots and Systems (IROS), 2011 IEEE/RSJ International Conference on*. IEEE, 2011, pp. 1919–1926.

[73] M. C. Carrozza, F. Vecchi, F. Sebastiani, G. Cappiello, S. Roccella, M. Zecca, R. Lazzarini, and P. Dario, “Experimental analysis of an innovative prosthetic hand with proprioceptive sensors,” in *Robotics and Automation, 2003. Proceedings. ICRA’03. IEEE International Conference on*, vol. 2. IEEE, 2003, pp. 2230–2235.

[74] B. S. Homberg, R. K. Katzschmann, M. R. Dogar, and D. Rus, “Haptic identification of objects using a modular soft robotic gripper,” in *Intelligent Robots and Systems (IROS), 2015 IEEE/RSJ International Conference on*. IEEE, 2015, pp. 1698–1705.

[75] N. Correll and C. Heckman, “Materials that make robots smart,” *arXiv preprint arXiv:1711.00537*, 2017.

[76] P. T. Mather, “Responsive materials: Soft answers for hard problems,” *Nature materials*, vol. 6, no. 2, p. 93, 2007.

[77] D. Beal, F. Hover, M. Triantafyllou, J. Liao, and G. Lauder, “Passive propulsion in vortex wakes,” *Journal of Fluid Mechanics*, vol. 549, pp. 385–402, 2006.

[78] T. Hatanaka, N. Chopra, and M. W. Spong, “Passivity-based control of robots: Historical perspective and contemporary issues,” in *Decision and Control (CDC), 2015 IEEE 54th Annual Conference on*. IEEE, 2015, pp. 2450–2452.

[79] F. Boyer, M. Porez, F. Morsli, and Y. Morel, “Locomotion dynamics for bio-inspired robots with soft appendages: Application to flapping flight and passive swimming,” *Journal of Nonlinear Science*, vol. 27, no. 4, pp. 1121–1154, 2017.

[80] I. Fantoni, R. Lozano, and M. W. Spong, “Energy based control of the pendubot,” *IEEE Transactions on Automatic Control*, vol. 45, no. 4, pp. 725–729, 2000.

[81] G. Yang, I.-M. Chen, W. Lin, and J. Angeles, “Singularity analysis of three-legged parallel robots based on passive-joint velocities,” *IEEE transactions on robotics and automation*, vol. 17, no. 4, pp. 413–422, 2001.

[82] J.-B. Mouret and S. Doncieux, “Encouraging behavioral diversity in evolutionary robotics: An empirical study,” *Evolutionary computation*, vol. 20, no. 1, pp. 91–133, 2012.

[83] N. Ulrich, R. Paul, and R. Bajcsy, “A medium-complexity compliant end effector,” in *Robotics and Automation, 1988. Proceedings., 1988 IEEE International Conference on*. IEEE, 1988, pp. 434–436.

[84] A. M. Dollar and R. D. Howe, “The highly adaptive sdm hand: Design and performance evaluation,” *The international journal of robotics research*, vol. 29, no. 5, pp. 585–597, 2010.

[85] H. Arai and S. Tachi, “Position control of manipulator with passive joints using dynamic coupling,” *IEEE transactions on Robotics and Automation*, vol. 7, no. 4, pp. 528–534, 1991.

[86] B. Roy and H. H. Asada, “Nonlinear feedback control of a gravity-assisted underactuated manipulator with application to aircraft assembly,” *IEEE Transactions on Robotics*, vol. 25, no. 5, pp. 1125–1133, 2009.

[87] S. Wolf and G. Hirzinger, “A new variable stiffness design: Matching requirements of the next robot generation,” in *Robotics and Automation, 2008. ICRA 2008. IEEE International Conference on*. IEEE, 2008, pp. 1741–1746.

[88] S. Wolf, G. Grioli, O. Eiberger, W. Friedl, M. Grebenstein, H. Höppner, E. Burdet, D. G. Caldwell, R. Carloni, M. G. Catalano *et al.*, “Variable stiffness actuators: Review on design and components,” *IEEE/ASME transactions on mechatronics*, vol. 21, no. 5, pp. 2418–2430, 2016.

[89] G. Palli and C. Melchiorri, “Robust control of robots with variable joint stiffness,” in *Advanced Robotics, 2009. ICAR 2009. International Conference on*. IEEE, 2009, pp. 1–6.

[90] A. Jiang, G. Xynogalas, P. Dasgupta, K. Althoefer, and T. Nanayakkara, "Design of a variable stiffness flexible manipulator with composite granular jamming and membrane coupling," in *Intelligent Robots and Systems (IROS), 2012 IEEE/RSJ International Conference on*. IEEE, 2012, pp. 2922–2927.

[91] ——, "Design of a variable stiffness flexible manipulator with composite granular jamming and membrane coupling," in *Intelligent Robots and Systems (IROS), 2012 IEEE/RSJ International Conference on*. IEEE, 2012, pp. 2922–2927.

[92] J.-y. Nagase, S. Wakimoto, T. Satoh, N. Saga, and K. Suzumori, "Design of a variable-stiffness robotic hand using pneumatic soft rubber actuators," *Smart Materials and Structures*, vol. 20, no. 10, p. 105015, 2011.

[93] J. Hughes, U. Culha, F. Giardina, F. Guenther, A. Rosendo, and F. Iida, "Soft manipulators and grippers: a review," *Frontiers in Robotics and AI*, vol. 3, p. 69, 2016.

[94] F. J. Valero-Cuevas, J.-W. Yi, D. Brown, R. V. McNamara, C. Paul, and H. Lipson, "The tendon network of the fingers performs anatomical computation at a macroscopic scale," *IEEE Transactions on Biomedical Engineering*, vol. 54, no. 6, pp. 1161–1166, 2007.

[95] C. Della Santina, M. Bianchi, G. Averta, S. Ciotti, V. Arapi, S. Fani, E. Battaglia, M. G. Catalano, M. Santello, and A. Bicchi, "Postural hand synergies during environmental constraint exploitation," *Frontiers in neurorobotics*, vol. 11, p. 41, 2017.

[96] ——, "Postural hand synergies during environmental constraint exploitation," *Frontiers in neurorobotics*, vol. 11, p. 41, 2017.

[97] M. Santello, M. Bianchi, M. Gabiccini, E. Ricciardi, G. Salvietti, D. Prattichizzo, M. Ernst, A. Moscatelli, H. Jörntell, A. M. Kappers *et al.*, "Hand synergies: integration of robotics and neuroscience for understanding the control of biological and artificial hands," *Physics of life reviews*, vol. 17, pp. 1–23, 2016.

[98] K. Kim, K. R. Lee, W. H. Kim, K.-B. Park, T.-H. Kim, J.-S. Kim, and J. J. Pak, "Polymer-based flexible tactile sensor up to 32×32 arrays integrated with interconnection terminals," *Sensors and Actuators A: Physical*, vol. 156, no. 2, pp. 284 – 291, 2009. [Online]. Available: http://www.sciencedirect.com/science/article/pii/S092442470900377X

[99] D. Goger, N. Gorges, and H. Worn, "Tactile sensing for an anthropomorphic robotic hand: Hardware and signal processing," *2009 IEEE International Conference on Robotics and Automation*, pp. 895–901, 2009.

[100] T. Sagisaka, Y. Ohmura, Y. Kuniyoshi, A. Nagakubo, and K. Ozaki, "High-density conformable tactile sensing glove," *2011 11th IEEE-RAS International Conference on Humanoid Robots*, pp. 537–542, 2011.

[101] G. H. Büscher, R. Kõiva, C. Schürmann, R. Haschke, and H. J. Ritter, "Flexible and stretchable fabric-based tactile sensor," *Robotics and Autonomous Systems*, vol. 63, pp. 244 – 252, 2015, advances in Tactile Sensing and Touch-based Human Robot Interaction. [Online]. Available: http://www.sciencedirect.com/science/article/pii/S0921889014001821

[102] M. Shimojo, A. Namiki, M. Ishikawa, R. Makino, and K. Mabuchi, “A tactile sensor sheet using pressure conductive rubber with electrical-wires stitched method,” *IEEE Sensors Journal*, vol. 4, no. 5, pp. 589–596, 2004.

[103] U. Culha, U. Wani, S. G. Nurzaman, F. Clemens, and F. Iida, “Motion pattern discrimination for soft robots with morphologically flexible sensors,” in *2014 IEEE/RSJ International Conference on Intelligent Robots and Systems*. IEEE, 2014, pp. 567–572.

[104] S. Russo, T. Ranzani, H. Liu, S. Nefti-Meziani, K. Althoefer, and A. Menciassi, “Soft and stretchable sensor using biocompatible electrodes and liquid for medical applications,” *Soft Robotics*, vol. 2, no. 4, pp. 146–154, 2017/06/21 2015. [Online]. Available: https://doi.org/10.1089/soro.2015.0011

[105] D. Anghinolfi, G. Cannata, F. Mastrogiovanni, C. Nattero, and M. Paolucci, “On the problem of the automated design of large-scale robot skin,” *IEEE Transactions on Automation Science and Engineering*, vol. 10, no. 4, pp. 1087–1100, 2013.

[106] U. Culha, S. G. Nurzaman, F. Clemens, and F. Iida, “Svas3: Strain vector aided sensorization of soft structures,” *Sensors*, vol. 14, no. 7, pp. 12 748–12 770, 2014. [Online]. Available: http://www.mdpi.com/1424-8220/14/7/12748

[107] D. Hughes and N. Correll, “Texture recognition and localization in amorphous robotic skin,” *Bioinspiration & Biomimetics*, vol. 10, no. 5, p. 055002, 2015. [Online]. Available: http://stacks.iop.org/1748-3190/10/i=5/a=055002

[108] V. Wall, G. Zöller, and O. Brock, “A method for sensorizing soft actuators and its application to the rbo hand 2,” in *Robotics and Automation (ICRA), 2017 IEEE International Conference on*. IEEE, 2017, pp. 4965–4970.

[109] E. Brown, N. Rodenberg, J. Amend, A. Mozeika, E. Steltz, M. R. Zakin, H. Lipson, and H. M. Jaeger, “Universal robotic gripper based on the jamming of granular material,” *Proceedings of the National Academy of Sciences*, vol. 107, no. 44, pp. 18 809–18 814, 2010.

[110] A. Jiang, T. Ranzani, G. Gerboni, L. Lekstutyte, K. Althoefer, P. Dasgupta, and T. Nanayakkara, “Robotic granular jamming: Does the membrane matter?” *Soft Robotics*, vol. 1, no. 3, pp. 192–201, 2017/06/21 2014. [Online]. Available: https://doi.org/10.1089/soro.2014.0002

[111] J. Amend, N. Cheng, S. Fakhouri, and B. Culley, “Soft robotics commercialization: Jamming grippers from research to product,” *Soft Robotics*, vol. 3, no. 4, pp. 213–222, 2017/06/21 2016. [Online]. Available: https://doi.org/10.1089/soro.2016.0021

[112] C. Mattmann, O. Amft, H. Harms, G. Troster, and F. Clemens, “Recognizing upper body postures using textile strain sensors,” in *2007 11th IEEE International Symposium on Wearable Computers*. IEEE, 2007, pp. 29–36.

[113] M. Amjadi, K.-U. Kyung, I. Park, and M. Sitti, “Stretchable, skin-mountable, and wearable strain sensors and their potential applications: A review,” *Advanced Functional Materials*, vol. 26, pp. 1678–1698, 2016.

[114] X. Xiao, L. Yuan, J. Zhong, T. Ding, Y. Liu, Z. Cai, Y. Rong, H. Han, J. Zhou, and Z. L. Wang, "High-strain sensors based on zno nanowire/polystyrene hybridized flexible films," *Advanced materials*, vol. 23, no. 45, pp. 5440–5444, 2011.

[115] Y. R. Jeong, H. Park, S. W. Jin, S. Y. Hong, S.-S. Lee, and J. S. Ha, "Highly stretchable and sensitive strain sensors using fragmentized graphene foam," *Advanced Functional Materials*, vol. 25, no. 27, pp. 4228–4236, 2015.

[116] M. Amjadi, A. Pichitpajongkit, S. Lee, S. Ryu, and I. Park, "Highly stretchable and sensitive strain sensor based on silver nanowire–elastomer nanocomposite," *ACS nano*, vol. 8, no. 5, pp. 5154–5163, 2014.

[117] J. R. Amend, E. Brown, N. Rodenberg, H. M. Jaeger, and H. Lipson, "A positive pressure universal gripper based on the jamming of granular material," *IEEE Transactions on Robotics*, vol. 28, no. 2, pp. 341–350, 2012.

[118] R. Fernandez, I. Payo, A. S. Vazquez, and J. Becedas, "Micro-vibration-based slip detection in tactile force sensors," *Sensors*, vol. 14, no. 1, pp. 709–730, 2014.

[119] M. Stachowsky, T. Hummel, M. Moussa, and H. A. Abdullah, "A slip detection and correction strategy for precision robot grasping," *IEEE/ASME Transactions on Mechatronics*, vol. 21, no. 5, pp. 2214–2226, 2016.

[120] D. D. Damian, T. H. Newton, R. Pfeifer, and A. M. Okamura, "Artificial tactile sensing of position and slip speed by exploiting geometrical features," *IEEE/ASME Transactions on Mechatronics*, vol. 20, no. 1, pp. 263–274, 2015.

[121] S. Shirafuji and K. Hosoda, "Detection and prevention of slip using sensors with different properties embedded in elastic artificial skin on the basis of previous experience," *Robotics and Autonomous Systems*, vol. 62, no. 1, pp. 46–52, 2014.

[122] R. A. Romeo, C. M. Oddo, M. C. Carrozza, E. Guglielmelli, and L. Zollo, "Slippage detection with piezoresistive tactile sensors," *Sensors*, vol. 17, no. 8, p. 1844, 2017.

[123] C.-H. Chuang, Y.-R. Liou, and C.-W. Chen, "Detection system of incident slippage and friction coefficient based on a flexible tactile sensor with structural electrodes," *Sensors and Actuators A: physical*, vol. 188, pp. 48–55, 2012.

[124] S. Teshigawara, T. Tsutsumi, S. Shimizu, Y. Suzuki, A. Ming, M. Ishikawa, and M. Shimojo, "Highly sensitive sensor for detection of initial slip and its application in a multi-fingered robot hand," in *Robotics and Automation (ICRA), 2011 IEEE International Conference on*. IEEE, 2011, pp. 1097–1102.

[125] D. V. Dao, S. Sugiyama, S. Hirai *et al.*, "Development and analysis of a sliding tactile soft fingertip embedded with a microforce/moment sensor," *IEEE Transactions on Robotics*, vol. 27, no. 3, pp. 411–424, 2011.

[126] F. Iida and S. G. Nurzaman, "Adaptation of sensor morphology: An integrative view of perception from biologically inspired robotics perspective," *Interface Focus*, vol. 6, no. 4, p. 20160016, 2016.

[127] L. Wang and F. Iida, "Physical connection and disconnection control based on hot melt adhesives," *IEEE/ASME Transactions on mechatronics*, vol. 18, no. 4, pp. 1397–1409, 2013.

[128] A. Bicchi and V. Kumar, "Robotic grasping and contact: A review," in *Robotics and Automation, 2000. Proceedings. ICRA'00. IEEE International Conference on*, vol. 1. IEEE, 2000, pp. 348–353.

[129] P. V. P. Reddy and V. Suresh, "A review on importance of universal gripper in industrial robot applications," *Int. J. Mech. Eng. Robot. Res*, vol. 2, no. 2, pp. 255–264, 2013.

[130] G. Mantriota, "Optimal grasp of vacuum grippers with multiple suction cups," *Mechanism and machine theory*, vol. 42, no. 1, pp. 18–33, 2007.

[131] K. Autumn, Y. A. Liang, S. T. Hsieh, W. Zesch, W. P. Chan, T. W. Kenny, R. Fearing, and R. J. Full, "Adhesive force of a single gecko foot-hair," *Nature*, vol. 405, no. 6787, pp. 681–685, 2000.

[132] K. Liu, J. Du, J. Wu, and L. Jiang, "Superhydrophobic gecko feet with high adhesive forces towards water and their bio-inspired materials," *Nanoscale*, vol. 4, no. 3, pp. 768–772, 2012.

[133] M. Osswald and F. Iida, "Design and control of a climbing robot based on hot melt adhesion," *Robotics and Autonomous Systems*, vol. 61, no. 6, pp. 616–625, 2013.

[134] J. Neubert, A. Rost, and H. Lipson, "Self-soldering connectors for modular robots," *IEEE Transactions on Robotics*, vol. 30, no. 6, pp. 1344–1357, 2014.

[135] T. Nishida, D. Shigehisa, N. Kawashima, and K. Tadakuma, "Development of universal jamming gripper with a force feedback mechanism," in *Soft Computing and Intelligent Systems (SCIS) 15th International Symposium*. IEEE, 2014, pp. 242–246.

[136] Y.-J. Park and H.-J. Kim, "Hot-melt adhesive properties of eva/aromatic hydrocarbon resin blend," *International journal of adhesion and adhesives*, vol. 23, no. 5, pp. 383–392, 2003.

[137] C. Gay and L. Leibler, "Theory of tackiness," *Physical review letters*, vol. 82, no. 5, p. 936, 1999.

[138] O. A, "The effect of molecular weight and temperature on tack properties of model polyisobutylenes," *Int. J. of Adhesion & Adhesives*, vol. 24, 2004.

[139] J. B. Enns and J. K. Gillham, "Time–temperature–transformation (ttt) cure diagram: Modeling the cure behavior of thermosets," *Journal of Applied Polymer Science*, vol. 28, no. 8, pp. 2567–2591, 1983.

[140] R. Bates, "Studies in the nature of adhesive tack," *Journal of Applied Polymer Science*, vol. 20, no. 11, pp. 2941–2954, 1976.

[141] I. H. Shames, *Elastic and inelastic stress analysis*. CRC Press, 1997.

[142] M. Sakai, "Time-dependent viscoelastic relation between load and penetration for an axisymmetric indenter," *Philosophical Magazine A*, vol. 82, no. 10, pp. 1841–1849, 2002.

[143] C. A. Tweedie and K. J. Van Vliet, "Contact creep compliance of viscoelastic materials via nanoindentation," *Journal of materials research*, vol. 21, no. 6, pp. 1576–1589, 2006.

[144] J. B. Enns and J. K. Gillham, "Time–temperature–transformation (ttt) cure diagram: Modeling the cure behavior of thermosets," *Journal of Applied Polymer Science*, vol. 28, no. 8, pp. 2567–2591, 1983.

[145] A. Naeemi and J. D. Meindl, "Physical modeling of temperature coefficient of resistance for single-and multi-wall carbon nanotube interconnects," *IEEE Electron Device Letters*, vol. 28, no. 2, pp. 135–138, 2007.

[146] J. Glatz-Reichenbach *et al.*, "Feature article conducting polymer composites," *Journal of Electroceramics*, vol. 3, no. 4, pp. 329–346, 1999.

[147] S. Ding, B. Han, X. Dong, X. Yu, Y. Ni, Q. Zheng, and J. Ou, "Pressure-sensitive behaviors, mechanisms and model of field assisted quantum tunneling composites," *Polymer*, vol. 113, pp. 105–118, 2017.

[148] T. Ding, L. Wang, and P. Wang, "Changes in electrical resistance of carbon-black-filled silicone rubber composite during compression," *Journal of Polymer Science Part B: Polymer Physics*, vol. 45, no. 19, pp. 2700–2706, 2007.

[149] W. Yi, Y. Wang, G. Wang, and X. Tao, "Investigation of carbon black/silicone elastomer/dimethylsilicone oil composites for flexible strain sensors," *Polymer Testing*, vol. 31, no. 5, pp. 677–684, 2012.

[150] D. Bloor, K. Donnelly, P. Hands, P. Laughlin, and D. Lussey, "A metal–polymer composite with unusual properties," *Journal of Physics D: Applied Physics*, vol. 38, no. 16, p. 2851, 2005.

[151] L. Wang and L. Cheng, "Piezoresistive effect of a carbon nanotube silicone-matrix composite," *Carbon*, vol. 71, pp. 319–331, 2014.

[152] A. Saleem, L. Frormann, and A. Soever, "Fabrication of extrinsically conductive silicone rubbers with high elasticity and analysis of their mechanical and electrical characteristics," *Polymers*, vol. 2, no. 3, pp. 200–210, 2010.

[153] A. Napierala, "Electrical behaviour of current conducting silicon rubber," *8th EEEIC*, 2009.

[154] F. Gubbels, R. Jérôme, P. Teyssie, E. Vanlathem, R. Deltour, A. Calderone, V. Parente, and J.-L. Brédas, "Selective localization of carbon black in immiscible polymer blends: a useful tool to design electrical conductive composites," *Macromolecules*, vol. 27, no. 7, pp. 1972–1974, 1994.

[155] P. Wang, T. Ding, F. Xu, and Y. Qin, "Piezoresistivity of conductive composites filled by carbon black particles." *Fuhe Cailiao Xuebao(Acta Mater. Compos. Sin.)*, vol. 21, no. 6, pp. 34–38, 2004.

[156] O. D. Lara and M. A. Labrador, "A survey on human activity recognition using wearable sensors," *IEEE Communications Surveys & Tutorials*, vol. 15, no. 3, pp. 1192–1209, 2013.

[157] A. Pantelopoulos and N. G. Bourbakis, "A survey on wearable sensor-based systems for health monitoring and prognosis," *IEEE Transactions on Systems, Man, and Cybernetics, Part C (Applications and Reviews)*, vol. 40, no. 1, pp. 1–12, 2010.

[158] P. Bonato *et al.*, "Wearable sensors/systems and their impact on biomedical engineering," *IEEE Engineering in Medicine and Biology Magazine*, vol. 22, no. 3, pp. 18–20, 2003.

[159] J. Bergmann and A. McGregor, "Body-worn sensor design: what do patients and clinicians want?" *Annals of biomedical engineering*, vol. 39, no. 9, pp. 2299–2312, 2011.

[160] Y. Mengüç, Y.-L. Park, H. Pei, D. Vogt, P. M. Aubin, E. Winchell, L. Fluke, L. Stirling, R. J. Wood, and C. J. Walsh, "Wearable soft sensing suit for human gait measurement," *The International Journal of Robotics Research*, p. 0278364914543793, 2014.

[161] A. Torres, L. Sarlabous, J. A. Fiz, J. Gea, J. M. Martínez-Llorens, J. Morera, and R. Jané, "Noninvasive measurement of inspiratory muscle performance by means of diaphragm muscle mechanomyographic signals in copd patients during an incremental load respiratory test," in *2010 Annual International Conference of the IEEE Engineering in Medicine and Biology*. IEEE, 2010, pp. 2493–2496.

[162] S. Coyle, D. Morris, K.-T. Lau, D. Diamond, and N. Moyna, "Textile-based wearable sensors for assisting sports performance," in *2009 Sixth International Workshop on Wearable and Implantable Body Sensor Networks*. IEEE, 2009, pp. 307–311.

[163] F. Michard, D. Chemla, C. Richard, M. Wysocki, M. R. Pinsky, Y. Lecarpentier, and J.-L. Teboul, "Clinical use of respiratory changes in arterial pulse pressure to monitor the hemodynamic effects of peep," *American journal of respiratory and critical care medicine*, vol. 159, no. 3, pp. 935–939, 1999.

[164] J. A. Luis, L. M. Roa Romero, J. A. Gómez-Galán, D. N. Hernández, M. Á. Estudillo-Valderrama, G. Barbarov-Rostán, and C. Rubia-Marcos, "Design and implementation of a smart sensor for respiratory rate monitoring," *Sensors*, vol. 14, no. 2, pp. 3019–3032, 2014.

[165] K. H. Shelley, "Photoplethysmography: beyond the calculation of arterial oxygen saturation and heart rate," *Anesthesia & Analgesia*, vol. 105, no. 6, pp. S31–S36, 2007.

[166] S. Gong, W. Schwalb, Y. Wang, Y. Chen, Y. Tang, J. Si, B. Shirinzadeh, and W. Cheng, "A wearable and highly sensitive pressure sensor with ultrathin gold nanowires," *Nature communications*, vol. 5, 2014.

[167] W. Tao, T. Liu, R. Zheng, and H. Feng, "Gait analysis using wearable sensors," *Sensors*, vol. 12, no. 2, pp. 2255–2283, 2012.

[168] K. Watanabe and M. Hokari, "Kinematical analysis and measurement of sports form," *IEEE Transactions on Systems, Man, and Cybernetics-Part A: Systems and Humans*, vol. 36, no. 3, pp. 549–557, 2006.

[169] S. Kimmeskamp and E. M. Hennig, "Heel to toe motion characteristics in parkinson patients during free walking," *Clinical biomechanics*, vol. 16, no. 9, pp. 806–812, 2001.

[170] O. Amft, H. Junker, P. Lukowicz, G. Troster, and C. Schuster, "Sensing muscle activities with body-worn sensors," in *International Workshop on Wearable and Implantable Body Sensor Networks (BSN'06)*. IEEE, 2006, pp. 4–pp.

[171] A. Bates, M. J. Ling, J. Mann, and D. Arvind, "Respiratory rate and flow waveform estimation from tri-axial accelerometer data," in *2010 International Conference on Body Sensor Networks*. IEEE, 2010, pp. 144–150.

[172] M. A. Brodie, T. R. Beijer, C. G. Canning, and S. R. Lord, "Head and pelvis stride-to-stride oscillations in gait: validation and interpretation of measurements from wearable accelerometers," *Physiological measurement*, vol. 36, no. 5, p. 857, 2015.

[173] E. Fortune, V. Lugade, M. Morrow, and K. Kaufman, "Validity of using tri-axial accelerometers to measure human movement–part ii: Step counts at a wide range of gait velocities," *Medical engineering & physics*, vol. 36, no. 6, pp. 659–669, 2014.

[174] M. Melzer, J. I. Mönch, D. Makarov, Y. Zabila, G. S. Cañón Bermúdez, D. Karnaushenko, S. Baunack, F. Bahr, C. Yan, M. Kaltenbrunner *et al.*, "Wearable magnetic field sensors for flexible electronics," *Advanced Materials*, vol. 27, no. 7, pp. 1274–1280, 2015.

[175] M. Stoppa and A. Chiolerio, "Wearable electronics and smart textiles: a critical review," *Sensors*, vol. 14, no. 7, pp. 11 957–11 992, 2014.

[176] E. Suaste-Gómez, D. Hernández-Rivera, A. S. Sánchez-Sánchez, and E. Villarreal-Calva, "Electrically insulated sensing of respiratory rate and heartbeat using optical fibers," *Sensors*, vol. 14, no. 11, pp. 21 523–21 534, 2014.

[177] Y. Wang, L. Wang, T. Yang, X. Li, X. Zang, M. Zhu, K. Wang, D. Wu, and H. Zhu, "Wearable and highly sensitive graphene strain sensors for human motion monitoring," *Advanced Functional Materials*, vol. 24, no. 29, pp. 4666–4670, 2014.

[178] S. Yao and Y. Zhu, "Wearable multifunctional sensors using printed stretchable conductors made of silver nanowires," *Nanoscale*, vol. 6, no. 4, pp. 2345–2352, 2014.

[179] O. Atalay and W. R. Kennon, "Knitted strain sensors: impact of design parameters on sensing properties," *Sensors*, vol. 14, no. 3, pp. 4712–4730, 2014.

[180] Y. Wang, L. Wang, T. Yang, X. Li, X. Zang, M. Zhu, K. Wang, D. Wu, and H. Zhu, "Wearable and highly sensitive graphene strain sensors for human motion monitoring," *Advanced Functional Materials*, vol. 24, no. 29, pp. 4666–4670, 2014.

[181] Y. Mengüç, Y.-L. Park, E. Martinez-Villalpando, P. Aubin, M. Zisook, L. Stirling, R. J. Wood, and C. J. Walsh, "Soft wearable motion sensing suit for lower limb biomechanics measurements," in *Robotics and Automation (ICRA), 2013 IEEE International Conference on*. IEEE, 2013, pp. 5309–5316.

[182] C. Mattmann, F. Clemens, and G. Tröster, "Sensor for measuring strain in textile," *Sensors*, vol. 8, no. 6, pp. 3719–3732, 2008.

[183] J. Cheng, O. Amft, and P. Lukowicz, "Active capacitive sensing: Exploring a new wearable sensing modality for activity recognition," in *International Conference on Pervasive Computing*. Springer, 2010, pp. 319–336.

[184] C.-C. Yang and Y.-L. Hsu, "A review of accelerometry-based wearable motion detectors for physical activity monitoring," *Sensors*, vol. 10, no. 8, pp. 7772–7788, 2010.

[185] S. Patel, H. Park, P. Bonato, L. Chan, and M. Rodgers, "A review of wearable sensors and systems with application in rehabilitation," *Journal of neuroengineering and rehabilitation*, vol. 9, no. 1, p. 1, 2012.

[186] R. Luttmann, D. G. Bracewell, G. Cornelissen, K. V. Gernaey, J. Glassey, V. C. Hass, C. Kaiser, C. Preusse, G. Striedner, and C.-F. Mandenius, "Soft sensors in bioprocessing: a status report and recommendations," *Biotechnology journal*, vol. 7, no. 8, pp. 1040–1048, 2012.

[187] H. Yousef, M. Boukallel, and K. Althoefer, "Tactile sensing for dexterous in-hand manipulation in robotics—a review," *Sensors and Actuators A: physical*, vol. 167, no. 2, pp. 171–187, 2011.

[188] A. J. Ijspeert, A. Crespi, D. Ryczko, and J.-M. Cabelguen, "From swimming to walking with a salamander robot driven by a spinal cord model," *science*, vol. 315, no. 5817, pp. 1416–1420, 2007.

[189] R. Pfeifer, F. Iida, and M. Lungarella, "Cognition from the bottom up: on biological inspiration, body morphology, and soft materials," *Trends in cognitive sciences*, vol. 18, no. 8, pp. 404–413, 2014.

[190] S. Wolf and G. Hirzinger, "A new variable stiffness design: Matching requirements of the next robot generation," in *Robotics and Automation, 2008. ICRA 2008. IEEE International Conference on*. IEEE, 2008, pp. 1741–1746.

[191] S. Haddadin, F. Huber, and A. Albu-Schäffer, "Optimal control for exploiting the natural dynamics of variable stiffness robots," in *Robotics and Automation (ICRA), 2012 IEEE International Conference on*. IEEE, 2012, pp. 3347–3354.

[192] J. Z. Wu, Z.-M. Li, R. G. Cutlip, and K.-N. An, "A simulating analysis of the effects of increased joint stiffness on muscle loading in a thumb," *Biomedical engineering online*, vol. 8, no. 1, p. 41, 2009.

[193] M. Manti, V. Cacucciolo, and M. Cianchetti, "Stiffening in soft robotics: A review of the state of the art," *IEEE Robotics & Automation Magazine*, vol. 23, no. 3, pp. 93–106, 2016.

[194] D. Trivedi, C. D. Rahn, W. M. Kier, and I. D. Walker, “Soft robotics: Biological inspiration, state of the art, and future research,” *Applied Bionics and Biomechanics*, vol. 5, no. 3, pp. 99–117, 2008.

[195] N. W. Bartlett, M. T. Tolley, J. T. Overvelde, J. C. Weaver, B. Mosadegh, K. Bertoldi, G. M. Whitesides, and R. J. Wood, “A 3d-printed, functionally graded soft robot powered by combustion,” *Science*, vol. 349, no. 6244, pp. 161–165, 2015.

[196] D. Rus and M. T. Tolley, “Design, fabrication and control of soft robots,” *Nature*, vol. 521, no. 7553, pp. 467–475, 05 2015. [Online]. Available: http://dx.doi.org/10.1038/nature14543

[197] T. Umedachi, V. Vikas, and B. A. Trimmer, “Highly deformable 3-d printed soft robot generating inching and crawling locomotions with variable friction legs,” in *Intelligent Robots and Systems (IROS), 2013 IEEE/RSJ International Conference on*. IEEE, 2013, pp. 4590–4595.

[198] C. Eppner and O. Brock, “Grasping unknown objects by exploiting shape adaptability and environmental constraints,” in *Intelligent Robots and Systems (IROS), 2013 IEEE/RSJ International Conference on*. IEEE, 2013, pp. 4000–4006.

[199] R. B. Gillespie, B. Yu, R. Grijalva, and S. Awtar, “Characterizing the feel of the piano action,” *Computer Music Journal*, vol. 35, no. 1, pp. 43–57, 2011.

[200] S. Sugano and I. Kato, “Wabot-2: Autonomous robot with dexterous finger-arm–finger-arm coordination control in keyboard performance,” in *Robotics and Automation. Proceedings. 1987 IEEE International Conference on*, vol. 4. IEEE, 1987, pp. 90–97.

[201] Y.-F. Li and C.-Y. Lai, “Intelligent algorithm for music playing robot—applied to the anthropomorphic piano robot control,” in *Industrial Electronics (ISIE), 2014 IEEE 23rd International Symposium on*. IEEE, 2014, pp. 1538–1543.

[202] D. Zhang, J. Lei, B. Li, D. Lau, and C. Cameron, “Design and analysis of a piano playing robot,” in *Information and Automation, 2009. ICIA’09. International Conference on*. IEEE, 2009, pp. 757–761.

[203] J.-C. Lin, H.-H. Huang, Y.-F. Li, J.-C. Tai, and L.-W. Liu, “Electronic piano playing robot,” in *Computer Communication Control and Automation (3CA), 2010 International Symposium on*, vol. 2. IEEE, 2010, pp. 353–356.

[204] A. Gustus, G. Stillfried, J. Visser, H. Jörntell, and P. van der Smagt, “Human hand modelling: kinematics, dynamics, applications,” *Biological cybernetics*, vol. 106, no. 11-12, pp. 741–755, 2012.

[205] D. Burke, S. Gandevia, and G. Macefield, “Responses to passive movement of receptors in joint, skin and muscle of the human hand.” *The Journal of physiology*, vol. 402, no. 1, pp. 347–361, 1988.

[206] Y. Zhang, H. Deng, and G. Zhong, “Humanoid design of mechanical fingers using a motion coupling and shape-adaptive linkage mechanism,” *Journal of Bionic Engineering*, vol. 15, no. 1, pp. 94–105, 2018.

[207] R. J. Schwarz and C. Taylor, "The anatomy and mechanics of the human hand," *Artificial limbs*, vol. 2, no. 2, pp. 22–35, 1955.

[208] C. C. Norkin and D. J. White, *Measurement of joint motion: a guide to goniometry*. FA Davis, 2016.

[209] A. Hollister, D. J. Giurintano, W. L. Buford, L. M. Myers, and A. Novick, "The axes of rotation of the thumb interphalangeal and metacarpophalangeal joints," *Clinical Orthopaedics and Related Research®*, vol. 320, pp. 188–193, 1995.

[210] R. L. Truby and J. A. Lewis, "Printing soft matter in three dimensions," *Nature*, vol. 540, no. 7633, p. 371, 2016.

[211] M. Wehner, R. L. Truby, D. J. Fitzgerald, B. Mosadegh, G. M. Whitesides, J. A. Lewis, and R. J. Wood, "An integrated design and fabrication strategy for entirely soft, autonomous robots," *Nature*, vol. 536, no. 7617, p. 451, 2016.

[212] R. J. Schwarz and C. Taylor, "The anatomy and mechanics of the human hand," *Artificial limbs*, vol. 2, no. 2, pp. 22–35, 1955.

[213] A. Hollister, D. J. Giurintano, W. L. Buford, L. M. Myers, and A. Novick, "The axes of rotation of the thumb interphalangeal and metacarpophalangeal joints," *Clinical Orthopaedics and Related Research®*, vol. 320, pp. 188–193, 1995.

[214] J. Calì, D. A. Calian, C. Amati, R. Kleinberger, A. Steed, J. Kautz, and T. Weyrich, "3d-printing of non-assembly, articulated models," *ACM Transactions on Graphics (TOG)*, vol. 31, no. 6, p. 130, 2012.

[215] R. R. Ma, L. U. Odhner, and A. M. Dollar, "A modular, open-source 3d printed underactuated hand," in *Robotics and Automation (ICRA), 2013 IEEE International Conference on*. IEEE, 2013, pp. 2737–2743.

[216] J. Friedman and T. Flash, "Task-dependent selection of grasp kinematics and stiffness in human object manipulation," *Cortex*, vol. 43, no. 3, pp. 444–460, 2007.

[217] H. Höppner, D. Lakatos, H. Urbanek, C. Castellini, and P. van der Smagt, "The grasp perturbator: Calibrating human grasp stiffness during a graded force task," in *Robotics and Automation (ICRA), 2011 IEEE International Conference on*. IEEE, 2011, pp. 3312–3316.

[218] T. E. Milner and D. W. Franklin, "Characterization of multijoint finger stiffness: dependence on finger posture and force direction," *IEEE Transactions on Biomedical Engineering*, vol. 45, no. 11, pp. 1363–1375, 1998.

[219] U. Culha, U. Wani, S. G. Nurzaman, F. Clemens, and F. Iida, "Motion pattern discrimination for soft robots with morphologically flexible sensors," in *2014 IEEE/RSJ International Conference on Intelligent Robots and Systems*. IEEE, 2014, pp. 567–572.

[220] M. Chepisheva, U. Culha, and F. Iida, "A biologically inspired soft robotic hand using chopsticks for grasping tasks," in *International Conference on Simulation of Adaptive Behavior*. Springer, 2016, pp. 195–206.

[221] J. C. Case, E. L. White, and R. K. Kramer, “Soft material characterization for robotic applications,” *Soft Robotics*, vol. 2, no. 2, pp. 80–87, 2015.

[222] ——, “Soft material characterization for robotic applications,” *Soft Robotics*, vol. 2, no. 2, pp. 80–87, 2015.

[223] F. Iida and R. Pfeifer, “Sensing through body dynamics,” *Robotics and Autonomous Systems*, vol. 54, no. 8, pp. 631–640, 2006.

[224] ——, “Structuring sensory information through body dynamics,” in *IROS05 Workshop on Morphology, Control and Passive Dynamics*, 2005.

[225] T. R. Farrell, R. F. Weir, C. W. Heckathorne, and D. S. Childress, “The effects of static friction and backlash on extended physiological proprioception control of a powered prosthesis,” *Journal of rehabilitation research and development*, vol. 42, no. 3, p. 327, 2005.

[226] S. G. Nurzaman, U. Culha, L. Brodbeck, L. Wang, and F. Iida, “Active sensing system with in situ adjustable sensor morphology,” *PLoS One*, vol. 8, no. 12, p. e84090, 2013.

Appendix A

Wrist Control for Playing

The details of how the wrist actuation is determined for playing of different sytles is detailed in this section.

The fingers used to play the three segments and the different repeated patterns within this phrases of music are shown in Fig. A.1. The fingers used have been chosen to achieved the correct conditional stiffness, but also to make the playing possible - for example by enabling jumps of slides to occur.

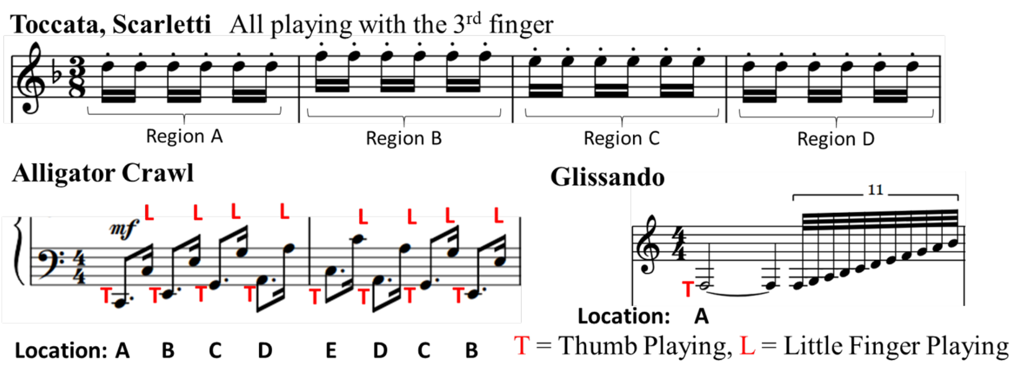

Figure A.1 Fingers used to play the different notes in the three pieces selected for playing.

The flow charts which corresponding to the sections of the music show in Fig. A.1 for the wrist movement planning is shown in Fig. A.2. This uses the note locations to determine the locations for each of the playing positions.

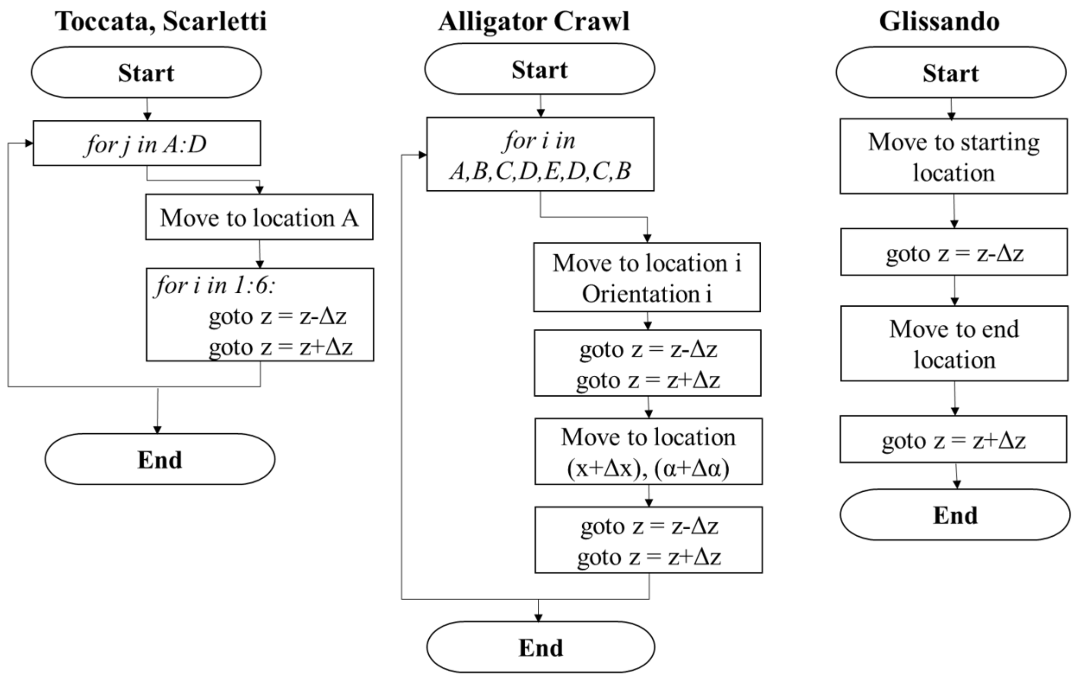

Figure A.2 Flow chart for the movement of the wrist for playing the three sections of music.

Appendix B

Related Work

B.1 Automated Robotic Lettuce Harvesting

Lettuce are currently harvested manually, which is highly labour intensive, unpleasant work and is becoming increasingly problematic due to the political and economic climate. Although there is significant automation in agricultural systems, iceberg lettuce is challenging as the crop is easily damaged when harvesting. However harvesting requires significant force and precision. This is therefore an opportunity for hybrid robotics systems to be used. To solve this problem an end effector for lettuce harvesting has been developed which uses a rigid guillotine system and a soft clamp system. Multiple iterations of the system have been developed, with the system tested in the lettuce fields. Achieving the correct balance between rigid force production and soft clamping to prevent damage whilst achieving a clean cut was critical to successful lettuce harvesting. The end effector has been integrated into a robot arm system, with a vision based lettuce localisation and classification system used to allow automated harvesting. Fig. B.1.a) shows the end effector developed mounted on the end of the arm system used for automated harvesting.

Although harvesting can be achieved with reasonable success. After harvesting, it can be necessary to remove the outer leaves of the lettuce, as some unwanted leaves remain after harvesting, be it manual or automated. The leaves are soft and fragile making this a challenging vision and manipulation task. An automatic lettuce removal system was developed[1]. The scenario considered is that of a lettuce placed in a random pose on a flat table where the outermost leaves must be peeled quickly without damaging the lettuce. Alongside a novel vision pipeline, a system for achieving leaf removal using vacuum pressure with a soft suction nozzle (again utilising soft-rigid hybrid design) was developed. This

(a)

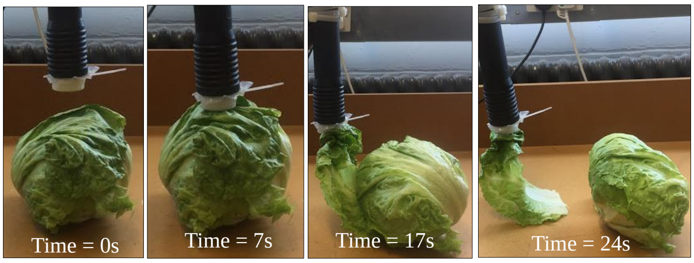

(b)

Figure B.1 a) Lettuce harvesting end-effector b) Time series of the leaf removal showing the time taken to complete the process.

enables the complete removal of the outer leaves in under 30 seconds (Fig. B.1.b). To our knowledge, this is the first automated lettuce leaf removal system.

B.2 Data Synthesis for Classification in Autonomous Robotic Grasping System[2]

The work in this thesis has considered grasping and manipulation where no vision is used. However, this is not entirely a realistic situation; vision has the ability to significantly aid grasping and manipulation when used alongside other tactile approaches. The generalised classification and localisation of objects for manipulation remains an unsolved problem.

In particular, the localisation and grasping of randomly placed objects where only a limited number of training images are available, remains a challenging problem. Approaches such as data synthesis have been used to synthetically augment data sets to aid performance. This research examines how limited data sets of product images of 'off the shelf' items can be used to generate a synthetic data set that can be used to train a neural network which allows classification, segmentation and grasping of the item. The pipeline developed is shown in Fig. B.2. Experiments investigating the effects of data synthesis were undertaken and using these results, the optimal data synthesis approaches used to train a network. This was then implemented in a robotic grasping system. This followed on from initial work using neural networks for grasping point identification[3].

---

[1]This work has been accepted for publication. I worked collaboratively to develop the concept, and worked on the development of the manipulation system, the experimental results, preparation of the figures and the writing of the paper:

- Josie Hughes, Luca Scimeca, Ioana Ifrim, Perla Maiolino and Fumiya Iida, "Achieving Robotically Peeled Lettuce", *Robotics and Automation Letters.*

[2]This work was was published, and includes the collaborative work of student M. Cheah and my supervisor F. Iida. I assisted with developing the problem statement, framework, the gripper development and the practical experiments, prepared the figures and collaboratively wrote the paper:

- Cheah, Michael, Hughes, Josie and Iida, Fumiya. "Data Synthesization for Classification in Autonomous Robotic Grasping System Using 'Catalogue'-Style Images" *Conference Towards Autonomous Robotic Systems. Springer, Cham, 2018.*

[3]This work was was published, and includes the collaborative work of student J. Watson and my supervisor F. Iida. I have assisted with the preparation of figures and the writing of the paper:

- Watson, Joe, Hughes, Josie and Iida, Fumiya. "Real-World, Real-Time Robotic Grasping with Convolutional Neural Networks." *Conference Towards Autonomous Robotic Systems. Springer, Cham, 2017.*

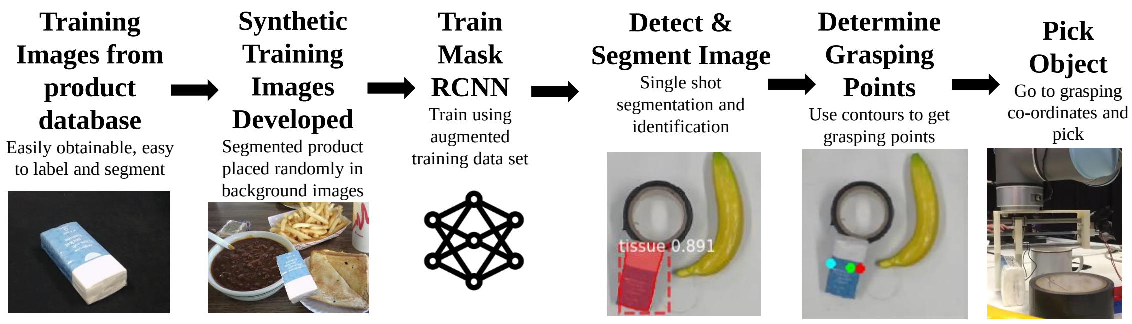

Figure B.2 Summary of the image identification pipeline from image acquisition to object grasping.

B.3 Flexible Assembly of Structures Using Autonomous Robotic Systems[4]

Understanding the applications and utility of manipulators and grippers it key to ubiquitous and efficient use. Construction is one area where robotic manipulations could make significant impact. Prefabrication of structures is currently used only in a limited capacity, due to the lack of flexibility in design, despite the potential cost and speed advantages. Autonomous flexible re-assembly enables structures to be developed which can be continuously and iteratively dis-assembled and re-assembled providing far more flexibility in comparison to single shot pre-fabrication methods. Dis-assembly of structures should be considered when assembling, due to the asymmetry of assembly and dis-assembly processes, to ensure structures can be recycled and re-assembled. This allows for agile development, significantly reducing the time and resource usage during the build process. In this research, a framework for flexible re-assembly is developed and a robotic platform is developed to implement and test this framework with simple Lego bricks. The trade-offs in terms of time, resource use and probability of success of this new assembly method can be understood by using a cost function to compare to alternative fabrication methods. This approach investigated developing structures using the building sub-structures which enable placement of more complex brick morphologies. This reflects the approach of thesis, where embodied mechanical intelligence is used to reduce the requirement for complex control.

[4] This work has been submitted for review. It is the work of K. Gilday, myself and my supervisor F. Iida. I have assisted with developing the problem statement, the theory developed and collaboratively prepared the figures and wrote the paper:

- Glday, Kieran, Hughes, Josie, and Fumiya Iida. "Achieving Flexible Assembly Using Autonomous Robotic Systems" *IROS, 2018*

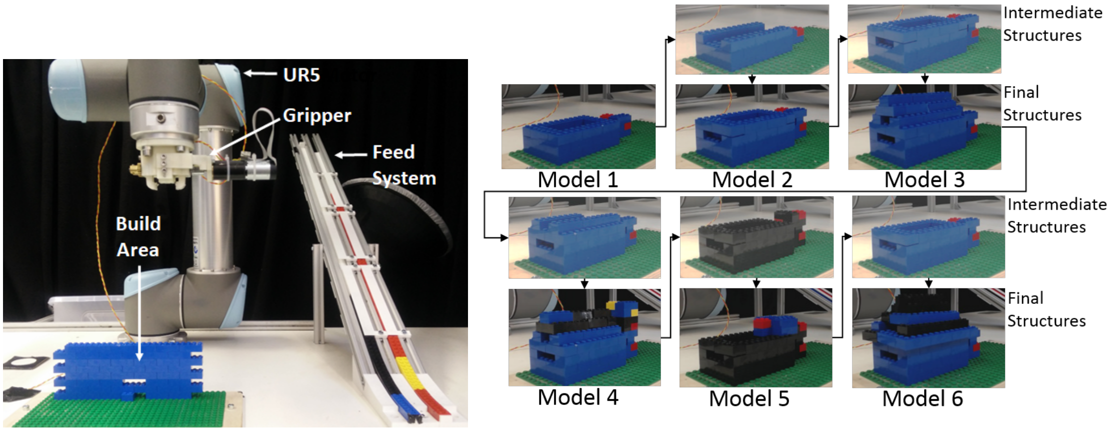

(a) (b)

Figure B.3 a) Automated robotic Lego fabrication system showing the arm, gripper and feed system, b) Wall built at each stage and the intermediate structure when re-assembling.